GENETIC ENGINEERING AND PURIFICATION OF THE HYDROGENASES FROM THE HYPERTHERMOPHILIC ARCHAEON *PYROCOCCUS FURIOSUS*

by

Patrick Michael McTernan

(Under the Direction of Michael W. W. Adams)

ABSTRACT

Due to the inevitable depletion of fossil fuels on earth, a major shift in research has occurred that emphasizes the generation of a renewable energy source. More specifically, this renewable energy source should be carbon neutral and capable of delivering a high energy yield upon use. Hydrogen gas meets these criteria as it can be produced in nature without the generation of greenhouse gases and the conversion of hydrogen to water yields three times more energy than gasoline on a weight basis. Although this may be true, more research is needed in order to understand the mechanisms and restrictions associated with biological hydrogen production. In order to gain this better understanding, the hydrogenase enzyme, which is responsible for hydrogen production in nature, has been investigated. The generation and analysis of hydrogenase can greatly help in understanding how these enzymes generate hydrogen and how these enzymes could be engineered for biofuel production. The hydrogenases from *Pyrococcus furiosus* are the focus of this study. *P. furiosus* is a hyperthermophilic *archaeon* that

optimally grows at 100^0 C and ferments both peptides and carbohydrates. It contains three [NiFe]-hydrogenases, two of which are found in the cytoplasm and are termed soluble hydrogenase I (SHI) and soluble hydrogenase II (SHII). The third is a 14-subunit membrane-bound hydrogenase (MBH) that is proposed to function as a novel respiratory system within the membrane. MBH shows a strong preference to evolve hydrogen, which is rare among [NiFe]-hydrogenases, and will be the focus of this dissertation. In the literature, previous attempts to purify MBH using standard purification techniques from *P. furiosus* lead to the purification of only five subunits of the fourteen-subunit complex. Herein, a new protocol is described that yields the entire 14-subunit MBH complex for biochemical and structural analyses. The genetic system that was recently developed for *P. furiosus* has been successfully used to place the SHI operon under a stronger promoter. This lead to the over-expression of the enzyme by 10-fold, and was used to engineer an affinity tag at the N-terminus of one of the subunits, which greatly improved the yield of the hydrogenase. This genetic system was also applied to MBH to split the native operon into two different transcriptional units. From the recombinant strain, both the 14-subunit intact MBH (S-MBH) and a completely soluble MBH sub-complex (C-MBH) were purified. Both forms of MBH were characterized at the enzymatic and structural level. From this analysis, the implications of a crystal structure of C-MBH on how other respiratory systems have evolved over time are discussed.

GENETIC ENGINEERING AND PURIFICATION OF THE HYDROGENASES FROM THE HYPERTHERMOPHILIC ARCHAEON *PYROCOCCUS FURIOSUS*

PATRICK MICHAEL MCTERNAN

B.S. Microbiology Louisiana State University 2007

A Dissertation Submitted to the Graduate Faculty of the University of Georgia in Partial Fulfillment of the Requirements for the Degree

DOCTOR OF PHILOSOPHY

ATHENS, GEORGIA

2015

GENETIC ENGINEERING AND PURIFICATION OF THE HYDROGENASES FROM THE HYPERTHERMOPHILIC ARCHAEON *PYROCOCCUS FURIOSUS*

by

Patrick Michael McTernan

Major Professor:
Michael W. W. Adams

Committee Members:
Michael Johnson
Robert Maier
William Lanzilotta

Electronic Version Approved:
Suzanne Barbour
Dean of the Graduate School
The University of Georgia
May 2015

DEDICATION

This dissertation is dedicated to my wonderful family that has been extremely supportive and helpful throughout my years in school. I will never forget the support and advice given to me to help me through this process of getting my degrees. I would like to recognize my wonderful wife, Misty McTernan, who has stayed with me throughout my time here in Athens and was always there to support me. I would like to thank my mother, Lynn Besch McTernan, for all her professional and motherly help throughout my time in Graduate School. I also dedicate this dissertation to my late father, Mark Stuart McTernan, whom passed away before I attended LSU for my undergraduate degree. He would never have imagined me pursuing the path of a Ph.D. in Biochemistry. He taught me a lot of lessons in life and I will always appreciate the time we had together.

ACKNOWLEDGEMENTS

I would like to thank Dr. Michael W. W. Adams for his support, oversight, and insight throughout my graduate school career. I would also like to express my gratitude to my committee members (Dr. Michael Johnson, Dr. Robert Maier, and Dr. William Lanzilotta) for their help and advice during my committee meetings. Additionally, I would also like to thank Dr. Sanjeev Chandrayan for his advice and help that contributed greatly to the success of my projects. Finally, I would like to thank the entire Adams lab for their individual help throughout my graduate career for all the countless challenges that come with working with anaerobic proteins.

TABLE OF CONTENTS

Page

Page

LIST OF TABLES

Page

LIST OF FIGURES

Page

LIST OF ABBREVIATIONS:

ATP- adenosine triphosphate

C-MBH – cytoplasmic MBH

COM1 - parent strain of *P. furiosus*

DDM- n-dodecyl-β-D-maltoside

DT- dithionite

Ech- energy conserving hydrogenase

EF1-α- elongation factor 1-alpha

EPPS- **(**4-(2-Hydroxyethyl)-1-piperazinepropanesulfonic acid

EPR- electron paramagnetic resonance

Fd_{ox}- oxidized ferredoxin

Fd_{red}- reduced ferredoxin

FHL- formate hydrogen lyase

FNOR- ferredoxin:$NADP^+$ oxidoreductase

GAP- glyceraldhyde-3-phosphate

GDH- glutamate dehydrogenase

His_9- 9x histidine tag

MBH- membrane bound hydrogenase

MV- methyl viologen

NAD- Nicotinamide adenine dinucleotide

NADPH- Nicotinamide adenine dinucleotide phosphate

OE-SHI- engineered strain of *P. furiosus*

PMSF- phenylmethylsulfonyl fluoride

POR- pyruvate ferredoxin oxidoreductase

SAXS- small angle x-ray scattering

SHI- soluble hydrogenase I

SHII- soluble hydrogenase II

S-MBH – Solubilized MBH

SLP- S-layer protein

Tris- tris(hydroxymethyl)aminomethane

CHAPTER 1

INTRODUCTION AND LITERATURE REVIEW

ARCHAEA

Three domains of life are known to exist and are annotated as the Eukarya, Bacteria and Archaea (1-4). These three domains of life have been organized into a phylogenic tree based on the work of Dr. Carl Woese in the late 1970's. Dr. Woese classified these organisms by comparing sequences of small-subunit ribosomal RNA as a molecular marker to distinguish the three domains of life (Figure 1.1). Archaea were originally thought to be bacteria. For example, the first Archaea to be studied were methane-producing microorganisms, which were originally classified in the domain 'archaebacteria', but later changed to archaea (5, 6). From this phylogenetic tree, it was determined that archaea were in fact more closely related to eukaryotes than bacteria, and it was thought that archaea may share a common heritage of information-processing systems due to this close relationship. This observation was further confirmed in the 1980's when it was observed that the archaeal DNA-dependent RNA polymerase is very similar to the eukaryotic version of the enzyme in both complexity and subunit composition (7). While Archaea share relationships with eukaryotic organisms, they also share characteristics with bacteria. Genome sequencing in the 1990's showed that archaea are in fact a "genetic mosaic" of both eukaryotes and bacteria. These information processing systems of archaea show significant homology to their eukaryotic counterparts, while the house-keeping proteins resemble the bacterial versions (8-10). Archaea are also believed to be the slowest-evolving organisms and may represent the most ancient form of life (3).

Figure 1.1

Universal phylogenetic tree of the three domains of life based on rRNA sequence. Blue lines indicate hyperthermophiles. Redrawn and modified from (6).

Phylogenetic Tree of three domains of life

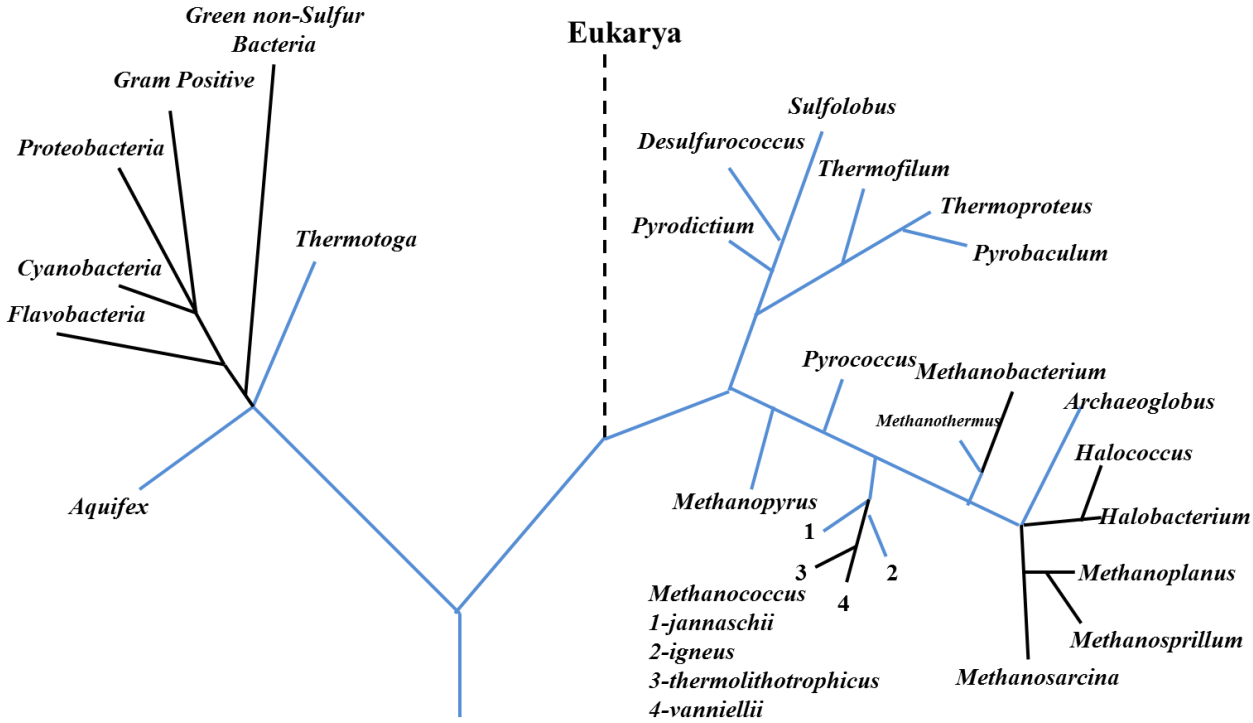

The majority of organisms belonging to the Archaeal domain have been isolated from extreme environments. The majority of this domain is split into two major phyla, which are classified as the *Crenarchaeota* and *Euryarchaeota* (2). A third phylum of archaea has been previously proposed that consists of only one organism and is referred to as the *Nanoarchaeota*, but is believed to be the result of a rapidly evolving Euryarchaeal lineage (11, 12). In 2008, a fourth archaeal phylum was proposed that included organisms that were similar to those found in the *Crenarchaeota*, but grew at much lower temperatures. This phylum was called the *Thaumarcheaota* and from sequence analysis has been proposed to be much different than the *Crenarchaeota* (13). Another phylum that harbors organisms only found at high temperature are the *Korarchaeota* and these are believed to be "ancient" archaea due to their deep branching that does not belong to the other major phyla, *Euryarchaeota* and *Crenarchaeota* (14, 15). The *Crenarchaeota* phylum harbors only high temperature species such as the orders of *Sulfolobales*, *Thermoproteales*, and *Desulfurococcales* organisms. The best studied example from this kingdom of archaea is the *Sulfolobales* (16-18).

The *Euryarchaeota* represent the most studied group of Archaea and harbors the most known species of all of the archaeal phyla. These include organisms that live in extreme salt conditions (halophiles), ones that produce methane (methanogens), and other organisms that live at high temperatures and low pH (thermoacidophiles) (19). The *Euryarchaeota* includes the sulfate-reducers (*Archaeoglobales*), the methanogens (*Methanococcales/Methanopyrales*), and the *Thermococcales* (sulfur-reducers) (20-22). All of the *Thermococcales* have been isolated from the shallow marine thermal springs or deep-sea hydrothermal vents. These are made up into three different genera classified as *Pyrococcus*, *Thermococcus*, and *Paleococcus*. *Thermococcales* are considered to be obligate heterotrophic anaerobes that assimilate peptides,

pyruvate, amino acids, and oligosaccharides coupled to the reduction of sulfur or hydrogen fermentation. *Thermococcus* contains the highest number of characterized isolates and ecological studies have shown that *Thermococcus* species are ubiquitous in deep-sea hydrothermal vents.

Hyperthermophiles live at temperatures above 80^0C and were discovered by the efforts of Stetter and his co-workers (23, 24). The most extreme example of a hyperthermophile is *Methanopyrus kandleri*, which is capable of growing under increased pressure at temperatures of 122^0C (25). These organisms survive near and above the boiling point of water and thrive in shallow marine and deep-sea volcanic hydrothermal vents (black smokers). Other habitats that hyperthermophiles have been discovered in include acidic, sulfur-containing fields like those found in Yellowstone National Park, USA. Hyperthermophiles have also been isolated from man-made environments such as coal refuse piles and hot outflows from geothermal power plants. However, most hyperthermophiles have been isolated from marine environments (19).

The most important variables for determining an ecological niche of an organism are temperature, salinity, pressure, and pH (26). The salinity requirement of hyperthermophiles varies drastically between species. Marine hyperthermophiles have a high salt requirement (~3% NaCl w/v) for optimal growth in the laboratory, while this salinity requirement is much lower (0.01-0.05% NaCl w/v) for those isolated from terrestrial areas. These environments that hyperthermophiles live in are generally anoxic due to the low solubility of O_2 at high temperatures (<2 mg L^{-1} at 90^0C). Thus, all known hyperthermophiles are anaerobes, with the exception of *Pyrobaculum* species and *Aeropyrum* species (27-29). Hyperthermophiles are grown in the laboratory without any high pressure constraints, and this includes organisms isolated from depths below 3500 meters where the pressure can exceed 350 atm. It is thought

hyperthermophiles can survive at temperatures well below that required for optimum growth for long periods until conditions become favorable for growth again (26).

The metabolism of hyperthermophiles is very diverse (30). They gain energy from both heterotrophic and lithotrophic reactions similar to what has been observed in mesophilic organisms, although some pathways are modified (30, 31). Most hyperthermophiles are obligate heterotrophs and can use complex protein-based substrates such as yeast, meat and bacterial-extracts, peptone, or tryptone, as well as peptides as carbon sources. Some hyperthermophiles are saccharolytic but typically use only a narrow range of oligomeric and polymeric sugars (32). One exception to this are members of the genus *Thermoproteus*, which are able to metabolize monosaccharides (33). Besides peptides and sugars, hyperthermophiles can also utilize pyruvate as a carbon source, and there is also an example of a hyperthermophile that can fix nitrogen (34). A methanogen was able to reduce nitrogen gas (N_2) to ammonia (NH_3) at 92^0C, which was 28^0 C degrees higher than the previous temperature limit for nitrogen fixation. One notable exception to the diverse metabolism by hyperthermophiles is that there is no known hyperthermophile that can perform photosynthesis, which could be due to the fragile nature of the photosystems at high temperature.

Other types of metabolism performed by hyperthermophiles include chemolithoautotrophy, where CO_2 and other inorganic compounds are utilized for growth (30). There are also examples of hyperthermophiles that are facultative autotrophs and can utilize organic and inorganic compounds. Autotrophic CO_2 fixation is carried out by the reductive citric acid cycle and the reductive acetyl-CoA/carbon monoxide dehydrogenase pathway within hyperthermophiles as none of their genomes encode the enzymes of the Calvin cycle. S^0 is another electron acceptor commonly used by hyperthermophiles. A few genera of

hyperthermophiles are known that cannot use S^0 during metabolism, which include include *Sulfophobococcus, Aeropyrum* and *Pyrolobus*. Indeed, the growths of some hyperthermophilic species are inhibited in the presence of S^0, which includes *Pyrobaculum aerophilum*, *Thermosphaera aggregans*, and *Pyrolobus fumarii* (27, 30, 35). Other electron acceptors that are used by hyperthermophiles include thiosulfate ($S_2O_3^{2-}$), sulfate (SO_4^{2-}), elemental sulfur (S^0), nitric oxide (NO), nitrogen dioxide (NO^{2-}), nitrate (NO^{3-}), nitrous oxide (N_2O), protons (H^+), carbon dioxide (CO_2), carbon monoxide (CO), iron (Fe(III)), manganese (Mn(IV)), molybdenum (Mo(VI)), and oxygen (O_2) (30, 36, 37).

The most studied methods of lithotrophy utilized by hyperthermophiles are O_2 respiration, methanogenesis, and the reduction of nitrate, sulfate (SO_4^{2-}) and S^0 (30). There are very few examples of hyperthermophiles that utilize oxygen as most of these organisms are obligate anaerobes. Hyperthermophiles that do reduce oxygen are typically microaerophiles and are able to grow in low oxygen concentrations (<3% v/v). The only example of an obligate aerobic hyperthermophile is *Aeropyrum pernix,* which belongs to the *Crenarchaeota* (38). Hyperthermophiles of the genera *Aquifex, Sulfolobus, Acidianus, Pyrobaculum*, *Pyrolobus* and *Sulfurisphaera* utilize the general Knallgas reaction (H_2 + ½ O_2 -> H_2O) in order to reduce oxygen (30). The proteins used for the reduction of oxygen are similar to those found in mesophiles. Hyperthermophilic methanogenesis is carried out by the genera of *Methanopyrus, Methanococcus* and *Methanothermus* (33). All known hyperthermophilic methanogens perform hydrogenotrophic methanogenesis and grow using H_2 and CO_2 as the sole carbon and energy source. The enzymes from these hyperthermophilic methanogens are similar to those used by mesophiles.

Nitrate reduction is rare among the hyperthermophiles and is found in only three genera of Archaea (*Pyrobaculum, Pyrolobus, Ferroglobus*) and in one bacterium (*Aquifex*) (39). On the other hand, the reduction or oxidation of sulfur compounds is a critical reaction for a number of Archaea (40). Within the Archaea, S^0 and SO_4^{2-} are reduced to H_2S using either organic or inorganic substrates. Most hyperthermophilic Archaea are obligate S^0 reducers, but one exemption is the genus *Archaeoglobus*, which obligately reduces SO_4^{2-} (41). All species of *Archaeoglobus* have been shown to grow lithotrophically with the reduction of sulfate to H_2S with exception of *A. fulgidis*, which is able to grow using organic electron donors. Based on studies of *Archaeoglobus* species, the mechanisms of sulfate reduction is similar to those found in mesophilic organisms such as the genus *Desulfovibrio*. The only other hyperthermophilic species that is able to reduce sulfate includes *Caldivirga* (42), although these species are also able to reduce other sulfur compounds such as thiosulfate and sulfate.

The reduction of S^0 is also an obligate process for many hyperthermophilic archaea (40). *Pyrodictium* has been extensively studied in order to better understand how energy is conserved during S^0 reduction (43, 44). Some species of *Pyrodictium*, such as *Pm. brockii* and *Pm. abysii*, contain a membrane electron chain that harbors a sulfur reductase and hydrogenase as the primary redox enzymes needed for S^0 reduction. Electrons are generated from the oxidation of hydrogen by a hydrogenase and are shuttled to the sulfur reductase via quinone and cytochromes.

PYROCOCCUS FURIOSUS

Pyrococcus furiosus is a hyperthermophilic *Euryarchaeota* that belongs to the order *Thermococcales* (45). It was isolated by Karl Stetter from geothermally-heated marine vents off the coast of Vulcano Island, Italy (Figure 1.2). *P. furiosus* is a strict anaerobic heterotroph with

Figure 1.2

Electron micrograph of *Pyrococcus furiosus*. Picture of platinum shadowed electron micrograph of *P. furiosus*, which shows the monopolar polytrichous flagellation. Modified from (45).

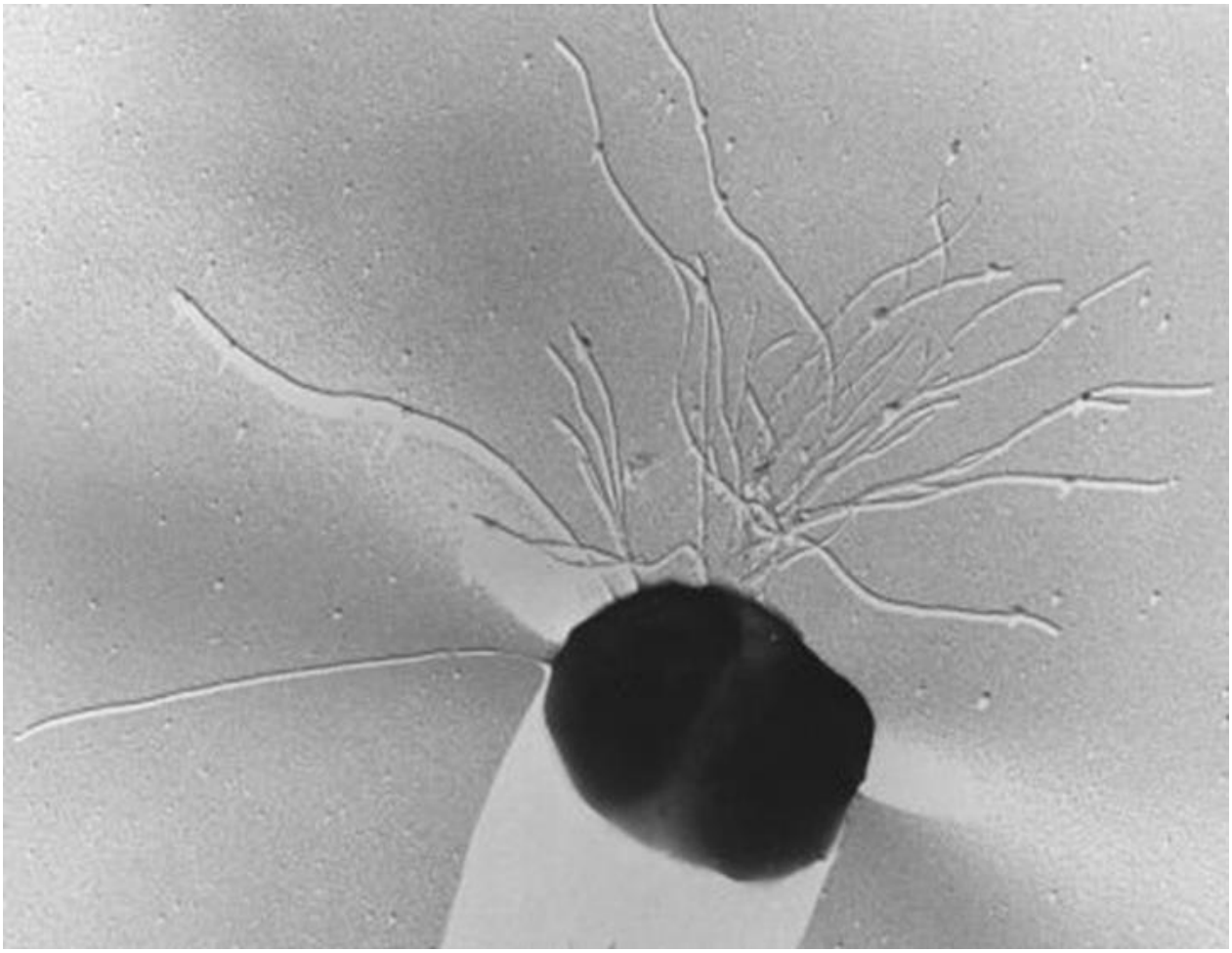

an optimal growth temperature near 100^0C and utilizes a variety of substrates such as starch, maltose, peptone, and complex organic substrates. *P. furiosus* converts these substrates to organic acids, CO_2 and H_2 as end products of metabolism when S^0 is not present (45, 46). In the presence of S^0, H_2 is not produced and is replaced by H_2S, which is the product of S^0 reduction. Alanine is also one of the end products of fermentation by *P. furiosus* (45). The genome of *P. furiosus* was sequenced in 2000 and is 1.91 Mb is size and encodes 2,196 open reading frames (47).

The metabolism of *P. furiosus* is very versatile as it can grow saccharolytically or proteolytically in the absence or presence of S^0 (45, 46). The exact role of S^0 in *P. furiosus* metabolism is still an open question. *P. furiosus* can grow well without S^0, but a major change in gene expression occurs when S^0 is added to the medium. This has been characterized as a primary (within 10 mins) or secondary (within 30 mins) response depending on the timing of the change in gene expression (48). One of the genes that were found to be up-regulated 7-fold within 10 mins of S^0 uses NADPH to reduce S^0 and is termed NADPH sulfur reductase (NSR). An operon up-regulated 16-fold within 10 mins of S^0 addition is termed MBX and is 13 subunits. MBX is believed to oxidize ferredoxin and reduce NADP, which is then used by NSR to reduce elemental sulfur (48). There is a regulator protein called SurR that is responsible for controlling the expression of many of the S^0-responsive genes (49). SurR binds a conserved $GTTn_3AAC$ motif and is responsible for down-regulating the operons encoding the three hydrogenases of *P. furiosus* when S^0, which prevents H_2 production, is present (49).

During saccharolytic metabolism, *P. furiosus* uses a combination of intracellular and extracellular hydrolytic enzymes to break down long polysaccharides into smaller sugar units in order to be incorporated into the cell (45, 46). *P. furiosus* utilizes a range of polysaccharides

including starch, glycogen, or disaccharides like maltose (α -1,4 glucose linked) or cellobiose (β -1,4 glucose linked). *P. furiosus* has also been shown to grow with the simple 3-carbon compound pyruvate as both its energy and carbon source (45, 46). *P. furiosus* is not able to metabolize polymers such as chitin or cellulose or monosaccharide sugars like glucose, fructose, ribose, or galactose (45, 46).

The overall end products of *P. furiosus* fermentation of glucose-based sugars, when sulfur is not present, includes 1.2 equivalents of acetate, 1.2 equivalents of CO_2, 2.6 equivalents of H_2, and 0.5 equivalents of alanine per C_6 glucose unit (50, 51). The unused carbon from metabolism is used for exo-polysaccharide formation. *P. furiosus* fermentation can be divided into four different steps: the uptake and hydrolysis of sugar, the central metabolic pathway, the fate of reductant generated from metabolism, and the mechanisms of energy conservation. The first step of *P. furiosus* metabolism is the uptake of sugars into the cell. *P. furiosus* employs a binding-protein dependent ATP-binding cassette system (ABC transporter) in order to incorporate sugars (52). It has also been reported that *P. furiosus* employs different transporters for the incorporation of these different sugars. For example, during the uptake of cellobiose, one gene is induced that encodes for a 70 kDa protein (CbtA), which is a high affinity transporter belonging to the Opp family of ABC transporters (52). Four other genes located downstream of CbtA are also up-regulated in the presence of cellobiose and have high sequence similarity with permease genes from ABC transporters.

P. furiosus contains two putative maltose transporter operons named Mal-I and Mal-II that have high sequence similarities to maltose/trehalose uptake operon of *Thermococcus litoralis* (53). *P. furiosus* is believed to have acquired these operons by horizontal gene transfer

(54). Mal-I is arranged into five different gene products, which are termed the maltose binding protein (MalE), two transmembrane proteins (MalF and G), an ATPase subunit (MalK), and a maltose-specific transcriptional regulator (TrmB). Another open reading frame is also believed to associate with Mal-I in *P. furiosus* and is annotated as a trehalose synthase. The Mal-II transporter operon (PF1933-1938) is similar to the Mal-I operon in that there are three genes present, but one gene next to the operon is annotated as an amylopullulanase rather than a trehalose synthase, as observed next to the Mal-I operon. Both the Mal-I and Mal-II operons are up-regulated in the presence of maltose and maltooligosaccharides (55). Not all *Pyrococcus* species have maltose transporter operons including *P. horikoshii* or *P. abyssi*, which do not grow on sugars (51).

Extracellular hydrolases have also been isolated and studied from *P. furiosus* including an α-amylase, a pullulanase, and an amylopullulanase (56). These hydrolases are α-1, 4 and α-1,6-glucose cleaving enzymes and do not cleave polysaccharides completely to their monomeric forms. These partially digested polysaccharides are incorporated into the cell and digested further by intracellular hydrolases (57). This observation helps explain why *P. furiosus* is not able to grow on monosaccharides as it only has transporters specific for polymeric or oligomeric sugars that have been partially digested by the extracellular hydrolases.

Once imported, the oligosaccharides are further hydrolyzed by a suite of different α- and β-hydrolases. The α-glucosidase found in *P. furiosus* is a 125 kDa monomeric enzyme that breaks down maltose into glucose (51, 57). There are two β-glucosidases found in *P. furiosus* that have different affinities for cellobiose and are annotated as CelA and CelB. The more abundant of the two is CelB and is a homotetramer of 58 kDa subunits (58). CelB comprises

91% of the intracellular β-glucosidase activity. CelA and CelB have also been observed to hydrolyze galactose to glucose, which is then used in the modified glycolytic pathway of *P. furiosus*.

P. furiosus utilizes a modified Embden-Meyerhof (EM) pathway in order to metabolize glucose for the organism's energy needs (59-62). This pathway is different from the conventional Embden-Meyerhof pathway in two different ways (Figure 1.3). The pathway starts with the phosphorylation of glucose by glucokinase (GK), which is then isomerized to fructose-6 phosphate by phosphoglucoisomerase (PGI). *P. furiosus* GK has been purified and is a dimer of 47 kDa, but it is dependent upon ADP rather than ATP for activity (32, 59). PGI has also been purified from *P. furiosus* and is a dimer of 23 kDa subunits with no sequence homology to other PGIs from bacteria and Eukarya (63). Fructose-6 phosphate is then converted to fructose-1, 6-bisphosphate by phosphofructokinase (PFK) (64). PFK has been purified from *P. furiosus* and expressed recombinantly in *Escherichia coli*. Both purified versions of PFK are tetramers of 52 kDa subunits. PFK, like GK, uses ADP rather than ATP. GK also used also GDP, but this had only 28% of the activity seen with ADP (64). Fructose-1,6-bisphosphate is then converted to glyceraldehyde-3-phosphate (GAP) and dihydroxyacetone by fructose bisphosphate aldolase (FBA) (32). Triose phosphate isomerase (TPI) is responsible for keeping a balance between these two different C-3 forms (32). Neither FBA nor TPI have been purified from *P. furiosus* so far, but their respective activities have been measured in cell extracts.

GAP is oxidized by the tungsten-containing enzyme glyceraldehyde-3-phosphate oxidoreductase (GAPOR) (60). GAPOR has a very high affinity for the electron-carrier ferredoxin, which is an iron-sulfur containing protein that is important for accepting electrons at the oxidative steps of the modified Embden-Meyerhof pathway of *P. furiosus* (60, 65). GAPOR

Figure 1.3

Proposed modified Embden-Meyerhof pathway found in *P. furiosus*. Numbers correlate to the proposed enzymes at each step. GAPOR represents glyceraldehyde-3-phosphate oxidoreductase. POR represents pyruvate oxidoreductase. Fdox and Fdred stand for the oxidized and reduced forms of ferredoxin, respectively. Modified from (193)

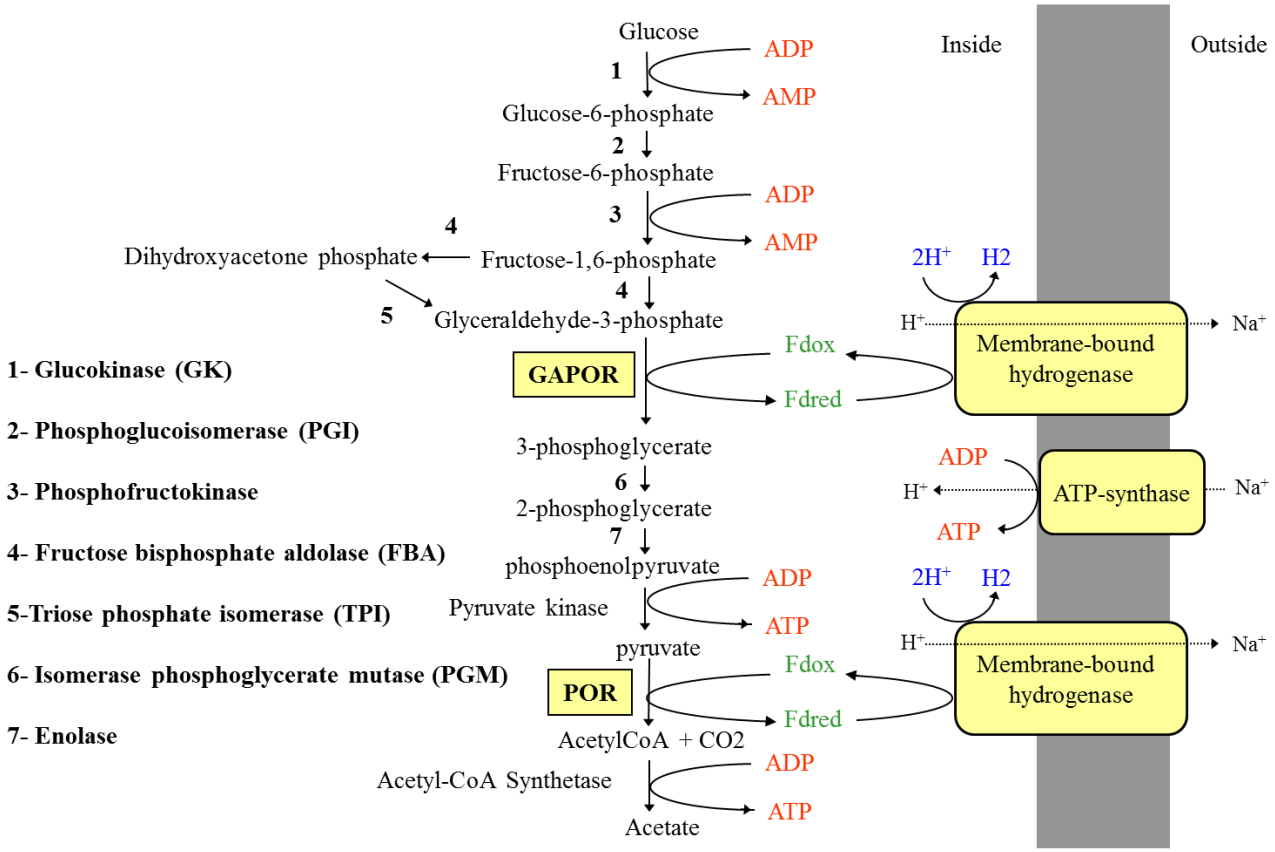
Glucose
ADP
1
AMP
Glucose-6-phosphate
2
Fructose-6-phosphate
ADP
3
AMP
4
Dihydroxyacetone phosphate
Fructose-1,6-phosphate
4
5
Glyceraldehyde-3-phosphate
Fdox
GAPOR
Fdred
3-phosphoglycerate
6
2-phosphoglycerate
7
phosphoenolpyruvate
ADP
Pyruvate kinase
ATP
pyruvate
Fdox
POR
Fdred
AcetylCoA + CO2
ADP
Acetyl-CoA Synthetase
ATP
Acetate
Inside
Outside
2H+
H2
H+
Na+
Membrane-bound hydrogenase
ADP
H+
ATP-synthase
Na+
ATP
2H+
H2
H+
Na+
Membrane-bound hydrogenase
1- Glucokinase (GK)
2- Phosphoglucoisomerase (PGI)
3- Phosphofructokinase
4- Fructose bisphosphate aldolase (FBA)
5-Triose phosphate isomerase (TPI)
6- Isomerase phosphoglycerate mutase (PGM)
7- Enolase

reduces ferredoxin instead of the nicotinamide nucleotides, which are the electron carriers in standard glycolysis pathways. This GAPOR step is very different from traditional glycolysis as this enzyme replaces both glyceraldehyde-3-phosphate dehydrogenase (GAPDH) and phosphoglycerate kinase (PGK). Thus, in *P. furiosus*, GAP is converted to 3-phosphoglycerate by GAPOR instead of the two conventional enzymes in one single enzymatic step. Importantly, 1,3 bisphosphoglycerate is not generated during glycolysis by *P. furiosus* and therefore ATP is not synthesized by the PGK reaction, as in the conventional pathway.

3-phosphoglycerate generated by GAPOR is then converted to 2-phosphoglycerate by phosphoglycerate mutase (PGM) (59-61). 2-phosphoglycerate is converted to phosphoenolpyruvate (PEP) by enolase, and PEP is then converted to pyruvate by the enzyme pyruvate kinase (PK) (32, 51). PK also couples this redox reaction to the conversion of ADP to ATP by substrate-level phosphorylation. This is the only step of ATP formation from the modified Embden-Meyerhof pathway of *P. furiosus*. Pyruvate, generated by glycolysis, is converted to acetyl-CoA and CO_2 by the enzyme pyruvate ferredoxin oxidoreductase (POR), which utilizes the electron-carrier ferredoxin, instead of nicotinamide nucleotide electron carriers (66). The acetyl-CoA is then used for the generation of acetate by the action of acetyl-CoA synthetases I and II in an ATP generating reaction via substrate level phosphorylation (67). The other key steps that are connected to the oxidation of glucose to acetate, which are important for energy conservation, occur with the GAPOR and POR steps (32, 62). The reduced ferredoxin generated from GAPOR and POR is used by a membrane-bound hydrogenase (MBH), which reduces protons with excess reductant and evolves molecular hydrogen (H_2) (Figure 1.3). This hydrogenase complex will be discussed in further detail below. This leads to the major end

products of metabolism of S^0, as discussed above, of acetate, CO_2 and H_2, when sulfur is not present in the medium.

P. furiosus can also utilize peptides as a sole carbon source for growth and generates different end products when compared to metabolism with sugars (45, 46). Pyruvate can be converted to alanine through the action of two alanine aminotransferases in *P. furiosus*, which oxidizes NADPH in order to perform this reaction. These enzymes serve an important role in maintaining the redox balance during metabolism (68). These enzymes are up-regulated in the presence of pyruvate, and change the relative flux of pyruvate to alanine. Pyruvate is thought to be a catabolic sink in *P. furiosus* metabolism and is converted to either acetate or alanine depending on the needs of *P. furiosus*. The other pathway that utilizes pyruvate in *P. furiosus* utilizes the proteolytic action of proteases (69). This action occurs by the help of intracellular and extracellular enzymes (69). These amino acids are then transaminated to 2-keto acids by transamination, which differs from mesophiles where these amino acids are dehydrated. 2-ketoglutarate is the primary amino acceptor in *P. furiosus* and is converted into glutamate by a suite of transaminases. Regeneration of 2-ketoglutarate occurs by the action of the enzyme glutamate dehydrogenase (GDH), which is responsible for the conversion of glutamate to 2-ketoglutarate and the reduction of $NADP^+$ (70). GDH is also the most abundant enzyme in *P. furiosus* and makes up 20% of the cytoplasmic proteins. *P. furiosus* contains 4 different ferredoxin-dependent 2-ketoacid oxidoreductases (KORs) that convert transaminated amino acids to their respective CoA derivatives (71-73). These four KORs include POR, indolepyruvate ferredoxin oxidoreductase (IOR), 2-ketoisovalerate ferredoxin oxidoreductase (VOR), and 2-ketoglutarate ferredoxin oxidoreductase (KGOR). IOR is responsible for the

conversion of aromatic 2-ketoacids. VOR is responsible for the conversion of branched chained 2-ketoacids, and KGOR is responsible for the conversion of 2-ketoglutarate.

Another oxidoreductase that has been discovered in *P. furiosus* is aldehyde ferredoxin oxidoreductase (AOR). This enzyme contains tungsten and catalyzes the oxidation of a range of aliphatic and aromatic aldehydes. The physiological function of AOR is believed to involve the oxidation of toxic aldehydes that are generated as side products of amino acid production (71-73). The two acyl CoA synthases (ACS I and II) are responsible for the connection of acetyl-CoA to acetate and also branched chain CoA-derivatives, but aryl CoAs are only utilized by ACS-II (67). Hence, substrate level phosphorylation also takes place during amino acid production and generates 1 ATP per reaction cycle (45). The reduced ferredoxin that is generated from the KOR reactions and by glycolysis is oxidized by a membrane-bound hydrogenase, the nature of which is discussed in the following section.

HYDROGENASE

Hydrogenases are found in all three domains of life (74, 75). These enzymes catalyze the simplest reaction in nature, the reversible interconversion of hydrogen gas to protons and electrons. They function in metabolism by either removing excess reductant through the production of hydrogen or oxidize hydrogen in order to give reducing power to the growing cell. *In vitro* studies of hydrogenase have shown that these enzymes can perform either reaction, but it is believed that *in vivo* hydrogenase catalysis is committed to only one direction. Hydrogenase research began in the 1920's, but these enzymes have been very difficult to work with due to a very complicated maturation pathway and are inactivated in the presence of oxygen. Hydrogenases are split into three different classes based on the metal content of the active site.

These three classes are the [NiFe]-hydrogenase, the [FeFe]-hydrogenase, and the [Fe]-only hydrogenases (74-77).

The [FeFe]-hydrogenases are only found in bacteria, such as clostridia, and anaerobic eukaryotes, such as green algae or fungi (74-76). The most studied [FeFe]-hydrogenases are from species of green algae, *Clostridia* and *Desulfovibrio* (76). There are [FeFe]-hydrogenase crystal structures available from three different organisms, which include the periplasmic [FeFe]-hydrogenase from *Desulfovibrio desulfuricans*, the cytoplasmic [FeFe]-hydrogenase from *Clostridium pasteurianum*, and HydA from *Chlamydomonas reinhardtii* (78-85). These hydrogenases have been characterized and show a bi-nuclear [FeFe] active site that is bound to a [4Fe-4S] cluster connected by the thiolate of a cysteine residue. A general model of the [FeFe] active site consists of the di-iron center with a di-sulfur bridge-head that is bound to both cyanides and carbon monoxide ligands. The two Fe atoms of the active site are designated as either the "proximal' or "distal" based on their position. The "proximal" Fe atom is linked to the cubane [4Fe-4S] cluster by a single thiolate bridge and is also bound to one CO and one CN. The "proximal" cluster is 4 Å from the bound [4Fe-4S] cluster. The "distal" Fe is also linked by only one CO and one CN and is further from the bound [4Fe-4S] cluster. There is a third CO ligand that acts as a bridging ligand that is bound to both active site Fe atoms. Most [FeFe]-hydrogenases are monomeric or dimeric in nature, for example the [FeFe]-hydrogenases of green algae only contain the H-cluster and no additional [FeS] clusters, but there are examples of multimeric subunit [FeFe]-hydrogenases, which include the NAD(P)H-dependent [FeFe]-hydrogenase from *Thermotoga maritima* that consists of three subunits, and the [FeFe]-hydrogenase from *Thermoanaerobacter tengcongensis* that consists of four subunits (74, 75). Other [FeFe]-hydrogenases can harbor additional types of [FeS] clusters such as [2Fe-2S] or

[4Fe-4S] clusters. All [Fe-Fe]-hydrogenases have been observed to be irreversible inactivated in the presence of oxygen (86, 87).

The maturation of the [FeFe] active site requires the action of three different accessory proteins termed as HydE, F, and G (88-92). These maturation factors were first identified in *Chlamydomonas reinhardtii* and are conserved in all organisms expressing [FeFe]-hydrogenases. Though the maturation of [FeFe]-hydrogenases has not been completely characterized, there are some steps of the maturation process that have been observed and discussed. HydF has a binding site at the C-terminus that harbors three conserved cysteine residues for the binding of a [4Fe-4S] cluster (93, 94). The N-terminus of HydF has a GTPase domain and both the N- and C-terminus of HydF have been shown to be important for proper maturation of the [FeFe] active site. HydE and G both belong to the radical SAM family (90, 95, 96). Members of the radical SAM family contain a [4Fe-4S] cluster near the N-terminus of the protein, where there is an opening in the protein for binding an S-adenosyl methionine (SAM) cofactor. Both HydE and G contain an additional [FeS] cluster binding site located at their C-terminus. This additional C-terminal [FeS] cluster differs in HydE and HydG. In HydE, it is believed that a [2Fe-2S] cluster is found at the C-terminus, while in HydG it is believed that a [4Fe-4S] cluster is present (97-99). The predicted order of assembly of the bi-nuclear Fe site starts with HydG (100-103). While no substrate is known for HydE, tyrosine has been found to be the substrate for HydG and is needed for generation of both the CO and CN ligands (104, 105). It is believed that HydG is responsible for the catalytic conversion of the CO and CN ligands as well as the bridging dithiol to the bi-nuclear [FeFe] site. HydG is thought to begin this process as the extra [4Fe-4S] cluster, which is found in this protein, is proposed to bind tyrosine before reacting in order to generate the CO and CN ligands. Then the assembled [FeFe] site is brought to HydF, which already harbors the

[4Fe-4S] cluster, and serves as a scaffold for the "H-cluster" site (106-110). HydF is thought to scaffold the "H-cluster" after assembly and has been shown to harbor an important histidine ligand for stabilization of the two Fe atoms. Therefore, the general consensus for maturation of the [FeFe] active site is that HydG is responsible for adding the diatomic ligands to the active site, while HydF serves as a scaffold.

The [Fe]-only hydrogenases or Hmd hydrogenases are the least studied of the three hydrogenase classes (111-113). These hydrogenases are found only in methanogens and catalyze hydrogen oxidation. The first hydrogenase was found in *Methanothermobacter marburgensis* and is the most studied (112). It is important for the reversible reduction of methenyltetrahydromethanopterin with H_2 to methylene-H4MPT and H^+ (114-116). This reaction is only important for methanogens where nickel is limited. Under these conditions, the F_{420}-reducing [NiFe]-hydrogenase, which is necessary for methanogenesis, is not present and Hmd is used to remove excess reductant. Hmd is composed of two identical subunits of 38 kDa in size. Some difference between Hmd hydrogenases and the other classes of hydrogenase include that the Fe atom found in the active site is not redox active (116). The primary and tertiary structures of Hmd hydrogenases show no homology to the other two hydrogenase classes and Hmd hydrogenases do not catalyze the reversible reduction of protons, but rather the reduction of the Hmd cofactor.

The first structural reports of this [Fe]-only hydrogenase were obtained by reconstituting the hydrogenase apoenzyme from *Methanothermobacter jannaschii* with an iron cofactor from *Methanothermobacter marburgensis* (117, 118). In this structure, it was found that a mono nuclear Fe site displays a square pyramidal geometry where it is bound to a pyridinol derivative, two carbon monoxide molecules, a cysteinyl thiolate, and an unknown ligand. Further analysis

of the active site of Hmd hydrogenases have indicated that the pyridinol ring has back-bonding properties to the Fe atom, in a similar way that cyanide binds to Fe in the active sites of the other hydrogenase classes. The two carbon monoxide molecules bind the Fe at a 90^0 angle, and the cysteinyl thiolate bound to the Fe atom is derived from Cys176 (117, 118). The fifth unknown ligand cannot be assigned as either a monoatomic or diatomic ligand, but is clearly bound to the Fe. The sixth coordination site of the iron is open and is believed to be where hydrogen and the competitive inhibitor carbon monoxide bind. The oxidation state of the active site Fe atom remains unknown, but there is some thought, based on Mossbauer analysis, that the oxidized Fe atom may be in the Fe(0) or Fe(II) state as the Fe atom is EPR-silent (119).

The third class of hydrogenase, the [NiFe]-hydrogenases are found in both eukaryotes and bacteria and are the most studied of the hydrogenases (74-76). The majority of these hydrogenases oxidize hydrogen in order to reduce their physiological electron partners. The basic structure of the [NiFe]-hydrogenase is a heterodimer composed of a large and small subunit (Figure 1.4; 120-123). The large subunit harbors the deeply buried [NiFe] catalytic site, which contains 4 critical cysteine residues that are important for binding this metal active site (120-124). These 4 cysteines are arranged into two CXXC motifs at the N- and C-terminus of the large subunit. Two of these cysteines coordinate the Ni atom, while the other two cysteines serve as bridging ligands between the Fe and Ni atoms. The Fe atom is further bound by three diatomic ligands, which are important for keeping the Fe atom in a low spin state (Fe^{2+}). The diatomic ligands are two cyanide (CN) ligands and one carbon monoxide (CO) ligand. This low spin state is important for the hydrogenase reaction and no activity will occur if these ligands are removed (120-126). Interestingly, both [Fe-Fe] hydrogenases and [Ni-Fe] hydrogenases use the same diatomic ligands CN and CO bound to the Fe atom of their respective active sites, but are

Figure 1.4

Crystal structure of dimeric [NiFe]-hydrogenase. Modified from (125). The large subunit is shown in blue and harbors the [NiFe] active site. The small subunit is shown in red and harbors three [FeS] clusters. The box to the right shows the [NiFe] active site bound by four cysteines and the diatomic ligands on the Fe atom.

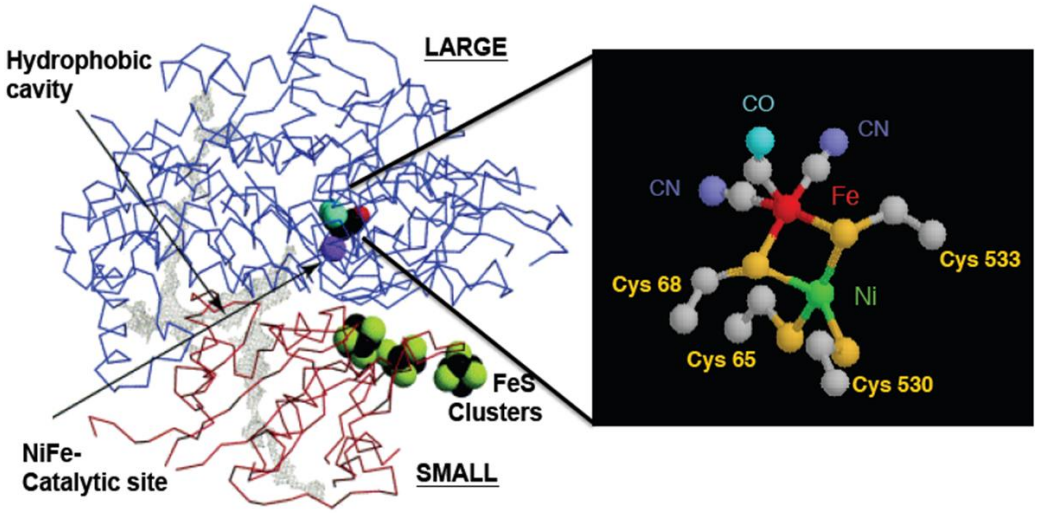
Hydrophobic cavity
LARGE
CO
CN
CN
Fe
Cys 533
Cys 68
Ni
Cys 65
Cys 530
FeS Clusters
NiFe- Catalytic site
SMALL

not believed to share an evolutionary history (74, 75). There are also hydrophobic tunnels that move throughout the large subunit. These tunnels allow for gas access to and from the active site. The large subunit contains five structural domains (labeled I_L, II_L, III_L, IV_L, V_L) and the small subunit contains two structural domains (labeled I_S and II_S) (120-126). The small subunit contains 3 [FeS] clusters, which are important for shuttling electrons to and from the [NiFe] active site. These clusters are referred to as proximal, medial and terminal depending on their position to the active site (120). [Ni-Fe] hydrogenases are reversibly inactivated in the presence of molecular oxygen (O_2), which is different compared to the Fe-Fe hydrogenases, and there is also a very complex maturation process that requires the concerted action of 8 maturation proteins for the proper assembly of the [NiFe] active site, which will be discussed in further detail below (127, 128).

MATURATION OF [NIFE] ACTIVE SITE

[NiFe]-hydrogenases require eight different maturation proteins for proper insertion of the $NiFe(CN)_2CO$ complex to the active site (Figure 1.5; 127, 128). These proteins were discovered based on knockout studies in *Escherichia coli*, where it was shown that when any of these 8 genes were knocked out, no hydrogenase activity was measured in the mutant strains (127-131). Thus, these proteins were named hydrogen pleiotrophy or Hyp proteins (HypABCDEFG and SlyD). The entire assembly pathway for the [NiFe] active site can be split into two different steps. The first step is the synthesis of the diatomic ligands on the Fe atom and the insertion of this ligand-bound Fe and Ni into the apoprotein. The second step is the C-terminus cleavage of the large subunit (127, 128). Cyanide ligands are generated by HypE and F from carbamoyl phosphate (132, 133). HypF begins the maturation process with the S-carbomylation of HypE, which occurs through the presence of two unstable intermediates. Based on the crystal structure

Figure 1.5

Maturation of the [NiFe] site of Hyd-3 from *E. coli* using eight different maturation proteins. HypC and HypD deliver the Fe atom. HypE and HypF add the diatomic ligands to the Fe atom. HypA, HypB, and SlyD deliver the Ni atom. HycI represents the protease for cleaving the C-terminal region of the large subunit, which is shown by a red box labeled as COOH. Modified from (127).

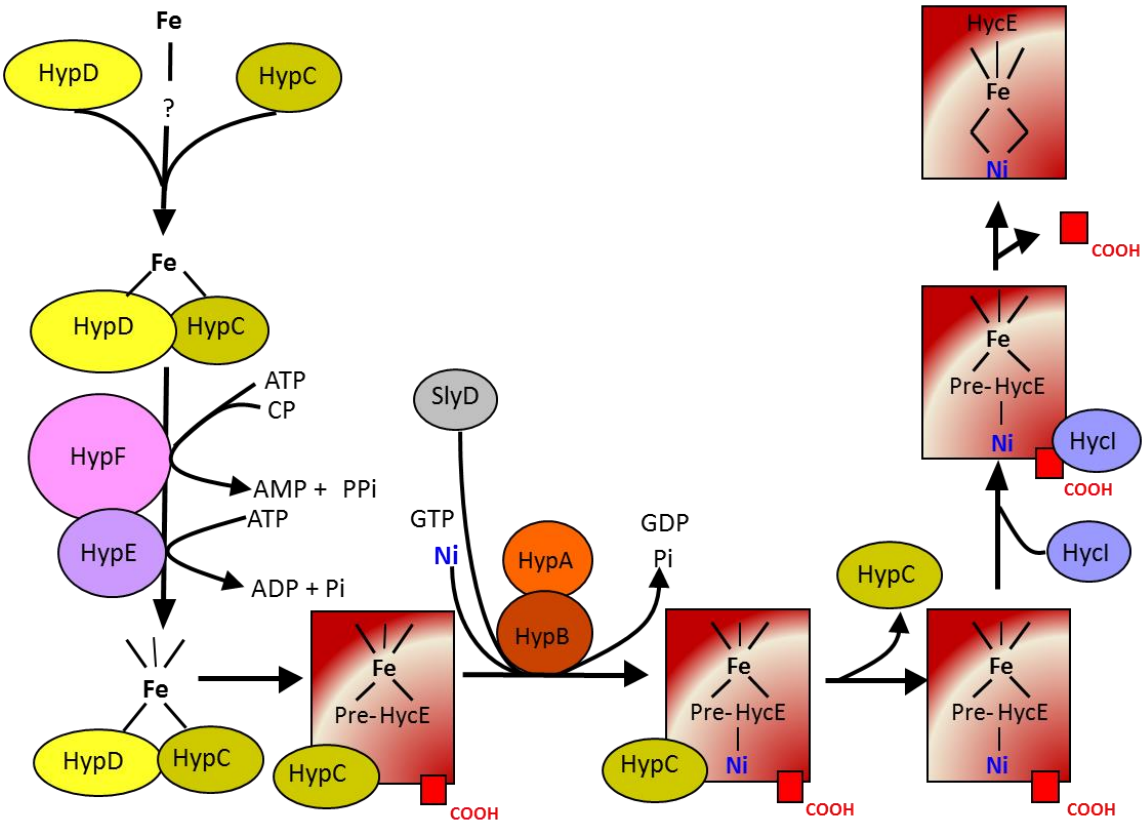
Fe
HypD
HypC
?
Fe
HypD
HypC
ATP
CP
HypF
AMP + PPi
ATP
HypE
ADP + Pi
Fe
HypD
HypC
SlyD
GTP
Ni
HypA
HypB
GDP
Pi
Fe
Pre-HycE
HypC
COOH
Fe
Pre-HycE
HypC
Ni
COOH
HypC
Fe
Pre-HycE
Ni
COOH
HycI
Fe
Pre-HycE
Ni
HycI
COOH
HycE
Fe
Ni
COOH

of HypE and F, it was observed that the C-terminus of HypE fits into HypF (134-137). The C-terminus of HypE contains a cysteine thiol that forms a thiocarboxamide, once in complex with HypF, which is converted into a thiocyanate in an ATP-dependent fashion. Once the cyanide ligand is generated, the ligand is transferred to the Fe atom, which is in complex with HypC and D, by HypE (138).

While the synthesis of CN from carbamoyl phosphate is well characterized and understood, the synthesis of CO is much less understood and is believed to be synthesized through a different route (139-141). Early labeling studies done with *Allochromatium vinosum* showed labeled CO was incorporated into the [NiFe]-hydrogenase when cells grown with labeled acetate. Further labeling studies in *Ralstonia eutropha* showed that when grown with either ^{13}C-labeled glycerol or fructose that the labeled CO came from the glycerol. Upon further experimentation with an excess of labeled CO gas, it was found that this labeled CO was also attached to the Fe atom. Unfortunately, the active site was only found to have this labeled CO in the presence of excess labeled CO. Thus, it is still unknown how CO is synthesized and incorporated into the [NiFe] active site. HypD serves as the main scaffold where the diatomic ligands are bound to the Fe atom (142, 143). HypC and D form a complex together in which HypE and F add the diatomic ligands to the Fe atom. It is believed that the two CN ligands are added first to the Fe atom by HypE before the addition of the CO ligand. Upon addition of CO to the Fe atom, HypD will hold the Fe atom with all three diatomic ligands bound. This $Fe(CN)_2CO$ complex is then added to the precursor large subunit before the addition of Ni.

The addition of Ni requires the action of three processing proteins, HypA, HypB, and slyD (sensitive to the lysis D) (144-150). HypB contains both a Ni and a Zn binding site with GTPase activity. HypA binds one Ni per monomer with a very high affinity and can also bind

the precursor large subunit without the other Hyp proteins present. It is believed due to this binding, that HypA directs the insertion of Ni to the precursor active site. SlyD has been shown to accelerate the transfer of Ni from HypB to HypA. Thus, Ni insertion begins with HypB binding Ni and transferring it to HypA using its GTPase activity with the help of SlyD. Upon relocation to HypA, the Ni is inserted into the premature active site after the insertion of the $Fe(CN)_2CO$ moiety.

After the insertion of both the Ni and Fe atom to the large subunit a proteolytic cleavage occurs at the C-terminus (127, 128). This cleavage occurs with a hydrogenase specific protease and the amount cleaved off the C-terminus can range from 4-40 amino acids. For example, in *E. coli* there are three different proteases that are responsible for the cleavage of the three different hydrogenases (128). This cleavage usually occurs after a histidine or arginine residue at a conserved motif DPCxxCxxH(R), where the CxxC are two of the cysteines responsible for binding the NiFe active site. High-resolution structural analysis of the [NiFe]-hydrogenases from *D. gigas* and *D. vulgaris* Miyazaki showed that an Mg^+ ion was bound to a C-terminal His536, where the C-terminal cleavage occurs during processing of the large subunit (76). In *D. vulgaris*, His536 residue is deeply buried within the large subunit, and upon cleavage of the large subunit, there is a large conformational change that occurs that results in the [NiFe] site becoming deeply buried within the large subunit. The crystal structure of one of the *E. coli* proteases HycI was determined and it was found that there are three metal binding sites that might also be required for cleavage (151-153).

STUDIES OF THE NI ATOM AND CATALYTIC CYCLE

Spectroscopic techniques such as electron paramagnetic resonance (EPR), Mossbauer and Fourier transform infrared (FTIR) spectroscopy were used in the early studies of the [NiFe] active site and the respected [FeS] clusters (154). Based on EPR and FTIR analysis of the Ni atom, it was observed that it is redox active and three different paramagnetic states could be detected (Figure 1.6). The Ni atom also displays EPR-silent states and these have been studied using FTIR spectroscopy (155-157). The three different EPR detectable states exhibit rhombic EPR spectra with three resolved *g* tensor components. The three detectable EPR states are labeled as Ni-A (g-values = 2.32, 2.24, 2.01), Ni-B (g-values = 2.33, 2.16, 2.01), and Ni-C (g-values = 2.20, 2.14, 2.01) based on the studies on the standard [NiFe]-hydrogenase from *Desulfovibrio vulgaris 'Miyazaki F'*. Ni-A and Ni-B are referred to as the "inactive" EPR detectable states, while Ni-C is considered the "active" state. All of the detectable and non-detectable EPR states will be discussed further below.

Under aerobic oxidizing conditions, the Ni atom is found to be in two different "inactive" paramagnetic EPR states, which are labeled as Ni-A and Ni-B (154-157). These two inactive states differ in the type of oxygen ligand bound to the [NiFe] active site. For example, in the case of the Ni-B state ("ready inactive state"), it has been predicted to harbor a hydroxide ligand bound in the active site, while the ligand bound in the Ni-A ("unready inactive") state is unknown (120). These two inactive states also differ in the time needed to reactivate the active site under reducing conditions. The Ni-A state has been observed to require hours in order to re-activate, while the Ni-B state can reactivate in reducing conditions within 10 minutes. Once re-activated, the Ni atom has been observed to show a third EPR detectable state called the Ni-C

Figure 1.6

Redox state of the Ni atom as it progresses through the catalytic cycle. The EPR active states are shown in red, while the EPR-silent states are shown in blue. The EPR-active states include Ni-A (unready state), Ni-B (ready state), Ni-C (reduced state), Ni-L (light-induced state), and Ni-CO (CO inhibited state). The EPR-silent states include Ni-SU (unready state), Ni-SI_r (ready state), Ni-SI_a (actjve state), Ni-SCO (CO inhibited state), and Ni-R (reduced state). Modified from (126).

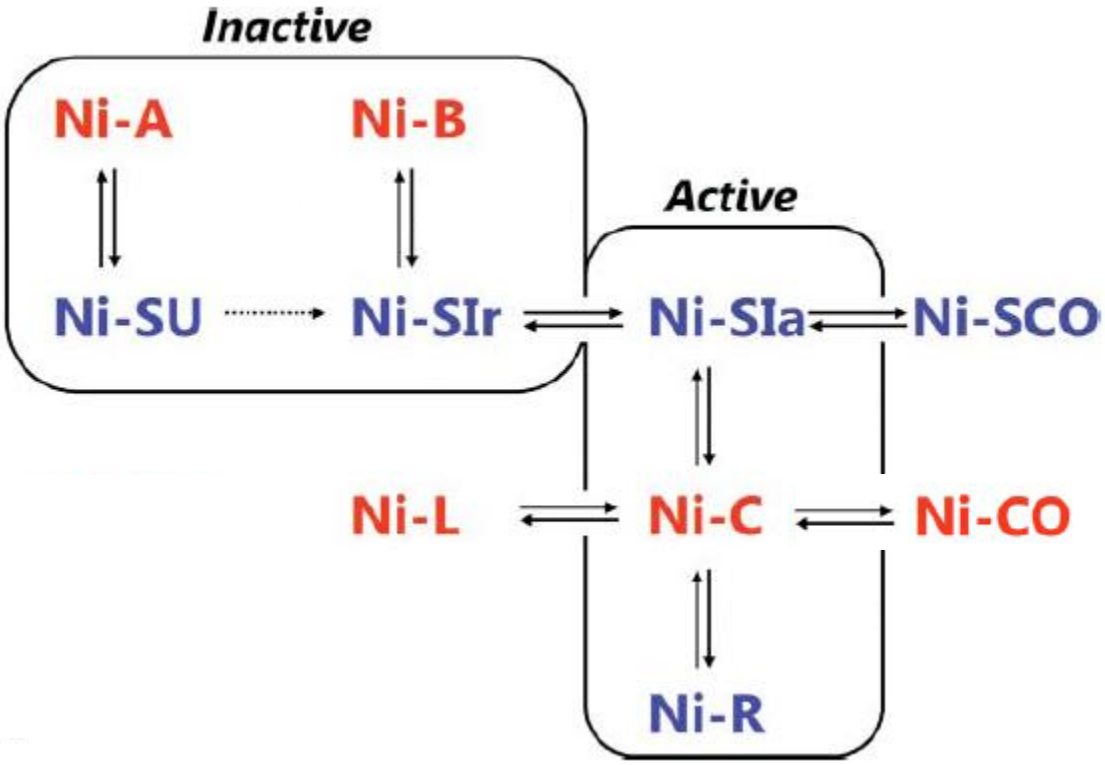
Inactive
Ni-A
Ni-B
Active
Ni-SU
Ni-SIr
Ni-SIa
Ni-SCO
Ni-L
Ni-C
Ni-CO
Ni-R

(ready active) state. This is the catalytically ready state of the enzyme and oxygen is replaced by hydrogen within the active site.

The Ni atom has also been observed by FTIR to have "EPR-silent" diamagnetic states that have been annotated as Ni-SU ("silent unready"), Ni-SI_r ("silent ready"), and Ni-SI_a (154-157; Figure 1.6). These states occur through the transition of the Ni atom between the different EPR detectable states (Ni-A, B, and C) under reducing conditions. For example, once the Ni atom, which is in the Ni-A state, is reduced it will form the Ni-SU state. For the Ni atom that is reduced, while in the Ni-B state, will result in the formation of the Ni-SI_r state. From here either the Ni-SU or the Ni-SI_r states are further reduced to the Ni-SI_a state. The Ni-SI_a state is then further reduced to the Ni-C state, which is the catalytically active state of the hydrogenase to perform the enzymatic reaction. CO is also an inhibitor of [NiFe]-hydrogenases and can bind at either the Ni-SI_a state or the Ni-C state to inhibit the enzyme. Ni-C can also be reduced by light to become the Ni-L state (g-values= 2.30, 2.12, 2.05), which cannot interact with the hydrogen. The Ni-C state can also be further reduced to a Ni-R state, which is "EPR-silent", but is believed to be part of the catalytic cycle with hydrogen. The [Fe-S] clusters have also been extensively studied by EPR studies and have confirmed the presence of three [FeS] clusters in the small subunit of "standard" hydrogenases. Not all hydrogenases follow this "standard" cycle of EPR active and silent states while performing the hydrogenase reaction. Some hydrogenases, which have been observed to be "oxygen tolerant", have shown a different transition of their Ni atom states in both oxidizing and reducing conditions (76). These "oxygen tolerant" hydrogenases will be discussed in further detail below.

OXYGEN TOLERANCE

[NiFe]-hydrogenases are reversibly inactivated in the presence of oxygen, but some carry out their respective enzymatic reaction in the presence of oxygen. These are all in Group 1 hydrogenases, which will be discussed further below, and have been classified as the "oxygen-tolerant" hydrogenases. These include the hydrogen-oxidizing membrane bound hydrogenase from *Aquifex aeolicus*, Hydrogenase 1 from *Escherichia coli*, the hydrogen-oxidizing membrane bound hydrogenase from *Hydrogenovibrio marinus*, and the hydrogenases from *Ralstonia eutropha* (124, 157-162). All of these hydrogenases have been reported to oxidize hydrogen in the presence of oxygen and can maintain their catalytic activity after initial exposure to oxygen. EPR studies on these hydrogenases have demonstrated that these do not show a signal for the Ni-A state. Thus, these "oxygen-tolerant" hydrogenases only show the EPR detectable signals for Ni-B and Ni-C and can reactivate much quicker in the presence of oxygen than the "standard" [NiFe]-hydrogenases.

The mechanism for oxygen-tolerance is still under investigation, but some structural results have been obtained that gives insight into understanding this tolerance. The crystal structures have been determined for the oxygen-tolerant hydrogenases from *E. coli* (PDB code: 4GD3), *H. marinus* (PDB code: 3AYX) and *R. eutropha* (PDB code: 3RGW) (124, 158, 159). It was found that these contained an unusual proximal cluster near the [NiFe] active site. This proximal cluster was a [4Fe-3S] cluster that is not found within the "standard" [NiFe]-hydrogenases. This cluster is ligated by 6 cysteine residues and is in a flexible open configuration. This configuration allows this cluster to transition to two different redox potentials that cannot be achieved by the proximal [4Fe-4S] cluster of "standard" hydrogenases. Thus, this proximal [4Fe-3S] cluster has the ability to convert between two different

conformations based on the reduction state of the cluster. In the ferricyanide-oxidized state, the deprotonated amide nitrogen of one the Fe coordinating cysteine residues breaks the bond with Fe and forms a new bond with the deprotonated backbone nitrogen of a nearby cysteine residue. Upon reduction of the cluster, the asymmetric cluster converts back to a cubane [4Fe-3S] shape (158, 160). The two electrons that are stored in this [4Fe-3S] cluster are important for making the cluster electron-rich, which in turn is used to detoxify oxygen. Oxygen is reduced by these stored electrons in order to form water (H_2O) and a hydroxyl group that bridges the [NiFe] active site (Ni-B state). Mutagenesis studies on the oxygen-tolerant hydrogenase membrane bound hydrogenase from *R. eutropha* determined which cysteine residues were important for oxygen tolerance (161). Cys19 and Cys120 were mutated to glycine residues in order to mimic standard [NiFe]-hydrogenases, and this converted the enzyme into an oxygen-sensitive hydrogenase. The authors were also able to show that Cys19 was more critical for oxygen tolerance.

The medial cluster [3Fe-4S] cluster has also been observed to be important for oxygen tolerance based on mutation studies on Hyd-1 from *E. coli*. It was observed that certain amino acid substitutions, which are important for binding the medial [3Fe-4S] cluster, resulted in a significant increase in oxygen sensitivity (124). In Hyd1, the medial cluster is around 20 Å from the active site and it was hypothesized that this cluster is important for the first stage of oxygen reduction where three electrons are shuttled from the cluster to the [NiFe] active site to form the Ni-B oxidized, active state (Ni(III)-OH) (124). Other features that help these hydrogenases maintain activity under an atmosphere of oxygen include the C-terminus of the small subunit, which is the anchor to the membrane and forms contacts with a membrane-bound cytochrome b. The distal cluster of the small subunit is in close contact to the heme of the cytochrome b and the proximity of this heme is believed to help in shuttling electrons to and from the active site in

order to reduce oxygen before it can inhibit the [NiFe] active site (124). The gas channels of the large subunit have also been investigated to see if these can attribute to the tolerance of oxygen. In previous studies, mutational analysis of residues in the gas channel (Ile and Phe) to smaller amino acids resulted in a faster inactivation by oxygen and carbon monoxide (162).

CLASSIFICATION OF [NIFE]-HYDROGENASES

[NiFe]-hydrogenases are classified into 4 different groups based on sequence comparison and their role in an organism's metabolism (Figure 1.7; 74, 75). Group 1 hydrogenases are classified as the membrane-bound uptake hydrogenases. These hydrogenases are found in both archaea and bacteria and are important for oxidizing hydrogen in order to reduce NO_3^-, SO_4^{2-}, fumarate, or CO_2. These hydrogenases have the typical large catalytic subunit and small subunit containing the three [Fe-S] clusters. Also present is a third subunit that connects the hydrogenase to a quinone pool. This third subunit is normally a di-heme cytochrome b that, with the help of the hydrophobic C-terminus of the small subunit, anchors the hydrogenase dimer to the cell membrane. Hydrogenases of this type are found in microorganisms such as *Wolinella succinogenes* and *Aquifex aeolicus* (163-165). Other organisms that contain a group 1 hydrogenase include the periplasmic Hyn hydrogenase from *Thiocapsa roseopersicina* and *Desulfovibrio* species (74). The Hyn hydrogenase from *Desulfovibrio gigas* was the first hydrogenase for which a crystal structure was available (PDB: 1FRV; 123). These group 1 uptake hydrogenases are characterized by the presence of a long signal peptide (35-50 amino acids) at the N-terminus of the small subunit. This signal peptide contains the conserved sequence [DENST]RRxFxK that is recognized by a specific membrane translocation and targeting pathway (mtt) or twin-arginine pathway (tat). This pathway works to

Figure 1.7

Phylogenetic tree of the [NiFe]-hydrogenases. Phylogentic tree was constructed using representative sequences from the catalytic subunits of [Ni-Fe] hydrogenases. Modified from (181).

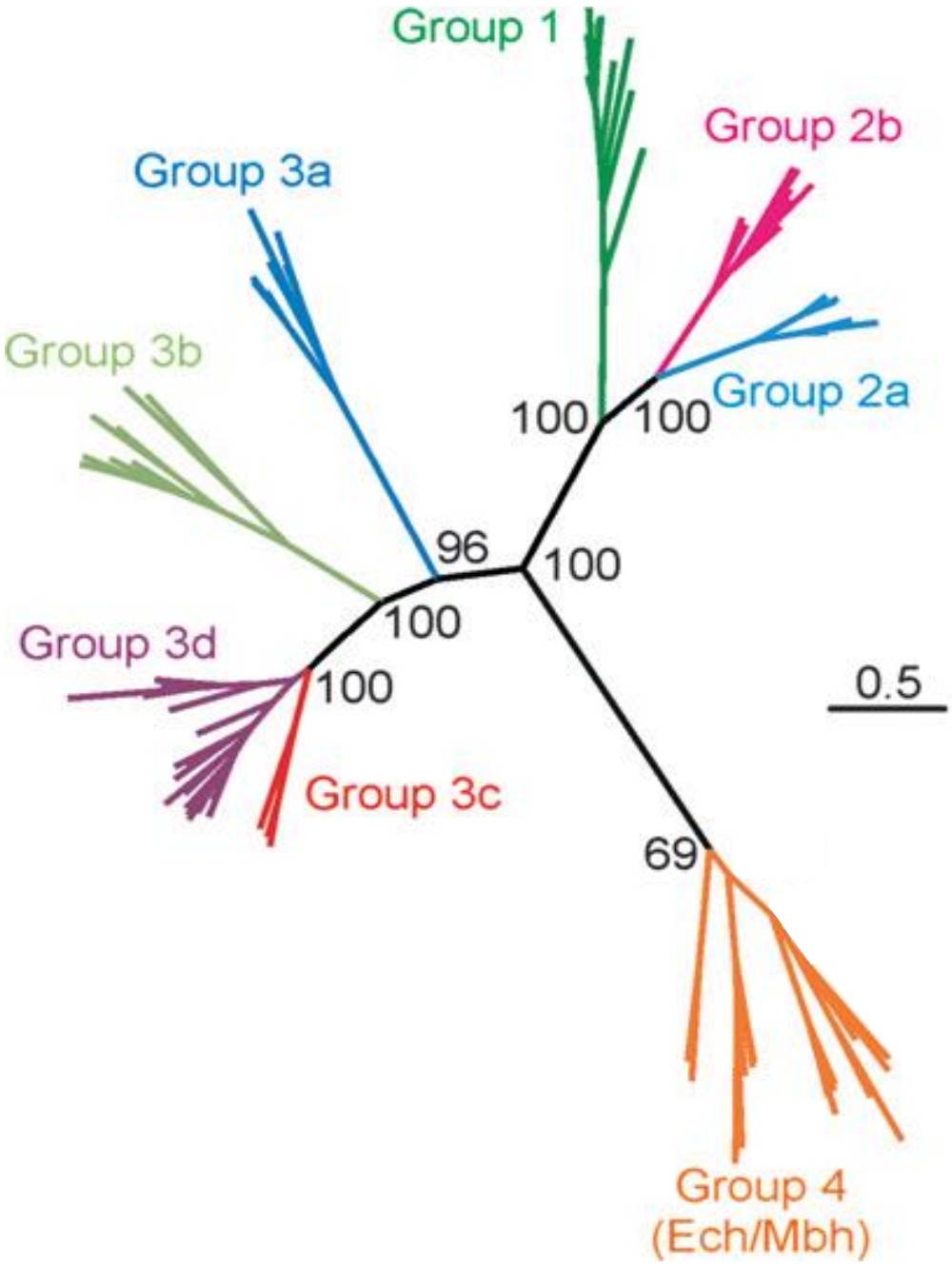
Group 1
Group 2b
Group 3a
Group 3b
Group 2a
100
100
96
100
100
Group 3d
0.5
Group 3c
69
Group 4
(Ech/Mbh)

target the hydrogenase complex to the membrane for proper assembly. Several hydrogenases from this group have been studied to understand the mechanism of membrane insertion. Membrane-bound hydrogenases from *E. coli*, *W. succinogenes*, and *R. eutropha* have been shown to be exported to the membrane by a hitchhiker mechanism (166). As discussed above, this group harbors the [NiFe]-hydrogenases that are classified as "oxygen-tolerant" hydrogenases (124, 158, 159).

Also present in group 1 is the subclass [NiFeSe]-hydrogenase from *D. vulgaris* hildenborough and *Desulfomicrobium baculatum* (167). These hydrogenases are unique in that one of the terminal cysteine ligands is replaced by a seleno-cysteine, which is encoded by the codon TGA. There are only two known organisms that have crystal structures reported for their [NiFeSe]-hydrogenases (167, 168). The observed structure of these resembles what has been previously seen in the [NiFe]-hydrogenases. Within the crystal structure of *D. gigas*, Cys530 is coordinated to the Ni atom of the active site. In the [NiSeFe] hydrogenases, it was found that this cysteine ligand is replaced by a seleno-cysteine. Besides this difference at Cys530, the structural differences between [NiFeSe]- and [NiFe]-hydrogenases include the C-terminal region of the large subunit, the [NiFe] active site, and the medial [FeS] cluster. The C-terminal region of the large subunit was found to be bound to a Fe atom based on X-ray anomalous dispersion experiments, instead of a Mg ion. Also, other metals are bound to the protein matrix that includes Ca and Cl, but it is unclear what functional role these metals have.

Group 2 [NiFe]-hydrogenases includes the cyanobacteria uptake hydrogenases and the H_2 sensors (74). There are two main features that distinguish this group from the other three [NiFe]-hydrogenase groups. The first is that there is no signal peptide at the N-terminus of the small subunit. The second feature is that there are numerous deletions of the primary amino acid sequence of the small subunit in this group, when compared to the Group 1 hydrogenase small subunit. There are two subgroups referred to as Group 2a and Group 2b. The Group 2a [NiFe]-

hydrogenases include the cyanobacterial uptake hydrogenases and are collectively encoded and referenced as HupSL. These hydrogenases are normally linked to nitrogenase and are induced under N_2 fixing conditions (169, 170). Hydrogenase III from *Aquifex aeolicus* is an example of this group and is thought to provide electrons to the reductive TCA cycle of the organism in order to fix carbon dioxide (164). Group 2b of the [NiFe]-hydrogenases includes the regulatory hydrogenases, which are termed either HupUV or HoxBC (74). These regulatory hydrogenases function as part of the regulatory cascade used to control the expression of the proteobacterial uptake hydrogenases in sensing the presence of hydrogen. These hydrogenases are unique in that they are completely insensitive to oxygen inactivation. Studies done on the Group 2b hydrogenases from *R. capsulatus* and *R. eutropha* revealed that the gas channels of these hydrogenases were full of bulky amino acids and mutational studies done to remove these bulky amino acids did result in increase oxygen sensitivity within these hydrogenases (171-173). From this observation it was postulated that these bulky amino acids restricted oxygen from accessing the active site. It was also found that the small subunit of these regulatory hydrogenases does not contain the typical 3 [4Fe-4S] clusters. Instead, they have two [2Fe-2S] clusters and a 4Fe species (174).

Group 3 [NiFe]-hydrogenases are split further into 4 different groups (74, 75). Group 3a hydrogenases include the F420-reducing hydrogenases, while the group 3b hydrogenases include the NADP-reducing hydrogenases. Group 3c includes MV-reducing hydrogenases, while group 3d includes the bidirectional NADP/NAD-reducing hydrogenases. The entire group 3 hydrogenases are composed of the two hydrogenase subunits (large and small) with other subunits associated that allow these hydrogenases to bind soluble cofactors such as F_{420}, NAD, or NADP. These enzymes can function bidirectionally and are able to physiologically re-oxidize

these cofactors under anaerobic conditions using protons as electron acceptors (74, 75). Recently, the first crystal structure of a group 3 hydrogenase was published (PDB: 4OMF; 175). The F_{420}-reducing [NiFe]-hydrogenase from *Methanothermobacter marburgensis* is the first structure of a [NiFe]-hydrogenase that does not belong to the group 1 type (175).

The NAD-dependent [NiFe]-hydrogenase from *R. eutropha* was the first example of a 3b-type enzyme, it has a tetrameric structure composed of two hydrogenase subunits (HoxYH) and two subunits (HoxFU), which are homologous to NADH dehydrogenases subunits. This can only be activated in the presence of NADH and not NADPH (176). A protein complex of this hydrogenase with a higher molecular weight has also been isolated that shows the presence of two additional HoxI subunits (176). Both NADH and NADPH activated this hydrogenase with the hexameric subunit composition. This suggests that the HoxI subunits provide a binding site for NADPH and are needed for interaction with NADPH. The soluble hydrogenases I (SHI) and II (SHII) from *P. furiosus* are also members of this 3b group and function to reduce NAD^+ and $NADP^+$ through the oxidation of hydrogen (74, 177, 178). Both SHI and SHII are encoded within 4 gene operons in *P. furiosus* and have been purified and characterized. SHI from the native organism is 10 times more active than SHII, and *in vitro* assays have shown that the preferred substrates for SHI are H_2 and $NADP^+$. From this analysis it was proposed that SHI functions *in vivo* to oxidize H_2 in order to regenerate NADPH, which can be used for biosynthetic purposes. *P. furiosus* will be discussed in more detail in Chapter 2.

Another well-studied example of a Group 3 hydrogenase is the enzyme from *Allochromatium vinosum*. This bidirectional hydrogenase is pentameric and consists of two hydrogenase-related subunits (HoxYH) and the diaphorase-containing subunits (HoxFUE). The HoxFUE subunits are homologous to subunits of complex I in the electron transport chain and

contain binding sites for FMN, NADP, and Fe-S clusters (74, 75). This homology to complex I is an example of how nature has utilized homologous subunits of a conserved complex in order to be used for metabolic purposes elsewhere in the cell.

The group 4 [NiFe]-hydrogenases are H_2-evolving, energy-conserving, membrane-associated enzyme (74, 75, 179-181). The basic composition of this group consists of six conserved subunits. Four encode hydrophilic proteins and the other two encode hydrophobic proteins (179, 180). These six conserved subunits are very homologous to the "core" subunits of complex I of the aerobic electron transport chain. There is very little homology between the group 1 and group 4 hydrogenases except for the residues that bind the [NiFe] active site and the proximal [FeS] cluster. Another difference found in this group of hydrogenase is that the small subunit contains only the "proximal" cluster rather than the typical three [FeS] clusters. There are no known crystal structures for group 4 hydrogenases. The physiological function of the Group 4 enzymes is to remove excess reductant generated from anaerobic metabolism by reducing protons with the excess electrons to evolve hydrogen, while also conserving energy through the generation of an electrochemical gradient. This gradient is then utilized by an ATP synthase in order to generate ATP. *E. coli* hydrogenase 3, the CODH:CooF complex from *Rhodospirillum rubrum* and Ech from *Methanosarcina barkeri* are some examples from this group (182-186).

Another example of a group 4 hydrogenase is the membrane-bound hydrogenase (MBH) from *Pyrococcus furiosus* (187, 188). This membrane-bound hydrogenase is encoded within a 14-gene operon and is believed to accept electrons from reduced ferredoxin generated during metabolism in order to reduce protons and evolve hydrogen, while also establishing a gradient

Figure 1.8

Schematic representation of the membrane bound hydrogenase (MBH) from *Pyrococcus furiosus*. The Mrp module is encoded by MbhA-H and the hydrogenase module by MbhI-N. MbhL harbors the [NiFe]-catalytic site, while MbhJ and N harbor the [FeS] clusters. Fd_{ox} and Fd_{red} represent the oxidized and reduced forms of ferredoxin, respectively.

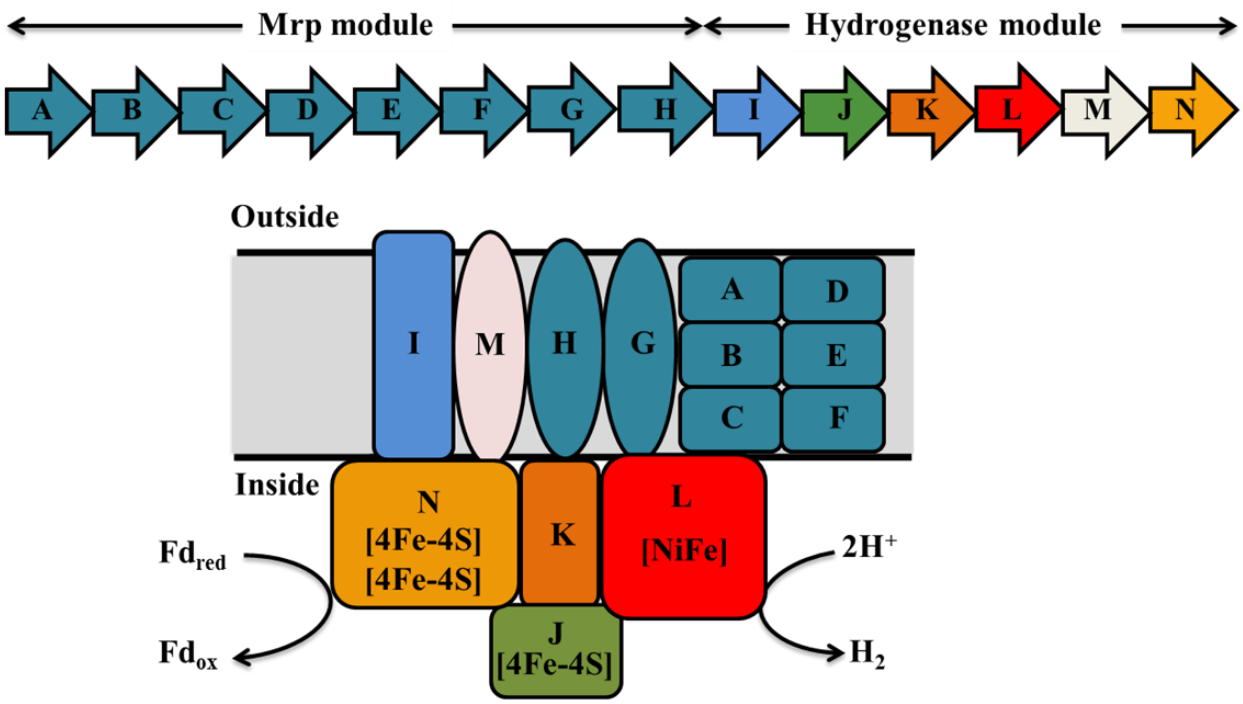
Mrp module
Hydrogenase module
A
B
C
D
E
F
G
H
I
J
K
L
M
N
Outside
I
M
H
G
A
B
C
D
E
F
Inside
N
[4Fe-4S]
[4Fe-4S]
K
L
[NiFe]
J
[4Fe-4S]
Fd$_{red}$
Fd$_{ox}$
2H$^+$
H$_2$

that is used to synthesize ATP by ATP synthase (187, 188; Figure 1.8). The reduction of protons is an exergonic reaction and this complex conserves energy by pumping ions across the membrane to create an electrochemical gradient. Based on sequence analysis, MBH has 8 subunits (MbhA-H) that are homologous to the Mrp H^+/Na^+ ion antiporter (MrpA-G) that is important in *Bacillus* species for alkaline resistance (189). Figure 9 shows a schematic representation of the 14-subunit MBH complex, and based on sequence analysis, MbhA-H shares homology to this Mrp complex. The 6 conserved subunits of MBH that have homology to complex I are MbhHJKLMN. These conserved subunits contain hydrophilic subunits MbhJKLN, while the hydrophobic subunits are MbhHM. MbhKL represent the large subunit of the group 1 enzymes that harbors the [NiFe] active site. MbhJ contains just the proximal [4Fe-4S] cluster, while MbhN contains the medial and terminal [4Fe-4S] clusters. Hence, MbhJN are equivalent to the small subunit of the group 1 enzymes. MbhH is believed to function in the antiporter process based on its homology to the Mrp antiporter and MbhM is thought to anchor the four soluble subunits to the membrane. Hence, MBH functions as a simple respiratory system and its properties are discussed in detail in chapters three and four.

ENERGY CONSERVATION IN P. FURIOSUS

P. furiosus, as mentioned in section 1.2, has two different mechanisms in which energy is conserved during metabolism. It has a simple "respiratory" system that involves the action of its membrane-bound hydrogenase, MBH, and an ATP synthase (190-192; Figure 1.9). MBH couples H_2 evolution to the pumping of ions, and this gradient is then utilized by ATP synthases in order to generate ATP for the cells energy needs (192, 193). Two different types of pumps exist in nature for the pumping of protons and ions across a membrane. Primary pumps function by coupling redox reactions to the formation of a gradient, while secondary pumps function by

Figure 1.9

Predicted physiological roles of the hydrogenases from *P. furiosus*. MBH stands for the membrane-bound hydrogenase. SHI and SHII stand for soluble hydrogenase I and II. Fd_{ox} and Fd_{red} represent the oxidized and reduced forms of ferredoxin, respectively. Modified from (192).

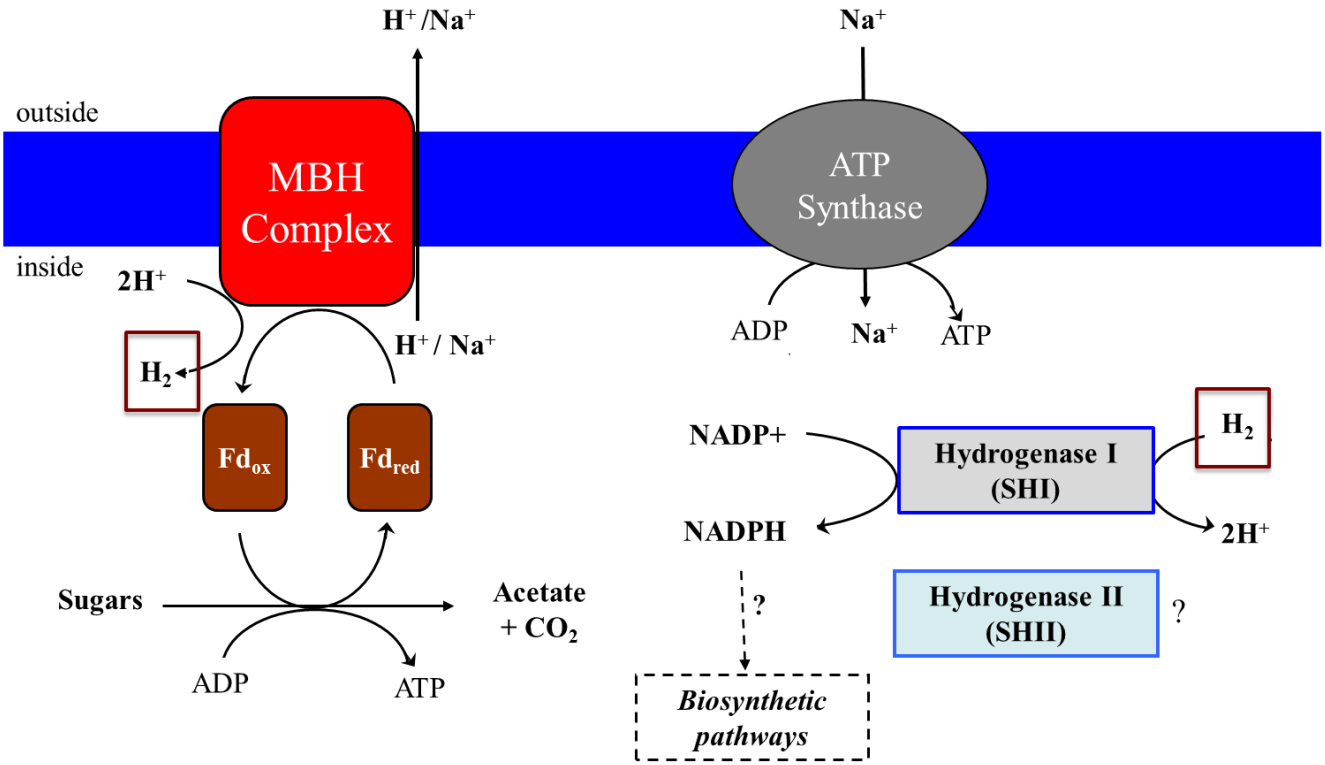
H+ /Na+
Na+
outside
MBH Complex
ATP Synthase
inside
2H+
H2
H+ / Na+
ADP
Na+
ATP
Fdox
Fdred
NADP+
Hydrogenase I (SHI)
H2
NADPH
2H+
Sugars
Acetate + CO2
?
Hydrogenase II (SHII)
?
ADP
ATP
Biosynthetic pathways

using an already established gradient to drive the transport of ions (194-195). An example of a secondary pump is the ATP synthase, which couples the thermodynamically favorable transport of ions to the generation of ATP. In *P. furiosus*, the MBH is the enzyme responsible for the generation of a Na^+ gradient that is then utilized by a Na^+-dependent A_1A_0 ATP synthase in order to generate ATP (190-193). The mechanism that is used to generate ATP is termed the chemiosmotic theory first proposed in 1961 by Mitchell (194). The two aspects of this gradient are $\Delta\psi$ and ΔpH. $\Delta\psi$ represents the electrical potential that forms as a result of the translocation of ions or charge across the membrane, while ΔpH represents the pH component that results in the translocation of these H^+ or Na^+ ions. The available energy that is conserved in this generated gradient is then utilized by ATP synthases for the generation of ATP.

ATP synthases are membrane-bound enzyme "motors" that can couple the transport of either H^+ or Na^+ across a membrane to the generation of ATP from ADP and inorganic phosphate (196, 197). These enzymes are found in all three domains of life and have been organized into 4 different groups called the A-type, V-type, F-type, and P-type ATP synthases (196-199). Based on sequence analysis, A-type, F-type and V-type ATP synthases all belong to the same family, while P-type ATP synthases are in a different class. ATP synthases contain an ion channel, which is made up of $A_0/V_0/F_0$ moieties, and a catalytic domain, which is made up of $A_1/V_1/F_1$ domain and is responsible for the conversion of ADP to ATP. F-type ATP synthases are the most studied type and utilize proton/ion gradients in order to generate ATP, while V-type ATP synthases function in maintaining the pH of the cell by hydrolyzing ATP in order to pump protons or ions outside of the cell. These ATP synthases also differ in the subunit size and number. F-type ATP synthases harbor at least 8 subunits, while V-type ATP synthases are composed of a minimum of 12 subunits. For A-type ATP synthases, the subunit number varies

and the reason is not well understood. The three-dimensional structure of the A_1A_0 ATP synthase from *P. furiosus* has recently been determined showing the "motor"-shape of the enzyme complex (191). Based on sequence comparisons, A-type and V-type ATP synthases are closely related, but catalytically, A-type ATP synthases function more like the F-type synthases. A-type ATP synthases are found exclusively in archaea and function similar to F-type ATP synthases.

P. furiosus also conserves energy by substrate-level phosphorylation. As discussed its glycolytic pathway does not contain the PGK step but does contain pyruvate kinase, which synthesizes ATP using PEP. In addition, reduced ferredoxin is generated in the modified Embden-Meyerhof pathway of *P. furiosus* by the action of GAPOR and POR (60, 61, 65, 66; Figure 3). This reduced ferredoxin is then used to reduce protons, by the membrane-bound hydrogenase (MBH) complex, in order to conserve energy by respiration. Another way that reduced ferredoxin becomes oxidized in *P. furiosus* is by the action of the ferredoxin $NADP^+$ oxidoreductase (FNOR) bifurcating enzyme complex (200). This enzyme complex conserves energy through a bifurcation mechanism that couples the oxidation of ferredoxin and NADH to the reduction of NADP in order to generate NADPH for biosynthesis, as NADP reduction is unfavorable due to the high NADP/NADPH ratio. FNOR is a heterodimer with subunits of 52,000 and 29,000 Dalton in size. The purified enzyme contains flavin but no active redox metals. The soluble hydrogenase I (SHI) in *P. furiosus* is also thought to generate NADPH (74, 177, 178, 192). However, the SHI deletion mutant has no phenotype so the function of SHI does not seem to be important under the usual laboratory conditions (201).

COMPLEX I HOMOLOGY AND FUNCTION

Complex I is an energy transducing membrane bound enzyme complex made up of at least 14 subunits that couples electron transfer from NADH to quinone to proton pumping across the membrane (202). Bacterial complex I is the minimal version of this enzyme complex and is around 550 kDa in size. It contains 8 to 10 iron-sulfur clusters and a flavin mononucleotide. The structure of complex I was recently solved using the enzyme from the thermophilic bacterium *Thermus thermophiles* (PDB: 3M9S; 202). This contained 16 subunits and has an L-shaped structure. It has been characterized into different modules depending upon function (202). The q-module represents those subunits responsible for accepting electrons from NADH and for shuttling these electrons to reduce quinone and is made up of four different subunits (NuoBCDI), all of which are hydrophilic. NuoD represents the catalytic subunit and is where quinone reduction occurs. NuoD is homologous to the catalytic subunits of the group 4 hydrogenases (MbhL) and the cavity where quinone is bound is believed to be similar to where the [NiFe] active site is found in these hydrogenases (See Chapter 4; 179, 180). NuoI harbors two [Fe-S] clusters and is homologous to MbhN. NuoB is homologous to MbhJ and harbors one [FeS] cluster named the N2 cluster, which is the cluster responsible for reducing quinone. NuoC is homologous to MbhK. This subunit does not contain any clusters, but is believed to be a part of the catalytic subunit. Other similarities between these enzyme complexes include the hydrophobic subunits NuoHLMN (179, 180). The membrane bound subunits of complex I are responsible for the translocation of a proton across the membrane as well as anchoring the hydrophilic subunits to the membrane. NuoH is homologous to MbhM is believed to anchor the hydrophilic subunits of Complex I to the membrane. NuoLMN are homologous to MbhH and are believed to be responsible for the pumping of protons in the generation of a gradient across

the membrane. Complex I also shares homology with the Mrp H^+/Na^+ antiporter complex (MrpA and D), like the group 4 hydrogenases (181), but does not have homology to the entire Mrp complex (Chapter 4, Figure 1).

NuoEFG represent the N-module and are responsible for oxidizing NADH. Electrons generated from the oxidation of NADH are shuttled to the q-module where quinone reduction can occur. The flavin mononucleotide is found in NuoF and is responsible for the oxidation of NADH. NuoF also harbors one [Fe-S] cluster which shuttles the electrons from NADH to NuoE, which harbors one [2Fe-2S] cluster. From there electrons are shuttled to NuoG, which harbors a [2Fe-2S] cluster and three [4Fe-4S] cluster, to the q-module. These subunits also show homology to group 3 hydrogenases (74, 75).

A large number of papers have been published discussing the evolutionary relationship between MBH and Complex I. These papers focused on the homology of the six conserved subunits of group 4 hydrogenases with the catalytic core of complex I, as well as the homology of these complexes with the Mrp H^+/Na^+ antiporter (74, 75, 179-181, 203). Based on the homology of these complexes, it can be seen that MbhH connects MBH to both complex I (NuoLMN) and the Mrp (MrpAD) antiporter (Chapter 4, Figure 1). This indicates that these genes share a conserved ion-translocating unit as they are each predicted to pump a proton based on the structural analysis of complex I. In addition, it has been proposed that Complex I may have evolved from an ancestral MBH complex (181). This ancestral MBH complex is also believed to be the progenitor of other membrane-bound hydrogenases such as Ech from methanogens. Since the progenitor of all of these complexes is believed to harbor both Mrp and hydrogenase type subunits, an ancestral MBH is believed to be the best candidate as it harbors a complete Mrp antiporter as well as the 6 “core” conserved subunits. Thus, the generation of a

crystal structure of MBH would give further insight into the structure and function of Complex I as well as shed insight into the evolutionary structural relationships shared between these complexes. This aspect is discussed further in Chapter 5.

PURIFICATION AND ANALYSIS OF GROUP 4 HYDROGENASES

As discussed above, very little is known about the structure and function of group 4 hydrogenases. This is due to the difficulty of purifying these membrane-bound complexes that contain at least six subunits. The simplest members include the 7-subunit hydrogenase 3 from *Escherichia coli*, which oxidizes formate and evolves H_2, the 8-subunit CO-induced hydrogenase of some CO-oxidizing bacteria that conserve energy from coupling the oxidation of CO to H_2 production, and the 6-subunit 'energy-conserving' hydrogenase (Ech) from the archaeon *Methanosarcina barkeri* (182-186). More complex members of the group 4 enzymes include the 18-subunit formate hydrogen lyase (FHL) system from *Thermococcus onnurineus* (204), which oxidizes formate and evolves hydrogen (80^0C). There are only four known reports of successful purifications of group 4 hydrogenases (182-186, 205, 206). These include the 6-subnit Ech from *Methanosarcina barkeri*, the 7-subunit CO-oxidizing COO hydrogenase complex from *Carboxydothermus hydrogenoformans*, the 6-subunit Ech from *Thermoanaerobacter tengcongensis*, and the 14-subunit MBH from *P. furiosus*.

The best characterized hydrogenase from group 4 is the Ech from *M. barkeri* and this was also the first group 4 hydrogenase to be purified (185, 186). Purified Ech contains six subunits corresponding to the products from the operon of *echA-F*. The enzyme contained 0.9 mol of Ni, 11.3 mol of nonheme-iron and 10.8 mol of acid-labile sulfur per mol of protein. Amino-acid sequence analysis of the cytoplasmic subunits of Ech identified two classical [4Fe-4S] clusters in EchF and one [4Fe-4S] cluster in EchC. EchC is homologous to the small subunit of [NiFe]-

hydrogenases and is significantly smaller than the traditional small subunit found in the other groups of [NiFe]-hydrogenases and contains only the "proximal" cluster. Electron paramagnetic resonance (EPR) and Fourier Transform Infrared Spectroscopy (FTIR) were used to study the [NiFe] site of the purified Ech enzyme. It was observed that the [NiFe] site in Ech had very similar properties compared to other [NiFe]-hydrogenases, which suggests that the architectures of the active sites are similar. The [FeS] clusters were also characterized by EPR and three different S= 1/2 species were observed that are believed to originate from three [4Fe-4S] clusters. The average g-signals that were observed for these clusters were g=1.92, g=1.89, and g=1.96. Redox titrations showed that the g=1.96 signal had the lowest redox potential (below -420 mV at pH 7.0). Magnetic interaction of the g=1.89 cluster with unpaired electrons from the [NiFe] active site showed that this signal belongs to the proximal cluster of Ech. The pH dependence of this cluster was also found to be similar to the proximal clusters of other [NiFe]-hydrogenases. As discussed below in the comparison of group 4 hydrogenases and complex I, this proximal cluster is equivalent to the N2 cluster of complex I, which is proposed to be important for ion pumping due to its unique redox properties. Further characterization and structural studies are needed to fully understand the relationship shared between these group 4 hydrogenases and complex I enzymes, and this is described further in Chapter 5.

HETEROLOGOUS EXPRESSION OF HYDROGENASES

Heterologous expression of proteins has been observed to have multiple difficulties. Some examples of these issues that arise include toxicity and low yields (207, 208). When toxicity occurs, the growth of the expression host will be inhibited and results in poor cell and protein yields. Toxicity effects can be limited by making sure the proper insertion of the correctly folded protein in the membrane, inclusion bodies, and cell-free synthesis approaches

(207-213). Heterologous expression of O_2-sensitive complexes such as hydrogenases has further difficulties due to both oxygen and the co-expression of accessory proteins (127, 128). As stated above, there are eight accessory proteins needed for proper maturation of the [NiFe]-hydrogenases and three accessory proteins are needed for [FeFe]-hydrogenase. These maturation proteins, which are required for both the assembly of the [NiFe] and [FeFe] active sites, are also oxygen-sensitive, which contributes further to the difficulty of successful heterologous expression of hydrogenases. There are a couple of different examples for successful heterologous expression of these enzymes that have been reported in the literature and will be discussed below.

For [NiFe]-hydrogenases, there have been a limited number of reports of successful heterologous expression and most of these have occurred using expression hosts similar to the native host organism. These include the heterologous expression of the three subunit hydrogen-oxidizing MBH from *R. eutropha*, which was expressed in *Pseudomonas stutzeri* using a broad host-range plasmid containing all the maturation proteins as well as a regulatory histidine kinase system that was needed for proper maturation (214). Another example of the successful heterologous expression of a [NiFe]-hydrogenase is the expression of the soluble hydrogenase I from *P. furiosus* in *E. coli* (215). This was significant as it was the first example of the successful heterologous expression of a hydrogenase in a distantly-related organism. Engineering of "minimal" versions of hydrogenases has also been met with limited success. Only one example exists, which was done in engineering a minimal version of SHI from *P. furiosus*, which was expressed in *P. furiosus*. A dimeric version of the heterotetrameric enzyme was expressed and purified using a histidine affinity tag (216). This "dimeric" version of SHI

was shown to accept electrons from an electron donor different from the physiological donor NADPH.

There are several examples of heterologous expression of [FeFe]-hydrogenases in genetically tractable hosts such as *E. coli*. Unlike [NiFe]-hydrogenase, there are examples of heterologous expression systems both *in vivo* and *in vitro*. One of the most studied [FeFe]-hydrogenase is the HydA1 from *Chlamydomonas reinhardtii* which has been natively purified and has been heterologously expressed in a couple different systems. These systems include expression in *E. coli* and *Clostridium acetobutylicum* (217-219). Affinity tags have also been used to assist in the purification of these heterologous proteins as demonstrated in the heterologous expression and Strep-Tactin affinity purification of HydA1 from *C. reinhardtii* expressed in *Shewanella oneidensis* (220). Another difference between the heterologous expression systems is the fact that cell-free synthesis systems have been developed for [FeFe]-hydrogenases (218, 221). Cell-free synthesis systems are important as they can be used in order to drastically increase the possibility of engineering a hydrogenase to become more oxygen-tolerant or increase the catalytic turnover. One example is the SIMPLEX (Single-Molecule PCR-Linked Expression) system, which uses directed evolution in an *in vitro* microtiter plate-based protein screening platform, was used to successfully synthesize a [FeFe]-hydrogenase that was four times more active than the wild-type enzyme (221).

GENETICALLY TRACTABLE ARCHAEA

There are only a few reports of genetic systems that have been established for members of the archaea (1). There are examples in both the *Crenarchaeota* and the *Euryarchaeota*, as well as the halophiles, methanogens, and thermophiles. In the thermophiles, genetic systems have been developed for members of the *Sulfolobales* and the *Thermococcales*. Within the

methanogens, genetic techniques are available for species of *Methanococcus* and *Methanosarcina*. More specifically, genetic techniques, such as transformations, shuttle vectors, and markerless genetic exchange have been successful in *M. maripaludas*, *M. acetivorans*, *M. voltae*, *M. barkeri*, and *M. mazei* (1). For example, in *Methanosarcina* the energy-conserving hydrogenase Ech was deleted showing that this enzyme was important for both methanogenesis and carbon fixation (222).

In the halophiles, there are two known organism that have genetic systems established, *Haloferax volcanii* and *Halobacterium salinarum*. Both are well established and there are advantages to using one or the other organism for genetic studies. *Hbt. salinarum* is typically used in order to study haloarchaeal cell biology, while *Hfx. volcanii* is used for traditional genetics (1). There are new systems being established in halophiles that are still in the beginning stages, including those for *Haloarcula marismortui*, *Halorubrum* sp., as well as *Haloferax mediterranei*, which is closely related to *Hfx. volcanii* (1, 223-225).

In the *Sulfolobales*, the development of a genetic system has met with limited success due to the availability of only two selectable markers, uracil auxotrophy and growth on lactose (1). The most genetically tractable strain is *S. solfataricus* P1 strain PH1-16, which is a uracil auxotroph and is grown on defined media lacking uracil in order to select mutants (226, 227). Two other established *Sulfolobus* species that have a genetic system is *S. islandicus* E233S1 and *S. acidocaldanus*, which are both uracil auxotrophs and have an established shuttle vector system available for genetic manipulation (228-230). These *Sulfolobus* species are the only *Crenarchaeota* that have genetic systems established for them (1).

In the Thermococcales, genetic systems exist for *Thermococcus kodakarensis, Pyrococcus abyssi* and *Pyrococcus furiosus* (1, 231-233). Genetic strategies that use auxotrophic

mutants in defined media are established for both *T. kodakarensis* and *P. furiosus*, while genetic strategies that use shuttle vectors have been established for all three *T. kodakarensis, P. furiosus* and *P. abyssi* (1). One interesting example of genetic techniques involving the thermococcales includes the report of a shuttle vector that can be used between *T. kodakarensis* and *E. coli* (232). The competent genetic strain for *P. furiosus* is referred to as COM1 and this will be the genetic strain that is used to manipulate hydrogenase for the goals of this thesis (201). This strain is a uracil auxotroph, and has been sequenced, and shows no difference in the regions that affect hydrogenase activity (201, 233).

HYDROGEN AS A BIOFUEL

Hydrogenases enzymatically generate the biofuel hydrogen. Hydrogen is a renewable, carbon neutral energy source that harbors a formidable amount of energy, as the conversion of hydrogen to water yields three times more energy than gasoline per kilogram (234-236). With the increasing demand for energy and limiting supply of fossil fuels, carbon neutral renewable energy sources are receiving increased attention. Hydrogen gas is a particularly attractive alternative fuel and although there are chemical methods to produce it, biological hydrogen production is also a potentially viable way to establish a hydrogen economy. One advantage for this is the replacement of expensive metals, such as palladium and platinum, which are used as catalysts in the chemical generation of hydrogen. Hence, any future cost-efficient hydrogen production method is likely to have biological or bio-inspired components. Although this may be true, more research is needed in order to understand the mechanisms and restrictions associated with hydrogen production.

As discussed above, [NiFe]-hydrogenases are extremely difficult enzymes to work with due to their inactivation in the presence of oxygen as well as the need for eight different proteins

for maturation of the active sites. In addition, techniques need to be developed that yield large amounts of the pure hydrogenase for in depth structure and function studies so that we can engineer these "biocatalysts" to improve their catalytic activity and become "oxygen-tolerant". Generation of "minimal" versions of hydrogenases could also give insights into their structure and function and shed light on which subunits are needed for an active enzyme or if the activity can be tailored to different substrates. The generation of such techniques for studying and engineering hydrogenase will be discussed below and will focus on the hydrogenases from *P. furiosus*

GOAL OF THIS WORK

The primary goal of this project is to gain a better understanding of the structure and function of the membrane-bound hydrogenase (MBH) from *Pyrococcus furiosus*. In order to accomplish this goal, the first objective was to develop a purification technique that would yield the entire 14-subunit complex. When this work was initiated, no such purification techniques were available, but due to the development of a genetic system in *P. furiosus*, such a technique was now possible through the engineering of an affinity tag (201). Before working on MBH, the capabilities of this genetic system was tested to see if it was possible to over-produce and affinity purify the soluble hydrogenase I (SHI) from *P. furiosus*. If successful, the next objective was to genetically manipulate MBH to see if it could be over-produced with an affinity tag to enable purification of the entire 14-subunit complex. The genetic system also potentially allowed for different variants of MBH to be constructed to better understand the structure and function of the different modules of MBH, such as the importance of the Mrp subunits on the physiological function of the entire complex. The construction of minimal versions of MBH were therefore attempted in order to generate a soluble sub-complex that could be purified without the use of

detergent. This detergent-free protein could then be used for structural analysis. Due to the lack of structural information on Group 4 hydrogenases, which show very little homology to group 1-3 hydrogenases, a structure of this complex would be instrumental in the understanding of how MBH is able to evolve hydrogen so effectively, while also conserving energy through the pumping of H^+/Na^+ to form a gradient. Such a structure would also provide great insight into the understanding of how MBH is related to the Complex I of the aerobic respiratory chain at the structural level.

CHAPTER 2

ENGINEERING THE HYPERTHERMOPHILIC ARCHAEON *PYROCOCCUS FURIOSUS* TO OVERPRODUCE ITS CYTOPLASMIC [NIFE]-HYDROGENASE[1]

[1]McTernan PM*, Chandrayan SK*, Hopkins RC, Sun J, Jenney FE, et al. 2012. Journal of Biological Chemistry 287: 3257-3264. Reprinted here with permission of the publisher.

*Both authors contributed equally to this work

ABSTRACT

The cytoplasmic hydrogenase (SHI) of the hyperthermophilic archaeon *Pyrococcus furiosus* is a NADP(H)-dependent hetero-tetrameric enzyme that contains a nickel-iron catalytic site, flavin and six iron-sulfur clusters. It has potential utility in a range of bioenergy systems *in vitro* but a major obstacle in its use is generating sufficient amounts. We have engineered *P. furiosus* to overproduce SHI utilizing a recently developed genetic system. In the over-expression OE-SHI strain, transcription of the four-gene SHI operon was under the control of a strong constitutive promoter, and a strep-tag II was added to the N-terminus of one subunit. OE-SHI and wild type *P. furiosus* strains had similar rates of growth and H_2 production on maltose. Strain OE-SHI had a 20-fold higher transcription of the polycistronic hydrogenase mRNA encoding SHI and the specific activity of the cytoplasmic hydrogenase was approximately ten-fold higher compared to the wild type strain, although the expression level of genes encoding processing and maturation of SHI were the same in both strains. Over-expressed SHI was purified by a single affinity chromatography step using the strep-tag II and it and the native form had comparable activities and physical properties. Based on protein yield per gram of cells (wet weight), the OE-SHI strain yields a 100-fold higher amount of hydrogenase compared to the highest homologous [NiFe]-hydrogenase system previously reported (from *Synechocystis*). This new *P. furiosus* system will allow further engineering of SHI and provide hydrogenase for efficient *in vitro* biohydrogen production.

INTRODUCTION

Hydrogenases catalyze the reversible reduction of protons to hydrogen gas (H_2) (1-3). Their physiological roles in microorganisms include the reduction of protons to evolve H_2 to remove excess reductant generated by oxidative metabolism or, in the reverse reaction, the oxidation of H_2 and its use as a source of reductant and energy. Structural and biochemical analyses have revealed that most hydrogenases contain either nickel and iron or only iron at their catalytic sites, and these are referred to as the [NiFe]- and [FeFe]-enzymes, respectively (4,5). [NiFe]-hydrogenases have been extensively studied from mesophilic organisms, particularly from species of *Desulfovibrio* (6-11). With the increasing demand for energy and limiting supply of fossil fuels, carbon neutral renewable energy sources are receiving increased attention. Biological H_2 production is a potentially viable alternative to establish a renewable and low carbon emitting hydrogen economy (12,13). One impetus for this is the replacement of expensive palladium- and platinum-based catalysts used in the current chemical generation of hydrogen gas (14). Hence, any future cost-efficient hydrogen production method is likely to have biological or bio-inspired components (15).

Efforts to over-produce hydrogenases in various heterologous systems in order to decipher their structural and biochemical properties have met with limited success (16). A major limitation is the complex oxygen-sensitive post-translational processing pathway that is required to give a functional [NiFe] catalytic subunit (17-19). For example, assembly of the Hyd3 hydrogenase of *E. coli*, a membrane bound [NiFe]-hydrogenase, requires the participation of at least eight processing proteins (17). Consequently, the majority of successful heterologous recombinant expression systems for hydrogenase have been achieved in closely-related hosts. For example, the hydrogenase from *Desulfovibrio gigas* was heterologously expressed in *D.*

fructosovorans (20), and a functional, NAD-dependent [NiFe]-hydrogenase from the gram-positive organism, *Rhodococcus opacus*, was produced in the gram-negative organism, *Ralstonia eutropha* (21). The membrane bound hydrogenase of *R. eutropha* was produced in *Pseudomonas stutzeri* using a broad-host-range plasmid containing all the accessory genes required for maturation of the [NiFe] active site (22). The one example of heterologous production of a [NiFe]-hydrogenase in a distantly-related organism was the production of the cytoplasmic hydrogenase I (SHI) from the hyperthermophilic archaeon *Pyrococcus furiosus*, which grows at 100°C, in the mesophilic bacterium *Escherichia coli* (23). Interestingly, assembly and maturation of *P. furiosus* SHI was accomplished by the processing proteins of *E. coli*, with the exception of the proteolytic C-terminal cleavage to give the functional catalytic subunit, which required the *P. furiosus* protease (FrxA) specific for SHI.

Unfortunately, however, none of the heterologous systems for hydrogenase have achieved significant over-production of the enzyme relative to the amount produced in the native host organism (16,23). An alternative approach is to homologously over-produce hydrogenase but this obviously requires a genetic system for the host organism. To date the only successful homologous over-expression of a [NiFe]-hydrogenase was reported with the enzyme from the mesophilic cyanobacterium *Synechocystis* sp. PCC6803 (24). This enzyme consists of five different subunits and utilizes NAD(P) as an electron carrier. To over-express the hydrogenase operon and incorporate an affinity strep-tag II, expression was controlled by a light-induced promoter *psb*AII. Simultaneously, five *hyp* accessory genes from the closely-related organism *Nostoc* sp PCC7120 were expressed using the same promoter (24). This resulted in increased expression of the hydrogenase operon by five-fold, but simultaneous over-expression of the

maturation genes was necessary to process the increased amounts of the enzyme, resulting in a 2-3-fold increase in the amount of active hydrogenase.

The goal of the current study was to develop a homologous expression system for *P. furiosus* SHI. This is a heterotetrameric enzyme that contains flavin and six iron-sulfur clusters, in addition to the [NiFe] catalytic site, and utilizes NADP(H) as an electron carrier (1-3,23,25-26). A diagrammatic representation of the enzyme is shown in Fig. 1, which is based on sequence analyses of the four subunits and the measured cofactor content of the purified enzyme. SHI has been shown to be very efficient in *in vitro* systems to produce H_2 from starch and cellulose in synthetic enzyme pathways (26). These approaches are limited, however, as they utilize SHI purified from *P. furiosus* biomass. Our goal is, therefore, to take advantage of the genetic system recently reported with *P. furiosus* (27) to overproduce the holoenzyme and various mutant forms lacking one or more subunit (28). Herein we describe the development of a one-step marked knock-in method using linear DNA fragments to construct a strain that over-produces SHI by at least an order of magnitude more than the wild-type strain. The recombinant hydrogenase has a strep-tag II affinity tag to facilitate purification and has properties that are comparable, although not identical, to those of SHI purified from wild-type *P. furiosus* (25). Surprisingly, even though an order of magnitude more fully-processed SHI was produced in the recombinant strain, expression of the maturation genes was at the same level as in the parent strain.

METHODS

Growth of P. furious - The strains used in this work are shown in Table 1. Cells were grown in defined medium for all the genetic manipulation work (27). Large scale growth was carried out using a 20 liter fermenter using maltose as the carbon source (29). Cells were grown at 90°C

with constant flushing of N_2/CO_2 at 90°C for 14 hr. Cells were harvested by centrifugation, flash frozen in liquid N_2, and stored at -80°C until used for protein purification.

Construction of a knock-in cassette by overlapping PCR - The knock-in cassette was created using overlapping PCR (30) where the primers used contained approximately 20-base pair overhangs (Supplemental Fig. S1A). The selectable marker and flanking regions were amplified from pGLW021 (27) and *P. furiosus* genomic DNA, respectively. The cassette also had a codon optimized 8 amino acid long strep-tag II with a two extra amino acid linker sequence (31). PCR products were purified using a commercial extraction protocol (Stratagene, Santa Clara, CA) and were used in overlapping PCR reactions using the *Pfx* supermix (Invitrogen, Carlsbad, CA). Final overlapping PCR products were gel purified and used for COM1 transformation as previously described (27). Standard molecular biology techniques were performed as described (32).

Pyrococcus furiosus transformation and construction of the OE-SHI strain - Transformations were carried out using freshly grown COM1 strain (uracil auxotroph), a competent strain of *P. furiosus* (27). For transformation, 200 ng DNA (knock in cassette, Supplemental Fig. S1A) was mixed with 100 µl of an overnight culture of COM1 cells and grown on defined medium. After incubation at 90°C for 72 hours, plates were examined for colonies on defined medium plates for gain of the *pyrF* marker as transformed cells are able to grow without uracil. Three colonies were picked from defined medium plates, grown overnight in 5 ml defined medium and 1.5 ml samples were used to isolate genomic DNA. PCR was used to confirm the correct insertion using the primers listed in Supplementary Table S1, which were designed to bind outside of the homologous flanking regions and amplified using the Prime Star HS polymerase Mix (Clontech, Mountain View, CA, USA). PCR-positive colonies were further purified by three separate

consecutive transfers in defined medium lacking uracil in order to confirm the culture phenotype. PCR screening was done after each round to ensure proper incorporation of the knock-in cassette was maintained. The PCR product amplified from genomic DNA of one positive clone was confirmed by sequencing (Macrogen Sequencing Facility, Rockville, MD).

RNA isolation and qPCR - Total RNA was extracted from 10 ml of mid-log phase cultures grown in rich maltose medium using the Absolute RNA prep kit (Stratagene) and quantified by Thermoscientific Nanodrop spectrophotometer. Before qPCR analyses, the RNA was treated with Turbo DNase (Ambion; Applied Biosystems, Bedford, CA, USA) for 30 min at 37°C and further purified using the DNAase inactivation reagent (Ambion; Applied Biosystems, Bedford, CA). cDNA was prepared using the Affinity Script quantitative PCR (qPCR) cDNA synthesis kit (Agilent Technologies, Santa Clara, CA). All quantitative reverse transcription-PCR (RT-qPCR) experiments were carried out with an Mx3000P instrument (Stratagene) with the Brilliant SYBR green qPCR master mix (Agilent Technologies). The genes encoding the house-keeping enzymes pyruvate ferredoxin oxidoreductase (gamma subunit, PF0971) and DNA polymerase sliding clamp (PF0983) were used as internal controls to normalize the amounts of cDNA that were used for qPCR (Supplemental Fig. S2)

Growth studies and purification of OE-SHI - Growth of and H_2 production by the OE-SHI strain were carried out in 250 ml cultures at 90°C in sealed bottles. At various times the medium was sampled (1ml) for protein estimation by Bradford Method (33) and the headspace was analyzed for H_2 by transferring samples (1 ml) into 10 ml vials containing 1 ml 0.5 M NaOH. After equilibration for 16 hr to remove any residual H_2S (which poisons the chromatography column), H_2 was estimated by using a 6850 network gas chromatograph (Agilent Technologies, Santa Clara, CA) (23,27). Samples of the medium were also removed throughout the growth

phase and the concentration of maltose was determined. OE-SHI was purified under strictly reducing and anaerobic conditions. Frozen cells (25 g) were thawed and lysed osmotically in 75 ml of Buffer A (50 mM Tris/HCL, pH 8.0, containing 2 mM sodium dithionite) and 50 µg/ml deoxyribonuclease I (Sigma Chemical, St. Louis, MO) with stirring for 1 hr at 23°C. The supernatant (S100, 40 ml, 11.7 mg protein/ml) was obtained after removal of cell debris by ultracentrifugation at 100,000 x g for 1 hour. Avidin (1.0 mg, Sigma) was added to the S100 and it was directly loaded using an AKTA Purifier system (GE Healthcare, Piscataway, NJ) on to three 5 ml StrepTactin Sepharose High Performance/StrepTrap HP columns (GE Healthcare) joined in series. The columns were pre-equilibrated and washed and OE-SHI was eluted using the binding and elution buffers described in the manufacturer's protocol, except that all buffers contained 2 mM sodium dithionite. In addition, to optimize the overall recovery, the flow through was reloaded on to the columns prior to washing and elution.

Other Methods - Maltose concentrations were measured spectrophotometrically using an assay kit (BioVision, CA,USA). Samples (50 µl) of the medium were diluted 500-fold with distilled water prior analysis. To measure protein stability using fluorescence spectroscopy, the hydrogenase (0.1 mg/ml in 100 mM EPPS, pH 8.4) was incubated at 90°C. Samples (50 µl) were periodically removed and the tryptophan emission spectrum were recorded using an RF-5301PC Spectroflurometer (Shimadzu, Columbia, MD). The excitation wavelength was 280 nm using a bandwidth of 5 nm.

Hydrogenase activity was routinely measured by H_2 production from methyl viologen (MV, 1 mM) reduced by sodium dithionite (10 mM) at 80°C in 100mM EPPS buffer, pH 8.4, using gas chromatography (23,25). One unit of hydrogenase activity is defined as 1 µmole of H_2 evolved min^{-1}. Assays were also carried out using NADPH (1 mM) as the electron donor in place of

reduced methyl viologen (23,25,34). H_2-oxidation activity was measured by the H_2-dependent reduction of NADP as described previously (35). Stability assays were performed by exposing hydrogenase samples to air at 23°C and thermal stability assays were carried out at 90°C under Ar. Samples of purified hydrogenase, OE-SHI and native SHI control (0.1 mg/ml) were incubated in 100 mM EPPS buffer, pH 8.0, containing 2 mM sodium dithionite at 90°C. Western blots were prepared and analyzed using a chemo-luminescent dye with the Genescript One-Step Western Kit (Genescript USA Inc; Piscataway, NJ) using antibodies for the catalytic subunit of SHI (PF0894) and antibodies to *P. furiosus* superoxide reductase SOR (PF1281) as the internal control. Nickel and iron were measured using a quadrupole-based ICP-MS (7500cc. Agilent Technologies, Tokyo, Japan), equipped with a MicroMist Nebulizer as described (36).

RESULTS

One-step marked insertion of P_{slp} with Strep-tag II in P. furiosus genome - The COM1 mutant *P. furiosus* strain was utilized in order to manipulate the native SHI operon. This strain has a deletion in its *pyrF* gene and cannot grow in a minimal medium lacking uracil (27). It was previously used for markerless gene deletion by selection for uracil prototrophy and counter selection using resistance to 5-fluoroorotic acid (5-FOA), an inhibitor of uracil biosynthesis. Herein we have developed a variation of that method for inserting a genetic element at any locus using linear DNA and a single double crossover event involving selection for uracil prototrophy. The promoter (P_{slp}), which in the parent strain drives expression of the gene encoding the S-Layer protein (PF1399), was inserted in front of the four gene operon (PF0891-PF0894) that encodes SHI. In addition, an affinity strep-tag II was inserted in frame with the N-terminus of the first gene (PF0891, Fig. 2). The genotypes of the COM1 parent and of the engineered strain, termed OE-SHI (for over-expressed SHI), are shown in Table 1. In wild-type cells the gene

encoding the S-layer protein is expressed by an order of magnitude higher than that of the SHI operon according to published DNA microarray data (37). The strep-tag II was chosen for affinity purification as its function is not affected by the chemical reductant, sodium dithionite, which is used to maintain anaerobic conditions during hydrogenase purification. In addition, this tag was assumed not to interfere with nickel incorporation into SHI, a potential problem with a polyhistidine tag.

Constructs were generated by overlapping PCR (Supplemental Fig. S1B and S1C), transformed into the COM1 parental strain, and transformants were selected on plates containing the minimal medium lacking uracil. Selected colonies were screened by PCR using primers specific for regions outside of the flanking region (Supplemental Table S1). A PCR product was expected for both the COM1 and OE-SHI strains, with the product for OE-SHI being approximately 1 kb larger than COM1, indicating correct insertion at the specified locus (Supplemental Fig. S1D). One colony was selected and designated as OE-SHI. Correct incorporation without mutation of the P_{slp}-Strep-tag II upstream of the SHI operon was confirmed by DNA sequencing.

Cytoplasmic fraction of the OE-SHI strain shows increased hydrogenase activity - Cytoplasmic extracts (S100) were prepared from fermenter-grown cells of the OE-SHI strain and of the parental strain and SHI activity was measured using the MV-linked hydrogenase assay (28). Approximately 20 µg of protein was used in the assays for both enzymes. The specific activity at 80°C of the OE-SHI strain extract was 7.96 ± 3.3 U/mg compared with 1.23 ± 0.3U/mg for the COM1 strain (Fig. 3). Hence, the OE-SHI strain had an approximately 7-fold higher level of SHI compared to the parental strain, assuming comparable activities for the native and recombinant enzymes (see below). Imunnoanalyses using a polyclonal antibody specific for

the catalytic subunit of SHI (PF0894; (23)) also confirmed an increased amount of the catalytic subunit in the OE-SHI strain when compared to the parent (Fig. 3). Quantitative PCR showed that the transcript for PF0894 (the fourth gene in the SHI operon) was 20.2 ± 6.2-fold higher in the OE-SHI strain compared to the parental strain (Fig. 4), in which transcription of the SHI operon is controlled by the P_{slp} system and by the native promoter, respectively.

Accessory genes encoding hydrogenase maturation proteins are not up-regulated in the OE-SHI strain-Since the OE-SHI strain contained 7-fold higher hydrogenase activity in its cytoplasm than the cytoplasm of COM1 cells, it was important to determine if genes encoding the accessory proteins required for assembly of the [NiFe] active site in the catalytic subunit of SHI (PF0894) were also up-regulated by some type of feedback mechanism. We focused on the hydrogenase protease *frxA* (PF0975), which specifically cleaves the C-terminus of the catalytic subunit (PF0894), and *hypF* (PF0559), which is involved is the assembly of the diatomic cyanide and carbon monoxide ligands on the Fe atom of the [NiFe]-catalytic site (17,19,23). Linkage between production of hydrogenase and the maturation process is shown by the fact that expression of the genes encoding these two proteins (PF0975 and PF0559) and those encoding SHI are all dramatically down-regulated when *P. furiosus* is grown on elemental sulfur (38). However, in the OE-SHI strain the expression of *frxA* or *hypF* were both unaffected (Fig. 4), in spite of an almost order of magnitude increase in the amount of their 'substrate', namely, unprocessed inactive SHI. The activities of these two maturation enzymes at their wild-type levels in the parental strain are apparently high enough to keep up with processing the increased amounts of the SHI protein. This includes the formation of iron-sulfur clusters as well as assembly and insertion of the [NiFe] site and proteolysis of the catalytic subunit (Fig. 1).

The OE-SHI strain has similar growth properties to the parental strain - P. furiosus grown on maltose produces H_2 as an end product of carbohydrate fermentation and SHI has been proposed to recycle the H_2 for biosynthetic purposes (3). However, the growth of the two strains using maltose as the carbon source was comparable (Fig. 5). Moreover, the amounts of H_2 produced by the two strains and the amounts of maltose consumed throughout the growth phase were also similar (Fig. 5). The dramatically increased amount of SHI in the OE-SHI strain might be expected to lead to an increased uptake of H_2 and perhaps an increase in cell yield. However, it is clear from these data that the growth of *P. furiosus* on the maltose-based medium is not limited by the ability of the organism to recycle H_2.

Affinity purification and characterization of the OE-SHI hydrogenase - The recombinant enzyme containing the strep-tag II (attached to the PF0891 subunit, Fig. 1), was purified from the OE-SHI strain using a strep-tactin column. The cytoplasmic fraction from the OE-SHI cells was applied directly to the column without any initial purification, and to optimize recovery of the hydrogenase, the material that flowed through the column was re-applied to column prior to washing the column with buffer. The hydrogenase was eluted with desthiobiotin as determined by its activity. The OE-SHI enzyme was purified 24-fold by the single affinity step with a 21% recovery of activity (Table 2). Note that this is an underestimate because the S100 fraction also contains hydrogenase II (SHII), which represents about 15% of the total cytoplasmic hydrogenase activity of wild-type cells (39). Approximately 4.2 mg of the OE-SHI enzyme was obtained with a specific activity of 120 units/mg from 25 g (wet weight) of cells of the OE-SHI strain by this one-step purification (Supplemental Fig. S3). A highly homogeneous preparation of the OE-SHI enzyme (Fig. 6) exhibiting a specific activity of 272 units/mg was obtained by including two additional steps of conventional chromatography (Supplemental Table S2), but

this yielded much less protein due to the relatively inefficient binding to the hydrophobic interaction column (Supplemental Table S2). The overall yield of recombinant OE-SHI enzyme after the single affinity step (4.2 mg/25 g of cells, wet weight) is significantly higher than that reported with SHI after four chromatography steps (0.6 mg/25 g of cells, wet weight (25)).

The properties of the hydrogenase purified from the OE-SHI strain were determined and compared with those of the native enzyme purified from biomass of wild type cells (25, 39). The results are summarized in Table 3. The specific activity of the recombinant enzyme was about 50% higher than that of the native enzyme in the standard MV-linked H_2-production assay measured at 80°C. This may be related to the finding that the OE-SHI enzyme was not quite as thermostable as the native form, with a half-time for inactivation of 6 rather than 14 hours at 90°C (Table 3). The thermal stability of OE-SHI was also assessed using the H_2-dependent reduction of NADP, which involves electron transfer by flavin and iron-sulfur centers and may be a more accurate reflection of protein stability. The results were in accord with those obtained using the H_2-evolution assay, with half-life values for OE-SHI and SHI of 5 and 10 hours, respectively, at 90°C (Table 3, Supplemental Fig. S6). The OE-SHI enzyme may therefore be more flexible and dynamic at 90°C compared to the native enzyme and hence more catalytically-active at higher temperatures (Supplemental Fig. S4). The lower thermal stability of OE-SHI at the growth temperature of the organism may also explain why there is no significant increase in H_2 uptake by the OE-SHI strain in comparison to the parental strain (Fig. 5B). Nevertheless, the high stability of the recombinant enzyme was shown by presence of the SDS-resistant and catalytically-active, high-molecular weight band (Fig. 6) that is evident after SDS electrophoresis of the native hydrogenase and represents undenatured holoenyzme (25,40). That the OE-SHI protein was fully folded and contained the full complements of flavin and iron-sulfur clusters

was shown by its ability to use NADPH as the electron donor for H_2 production and H_2 oxidation (Table 3, Supplemental Fig. S6). Furthermore, the tryptophan emission spectrum of both proteins showed the same emission maxima (λ^{max} of 355 nm) with almost the same fluorescence yield (Supplemental Fig. S7), which suggest that both have a similar three dimensional structure. However, both proteins showed little change in their emission spectra even after 16 hr at 90°C, suggesting that the difference in their residual activities after prolonged is not due to gross structural changes.

SHI is predicted to contain 23 iron atoms/heterotetramer together with a single nickel atom (Fig. 1) and the measured ratio for the OE-SHI hydrogenase (27 ± 2.84:1) is slightly higher than that of the native (21 ± 3.23:1, Table 3). However, given the high specific activity of the recombinant enzyme it would seem unlikely that it contains a significant amount of enzyme lacking a [NiFe]-catalytic site. The sensitivity of the OE-SHI enzyme to inactivation by oxygen (air) was also similar to that of the native enzyme with a half-life of about one day (Table 3), indicating that the catalytic sites of the two forms of the enzyme are in virtually identical environments within the protein.

DISCUSSION

The development of a genetic system for *P. furiosus* has important implications for this organism as we now have a tool to manipulate any gene within its genome. In the present study we focused on SHI, one of three hydrogenases of *P. furiosus* (3). Over-expression of the four genes encoding this enzyme, which are arranged in a single operon, led to several unexpected results. First, more than a 7-fold increase in specific hydrogenase activity was observed in the OE-SHI strain but this had little effect on the growth of the organism in closed (non-sparged) cultures, conditions under which H_2 accumulates. In fact, the recombinant strain if anything grew

marginally better than the COM1 parent (Fig. 5 and Supplemental Fig. S5). The physiological effect of an increased amount of SHI is presumably an increase in the amount of NADPH produced, but this is clearly not significant under the growth conditions studied.

We successfully increased the amount of SHI produced by *P. furiosus* generating an enzyme that can be obtained in a highly purified form by a single affinity step. Remarkably, in comparison with other homologous expression systems for [NiFe]-hydrogenases, that of *P. furiosus* represents a 100-fold higher yield of the hydrogenase. For the homologous expression system of *Synechocystis* sp. PCC 6803, a total of 25 g of cells yielded only 0.04 mg of hydrogenase protein, which compares to 4.2 mg from the OE-SHI strain (24). One step affinity purification based on the strep-tag II tag was used to purify both types of recombinant enzyme from their cytoplasmic extracts and in both cases the recovery of activity was approximately 20%. However, there were some important differences between the strategies employed with these two over-expression systems. With *Synechocystis* sp. PCC 6803, a five-fold increase in the production of the hydrogenase was obtained but this also required over-expression of the five *hyp* genes encoding the maturation and accessory proteins. In contrast, no attempt was made to over-express the genes encoding the maturation proteins for *P. furiosus* SHI. In fact, the wild-type expression levels of the genes encoding the protease (*frxA*) that processes the C-terminus of the SHI catalytic subunit and the key processing protein, *hypF* (17,19) were unaffected, even though expression of the SHI operon increased 20-fold. How the hydrogenase maturation process is regulated is not understood but clearly *P. furiosus* can respond to the increased production of SHI to give the fully functional protein with a full complement of cofactors, including the [NiFe]-catalytic site, flavin and multiple [FeS] clusters. However, the slightly lower Fe:Ni ratio in the OE-SHI enzyme compared to the native form (Table 3) suggests that the

limit may have been reached in processing this amount of the catalytic subunit of the OE-SHI enzyme. Consequently, even more OE-SHI might be produced if frxA and/or hypF, and/or one or more the other six processing proteins in *P. furiosus,* are also over-produced, and such studies are planned.

The properties of the recombinant affinity-tagged hydrogenase of *Synechocystis* sp. PCC 6803 were directly compared with that of the unmodified native enzyme since the latter has not been characterized (24). The properties of the purified OE-SHI enzyme from *P. furiosus* were very similar to those of the native enzyme, although recombinant form was slightly more active and also slightly less thermostable, suggesting that the OE-SHI hydrogenase was folded differently, even though the oxygen sensitivity of the two enzymes forms were the same. These differences in stability and activity of the OE-SHI enzyme are presumably the result of the eight amino acid strep-tag II and linker, which interferes with the folding process. The diffrence in thermal stability is also very evident in its H_2 oxidation activity (Supplemental Fig. S6). This has been previously reported using the same affinity tag with the D-arabitol dehydrogenase from the hyperthermophilic bacterium *Thermotoga maritima.* In this case the enzyme was heterologously produced in *E. coli* and the tagless form retained 90% of its original activity after 90 min at 85 °C while the step-tagged version had a half life of only 5 min (41).

The availability a *P. furiosus* strain that over produces the SHI hydrogenase affords many opportunities for those interested in research on such enzymes. For example, it will now be possible to generate site-directed mutants and active forms lacking one or more subunit of SHI (28). In addition, it provides a means to investigate the roles of the accessory genes *hypF* and *frxA* in processing SHI as these are poorly understood. There is also only limited insight into the functions of hyp C, D and E and SlyD in the maturation mechanism (5,19,42). In the engineered

P. furiosus OE-SHI strain, the production of the hydrogenase is under control at the transcriptional level by a strong, constitutive promoter (that for the gene encoding the S-layer protein), which is not known to be down-regulated by conditions that regulate the hydrogenase activity in this organism, such as elemental sulfur (S°) (37). Hence the addition of S° to maltose-grown cells would dramatically down-regulate the expression of *hypF* (PF0559) and *frxA* (PF0975) significantly (37), but production of OE-SHI would not be affected. It should therefore be possible to trap processing intermediates in SHI maturation by simply adding S° to the OE-SHI strain, with and without constitutive expression of one or more the processing genes that would normally be down-regulated by S°. Such an approach might allow the isolation of incompletely processed OE-SHI containing its C-terminal peptide by a single affinity purification step, and permit a study of its [NiFe] site and the nature of the other three subunits of the enzyme and their cofactor contents.

In conclusion, we have successfully over-expressed the heterotetrameric metalloenzyme SHI complex by using a marked knock-in method in order to insert a stronger promoter and an affinity tag for purification purposes. Despite the complex maturation process involved with the [NiFe] active site, the producion of SHI was increased by almost an order of magnitude. This is the first example of the over-production of a thermostable [NiFe]-hydrogenase and provides a method to obtain high amounts of the enzyme necessary for further development of *in vitro* H_2 production systems (15,43).

REFERENCES

1. Vignais, P. M., and Billoud, B. (2007) *Chem. Rev.* **107**, 4206-4272

2. Vignais, P. M., and Colbeau, A. (2004) *Curr. Issues Mol. Biol.* **6**, 159-188

3. Jenney, F. E., Jr., and Adams, M. W. (2008) *Ann. N. Y. Acad. Sci.* **1125**, 252-266

4. Fontecilla-Camps, J. C., Volbeda, A., Cavazza, C., and Nicolet, Y. (2007) *Chem. Rev.* **107**, 4273-4303

5. Pandelia, M. E., Ogata, H., and Lubitz, W.(2010) *Chemphyschem.* **11**, 1127-1140

6. Volbeda, A., Charon, M. H., Piras, C., Hatchikian, E. C., Frey, M., and Fontecilla-Camps, J. C. (1995) *Nature.* **373**, 580-587

7. Volbeda, A., Martin, L., Cavazza, C., Matho, M., Faber, B. W., Roseboom, W., Albracht, S. P., Garcin, E., Rousset, M., and Fontecilla-Camps, J. C. (2005) *J. Biol. Inorg. Chem.* **10**, 239-249

8. Ogata, H., Hirota, S., Nakahara, A., Komori, H., Shibata, N., Kato, T., Kano, K., and Higuchi, Y. (2005) *Structure.* **13**, 1635-1642

9. Marques, M. C., Coelho, R., De Lacey, A. L., Pereira, I. A., and Matias, P. M. (2009) *J. Mol. Biol.* **396**, 893-907

10. Ogata, H., Kellers, P., and Lubitz, W. (2010) *J. Mol. Biol.* **402**, 428-444

11. Lubitz, W., Reijerse, E., and van Gastel, M. (2007) *Chem. Rev.* **107**, 4331-4365

12. Cammack, R., Frey, M., and Robson, R. (2001) *Hydrogen as a fuel : learning from nature*, Taylor & Francis, London ; New York

13. Gupta, R. B. (2009) *Hydrogen fuel : production, transport, and storage*, CRC Press, Boca Raton

14. Lee, H. S., Vermaas, W. F., and Rittmann, B. E. *Trends. Biotechnol.* **28**, 262-271

15. Krassen, H., Schwarze, A., Friedrich, B., Ataka, K., Lenz, O., and Heberle, J. (2009) *ACS Nano.* **3**, 4055-4061

16. English, C. M., Eckert, C., Brown, K., Seibert, M., and King, P. W. (2009) *Dalton Trans.*, 9970-9978

17. Blokesch, M., and Bock, A. (2002) *J. Mol. Biol.* **324**, 287-296

18. Blokesch, M., Albracht, S. P., Matzanke, B. F., Drapal, N. M., Jacobi, A., and Bock, A. (2004) *J. Mol. Biol.* **344**, 155-167

19. Bock, A., King, P. W., Blokesch, M., and Posewitz, M. C. (2006) *Adv. Microb. Physiol.* **51**, 1-71

20. Rousset, M., Magro, V., Forget, N., Guigliarelli, B., Belaich, J. P., and Hatchikian, E. C. (1998) *J. Bacteriol.* **180**, 4982-4986

21. Porthun, A., Bernhard, M., and Friedrich, B. (2002) *Arch. Microbiol.* **177**, 159-166

22. Lenz, O., Gleiche, A., Strack, A., and Friedrich, B. (2005) *J. Bacteriol.* **187**, 6590-6595

23. Sun, J., Hopkins, R. C., Jenney, F. E., McTernan, P. M., and Adams, M. W. (2010) *PLoS One.* **5**, e10526

24. Germer, F., Zebger, I., Saggu, M., Lendzian, F., Schulz, R., and Appel, J. (2009) *J. Biol. Chem.* **284**, 36462-36472

25. Bryant, F. O., and Adams, M. W. (1989) *J. Biol. Chem.* **264**, 5070-5079

26. Zhang, Y. H., Evans, B. R., Mielenz, J. R., Hopkins, R. C., and Adams, M. W. (2007) *PLoS One.* **2**, e456

27. Lipscomb, G. L., Stirrett, K., Schut, G. J., Yang, F., Jenney, F. E., Jr., Scott, R. A., Adams, M. W., and Westpheling, J. (2011) *Appl. Environ. Microbiol.* **77**, 2232-2238

28. Hopkins, R. C., Sun, J., Jenney, F. E., Chandrayan, S., K., McTernan, P. M. and Adams, M. W. W. (2011) *PLOS One.* (*In press*)

29. Verhagen, M. F., Menon, A. L., Schut, G. J., and Adams, M. W. (2001) *Methods Enzymol.* **330**, 25-30

30. Horton, R. M., Hunt, H. D., Ho, S. N., Pullen, J. K., and Pease, L. R. (1989) *Gene.* **77**, 61-68

31. Maier, T., Drapal, N., Thanbichler, M., and Bock, A. (1998) *Anal Biochem* **259**, 68-73

32. Sambrook, J., and Russell, D. W. (2001) *Molecular cloning: a laboratory manual*, 3rd ed., Cold Spring Harbor Laboratory Press, Cold Spring Harbor, N.Y.

33. Bradford, M. M. (1976) *Anal. Biochem.* **72**, 248-254

34. Silva, P. J., van den Ban, E. C., Wassink, H., Haaker, H., de Castro, B., Robb, F. T., and Hagen, W. R. (2000) *Eur. J. Biochem.* **267**, 6541-6551

35. Ma, K., Zhao, Z. H., and Adams, M. W. W. (1994) FEMS Micro. letters.. **122**, 245-250

36. Cvetkovic, A., Menon, A. L., Thorgersen, M. P., Scott, J. W., Poole, F. L., 2nd, Jenney, F. E., Jr., Lancaster, W. A., Praissman, J. L., Shanmukh, S., Vaccaro, B. J., Trauger, S. A., Kalisiak, E., Apon, J. V., Siuzdak, G., Yannone, S. M., Tainer, J. A., and Adams, M. W.(2010) *Nature.* **466**, 779-782

37. Lee, H. S., Shockley, K. R., Schut, G. J., Conners, S. B., Montero, C. I., Johnson, M. R., Chou, C. J., Bridger, S. L., Wigner, N., Brehm, S. D., Jenney, F. E., Jr., Comfort, D. A., Kelly, R. M., and Adams, M. W. (2006) *J. Bacteriol.* **188**, 2115-2125

38. Schut, G. J., Bridger, S. L., and Adams, M. W. (2007) *J. Bacteriol.* **189**, 4431-4441

39. Ma, K., Weiss, R., and Adams, M. W. (2000) *J. Bacteriol.* **182**, 1864-1871

40. Mukherjee, S., Sharma, S., Kumar, S., and Guptasarma, P. (2005) *Anal. Biochem.* **347**, 49-59

41. Kallnik, V., Schulz, C., Schweiger, P., and Deppenmeier, U. (2011) *Appl. Microbiol. Biotechnol.* **90**, 1285-1293

42. Forzi, L., and Sawers, R. G. (2007) *Biometals.* **20**, 565-578

43. Zhang, Y. H., Sun, J., and Zhong, J. J. (2010) *Curr. Opin. Biotechnol.* **21**, 663-669

TABLE 2.1. Properties of *P. furiosus* strains used in this study. COM1 is the parent strain that was engineered to generate the OE-SHI strain to over-produce the SHI enzyme.

Strain Designation	Genotype	Deleted or Inserted ORF/Elements	Source
COM1	Δ*pyrF*	PF1114	Ref . 27
OE-SHI	P_{slp}*Strep-tagII-shIβγδα*	P_{slp}*Strep-tagII*	This study

TABLE 2.2. One-step purification of the over-produced affinity-tagged OE-SHI enzyme. The cytoplasmic extract from cells of the OE-SHI strain was purified using a Strep-Tactin affinity column. Hydrogenase activity was measured by H_2 production from reduced methyl viologen, where U is one unit of activity.

Step	Units (U)	Protein (mg)	Specific Activity ($U.mg^{-1}$)	Yield (%)	Fold Purification
S100	2536	468	5.4	100	1
Strep-Tactin	530	4.2	126	21	24

TABLE 2.3. Properties of affinity-tagged SHI purified from the OE-SHI strain and SHI purified from native biomass.

Property	OE-SHI	SHI
MV-linked specific activity ($U.mg^{-1}$)	272	190
NADPH linked specific activity ($U.mg^{-1}$)	2.0	1.5
Half-life ($t_{1/2}$, hr) at 90° C under argon (H_2 evolution)	6.0	14
Half-life ($t_{1/2}$, hr) at 25° C under air (H_2 evolution)	25	21
Half-life ($t_{1/2}$, hr) at 90°C under argon (H_2 oxidation)	5.0	10
Fe:Ni ratio	27:1	21:1

FIGURE 2.1

Model of affinity-tagged SHI showing subunit and cofactor content. The Strep-tag II is located at the N-terminus of PF0891. Adapted from ref. (25)

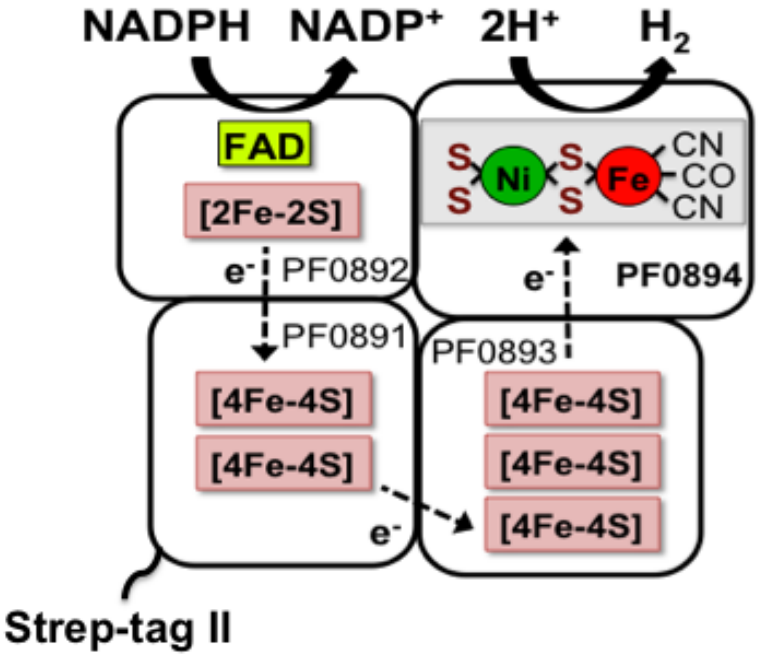
NADPH
NADP+
2H+
H2
FAD
[2Fe-2S]
e-
PF0892
PF0891
[4Fe-4S]
[4Fe-4S]
e-
Strep-tag II
S
S
Ni
S
S
Fe
CN
CO
CN
e-
PF0894
PF0893
[4Fe-4S]
[4Fe-4S]
[4Fe-4S]

FIGURE 2.2

Marked knock-in strategy to modify the operon (PF0891-0894) encoding SHI. A schematic representation of the knock-in cassette is presented. The abbreviations are: UFR, upstream flanking region; P*gdh-pyrF*, marker driven by the promoter for the glutamate dehydrogenase gene; P_{slp}-*strep-tagII:* S-Layer promoter with codon-optimized 8-amino acid strep tagII sequence; DFR, downstream flanking region.

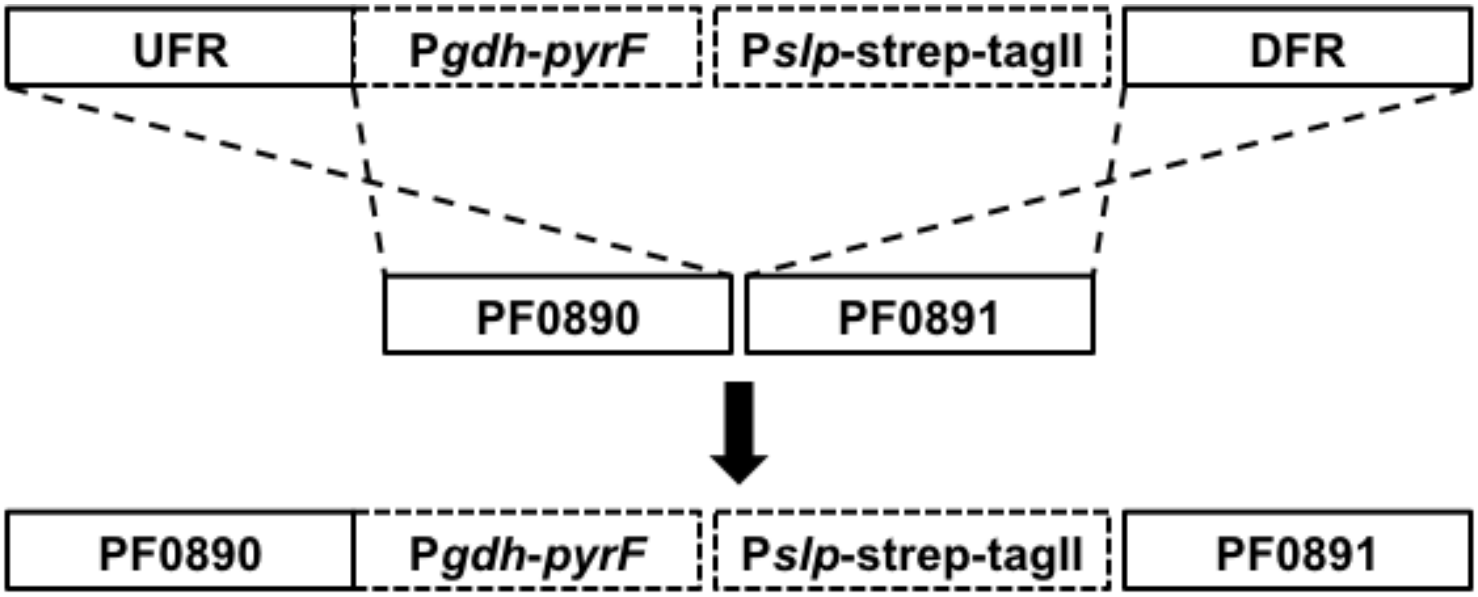
UFR
Pgdh-pyrF
Pslp-strep-tagII
DFR
PF0890
PF0891
PF0890
Pgdh-pyrF
Pslp-strep-tagII
PF0891

FIGURE 2.3

Increased catalytic activity and amount of catalytic subunit of SHI in the OE-SHI strain. The bar graph compares the MV-linked hydrogenase activity in cytoplasmic extracts (S100) of the parent COM1 and OE-SHI strains. Error bars represent standard deviations obtained from three independent experiments. The corresponding immunoanalysis of the extracts is shown below using anti-PF0894 (catalytic subunit, see Figure 1) with anti-PF1281 (superoxide reductase) as the internal loading control.

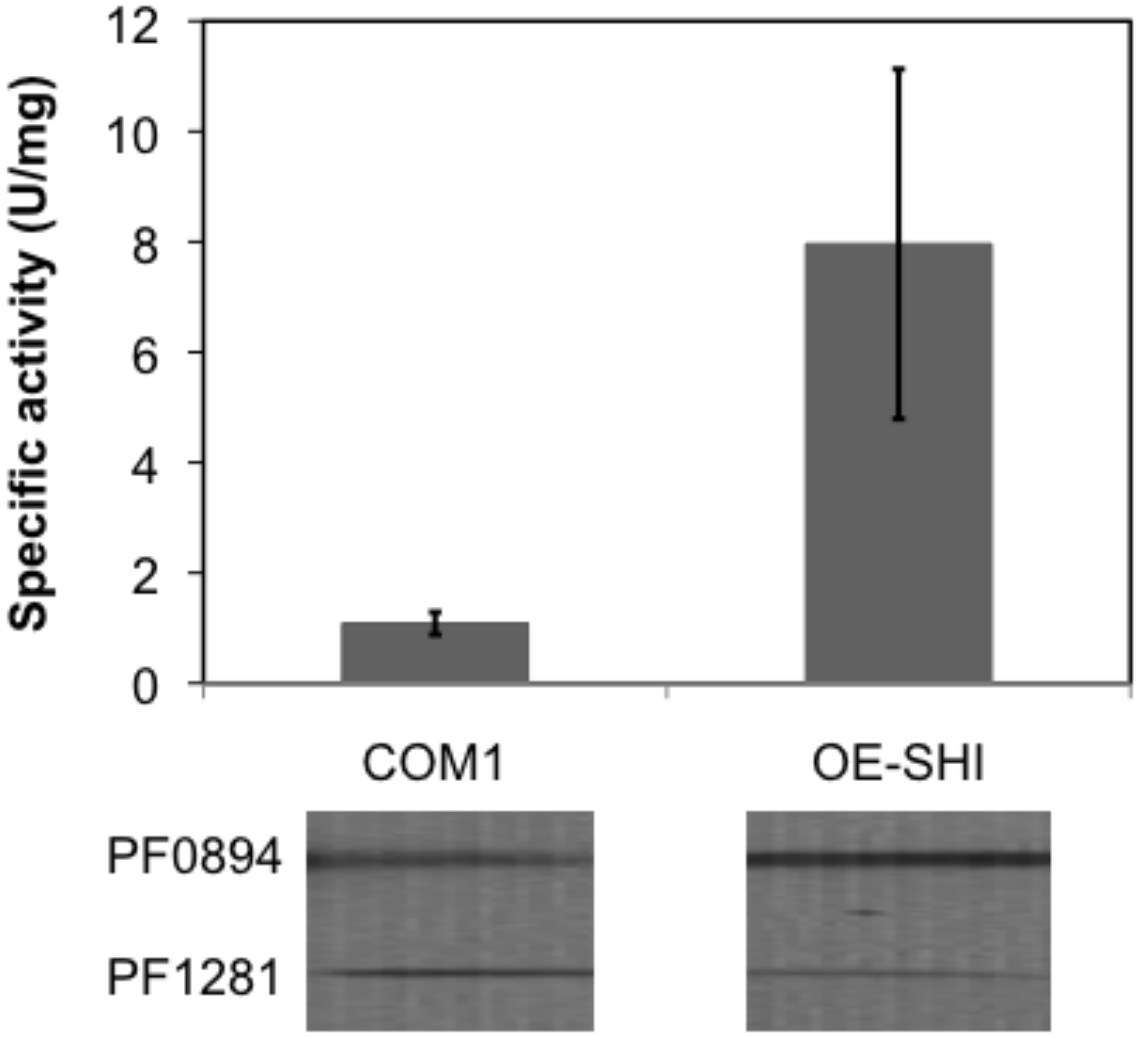
Specific activity (U/mg)
12
10
8
6
4
2
0
COM1
OE-SHI
PF0894
PF1281

FIGURE 2.4

Relative mRNA abundance in the OE-SHI and COM1 strains. The relative levels were determined by qPCR of the **mRNA encoding PF0894 (the catalytic subunit of SHI)**, PF0975 (frxA), and PF0559 (hypF). The error bars represent standard deviations obtained using triplicate independent samples.

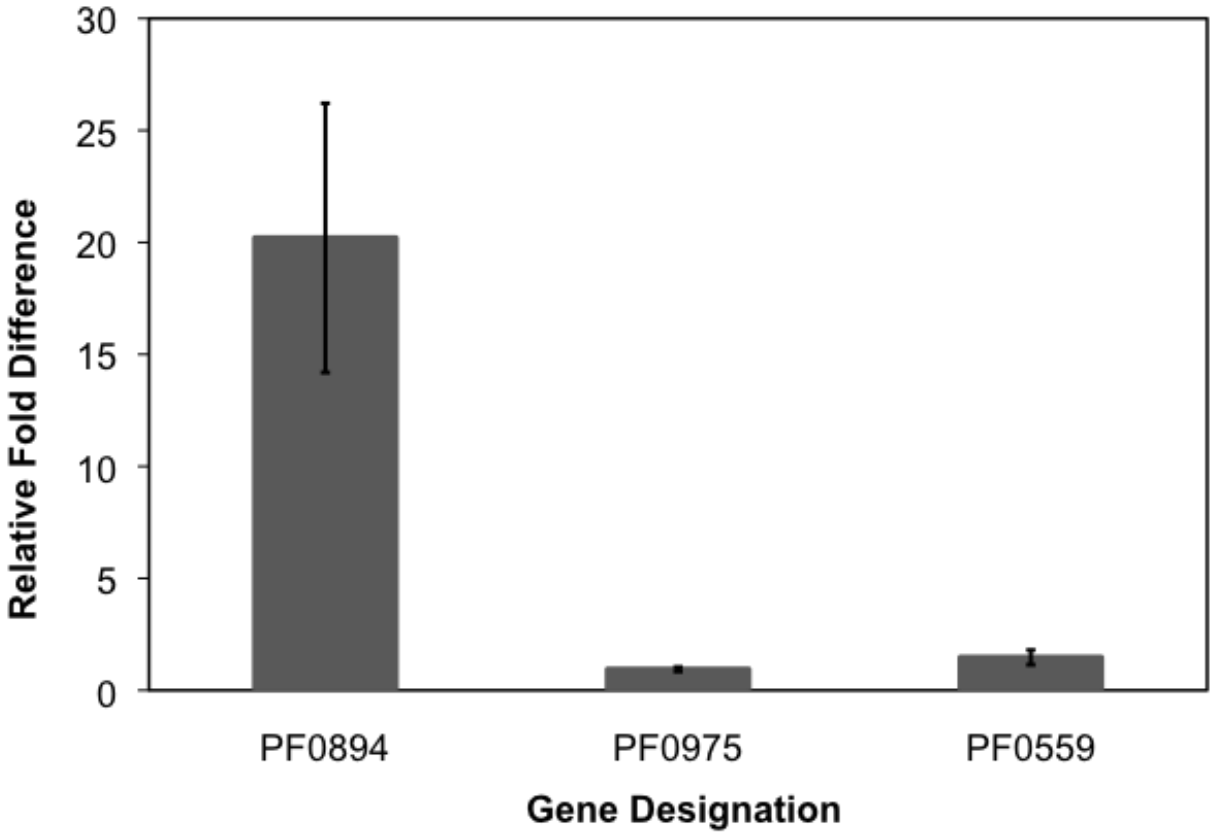
30
25
20
15
10
5
0
Relative Fold Difference
PF0894
PF0975
PF0559
Gene Designation

FIGURE 2.5

Comparison of growth and H_2 production and maltose consumption by the OE-SHI and COM1 strains.

A) Growth of the two strains using maltose as the carbon source and consumption of maltose during growth in closed bottles at 95°C. B) Corresponding production of H_2 during growth. The error bars represent standard deviation obtained from three independent samples.

A

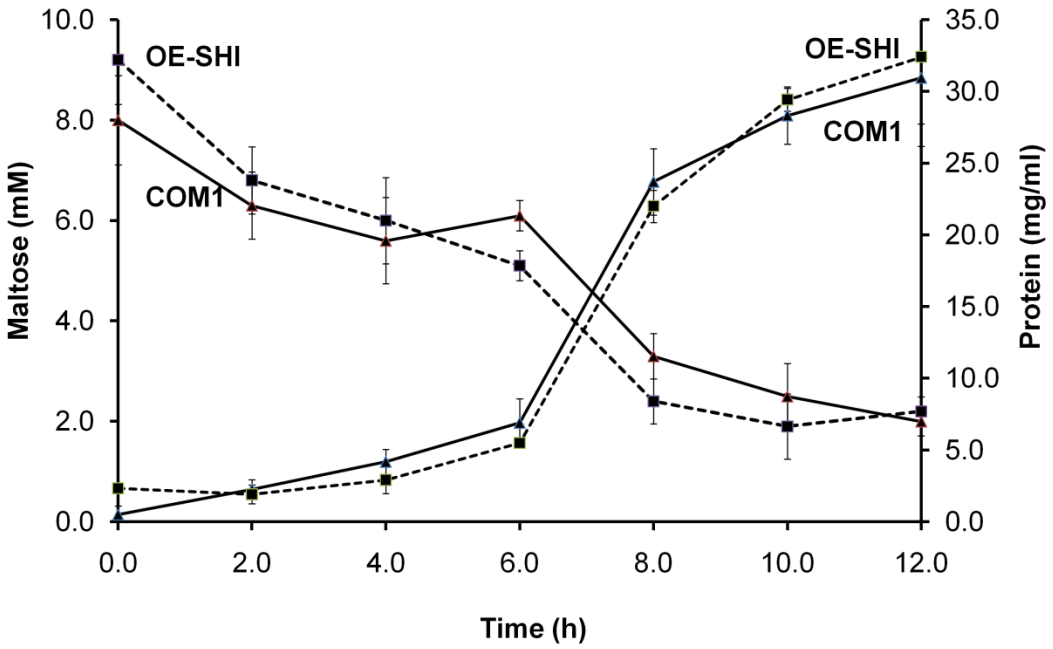
10.0
8.0
6.0
4.0
2.0
0.0
Maltose (mM)
35.0
30.0
25.0
20.0
15.0
10.0
5.0
0.0
Protein (mg/ml)
OE-SHI
COM1
OE-SHI
COM1
0.0
2.0
4.0
6.0
8.0
10.0
12.0
Time (h)

B

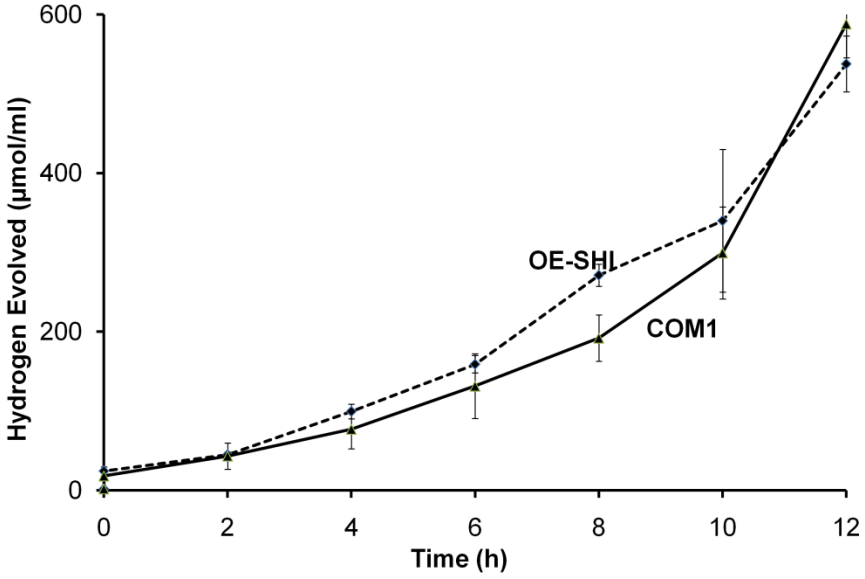
600
400
200
0
Hydrogen Evolved (µmol/ml)
OE-SHI
COM1
0
2
4
6
8
10
12
Time (h)

FIGURE 2.6

Electrophoretic analysis of the OE-SHI hydrogenase. The purified enzyme was analyzed by conventional SDS-PAGE except that the protein was incubated with the SDS-loading buffer for 10 min (lane 1) or for 60 min (lane 3) prior to electrophoresis. Native SHI (treated for 10 min) is shown in lane 2. The arrow indicates the high molecular catalytically-active protein band seen in lanes 1 and 2 (see ref. (25)). The center lane (M) contains the protein molecular weight ladder (Invitrogen) with corresponding masses as indicated in kDa.

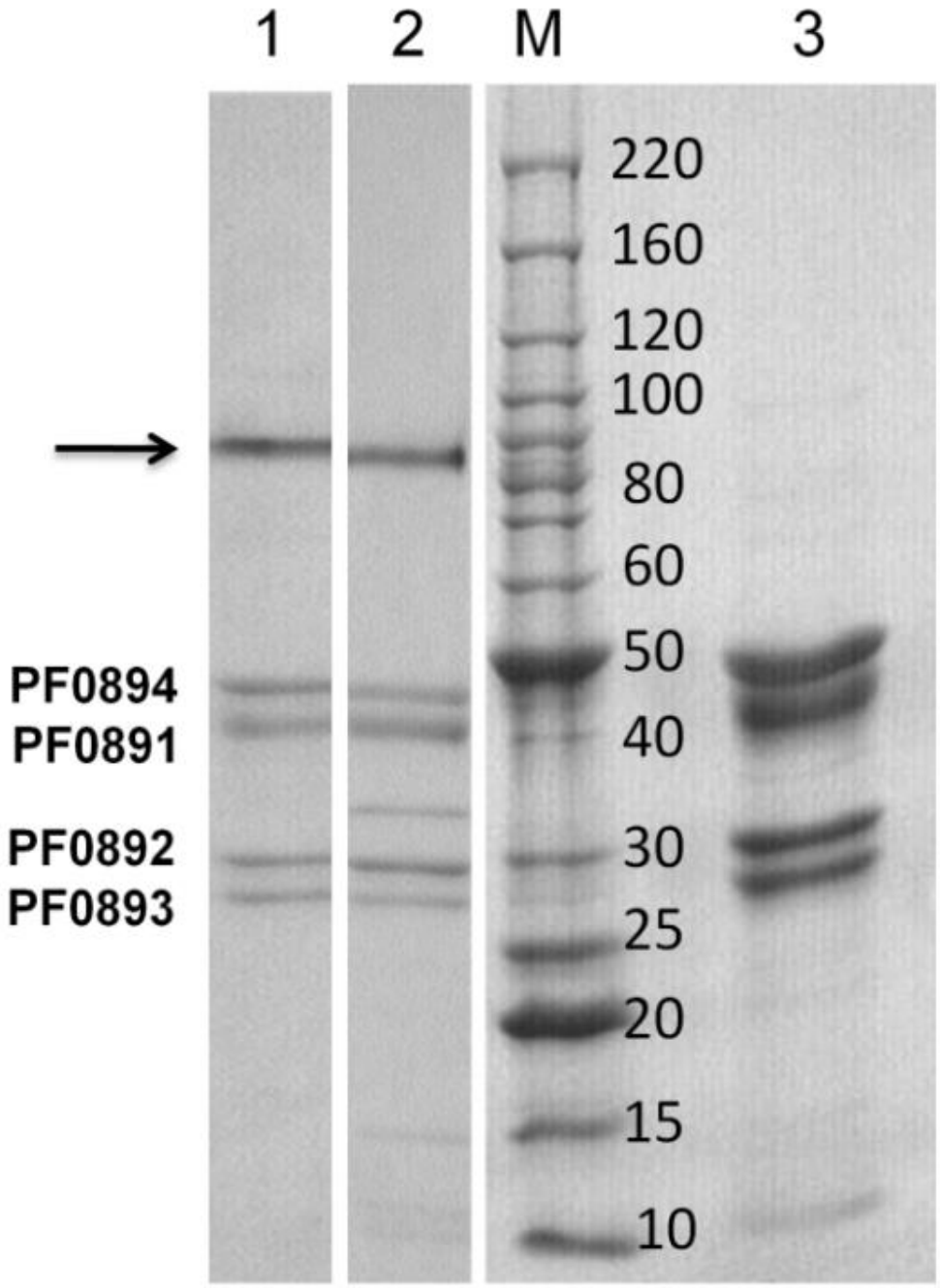
1
2
M
3
220
160
120
100
80
60
50
40
30
25
20
15
10
PF0894
PF0891
PF0892
PF0893

CHAPTER 3

INTACT FUNCTIONAL FOURTEEN-SUBUNIT RESPIRATORY MEMBRANE BOUND [NIFE]-HYDROGENASE COMPLEX OF THE HYPERTHERMOPHILIC ARCHAEON *PYROCOCCUS FURIOSUS*[1]

---

[1]McTernan PM, Chandrayan SK, Wu C-H, Vaccaro BJ, Lancaster WA, et al. 2014. Journal of Biological Chemistry 289:19364-19372. Reprinted here with permission of the publisher.

ABSTRACT

The archaeon *Pyrococcus furiosus* grows optimally at 100 degrees C by converting carbohydrates to acetate, CO_2 and H_2, obtaining energy from a respiratory membrane-bound hydrogenase (MBH). This conserves energy by coupling H_2 production to oxidation of reduced ferredoxin with generation of a sodium ion gradient. MBH is encoded by a 14-gene operon with both hydrogenase and Na^+/H^+ antiporter modules. Herein a His-tagged MBH was expressed in *P. furiosus* and the detergent-solubilized complex purified under anaerobic conditions by affinity chromatography. Purified MBH contains all 14 subunits by electrophoretic analysis (13 subunits were also identified by mass spectrometry) and had a measured Fe:Ni ratio of 15:1, resembling the predicted value of 13:1. The as-purified enzyme exhibited a rhombic EPR signal characteristic of the ready Ni-B state. The purified and membrane bound forms of MBH both preferentially evolved H_2 with the physiological donor (reduced ferredoxin) as well as with standard dyes. The O_2 sensitivities of the two forms were similar (half-lives of ~15 hr in air), but the purified enzyme was more thermolabile (half-lives at 90 degrees C of 1 hr and 25 hr, respectively). Structural analysis of purified MBH by small angle x-ray scattering (SAXS) indicated a Z-shaped structure with a mass of 310 kDa, resembling the predicted value (298 kDa). The SAXS analyses reinforce and extend the conserved sequence relationships of group 4 enzymes and Complex I (NADH quinone oxidoreductase). This is the first report on the properties of a solubilized form of an intact respiratory MBH complex that is proposed to evolve H_2 and pump Na^+ ions.

INTRODUCTION

Over the past decade there has been a major initiative to generate alternative non-fossil fuels to fulfill increasingly critical energy needs. Yet, such fuels must be energy efficient as well as carbon neutral, and biohydrogen production can meet these criteria (1). Hydrogen is metabolized by microbes from all three domains of life (2). Notably, they all contain the enzyme hydrogenase that functions to catalyze the reversible reduction of protons to molecular hydrogen (H_2). Hydrogenases are classified based on the metal content of their active site into the [NiFe]-hydrogenase, [FeFe]-hydrogenase, and the [FeS]-cluster free hydrogenases. The [NiFe]-hydrogenases are ubiquitous in the microbial world and have been extensively studied from numerous mesophilic bacteria (3-5). The minimum structure is a heterodimer composed of a large and small subunit. The large subunit contains the [NiFe] catalytic site that is coordinated by the sulfur atoms of four cysteine residues organized into two –CxxC– motifs near the N- and C-termini. The [NiFe] active site has been extensively studied by electron paramagnetic resonance (EPR) spectroscopy (6). The small subunit typically contains three iron-sulfur clusters invariably of the [4Fe-4S] type that shuttle electrons between an acceptor/donor for the enzyme and its active site. [NiFe]-hydrogenases are classified into four groups based on the phylogeny of their catalytic subunits (2). Crystal structures for [NiFe]-hydrogenases are available for group 1 hydrogenases (7,8), but no structural information is available for the other three hydrogenase groups.

The least studied of the [NiFe]-hydrogenases fall into group 4, and these are defined as the H_2-evolving energy-conserving membrane-associated hydrogenases (2). These group 4 enzymes show little sequence similarity to other [NiFe]-hydrogenases, except for the conserved residues that bind the [NiFe] catalytic site and its proximal [4Fe-4S] cluster (9,10), indicating a

distinct evolutionary history (11). Group 4 hydrogenases play an important role in conserving energy by establishing ion gradients across membranes that can be used to generate adenosine triphosphate (ATP). These enzymes are much more complex than the characterized dimeric hydrogenases and contain at least six subunits. The simplest members include the 7-subunit hydrogenase 3 from *Escherichia coli*, which oxidizes formate and evolves H_2 (12,13), the 8-subunit CO-induced hydrogenase of some CO-oxidizing bacteria that conserve energy from coupling the oxidation of CO to H_2 production (10,14), and the 6-subunit 'energy-conserving' hydrogenase (Ech) from the archaeon *Methanosarcina barkeri,* which functions in methanogenesis (15,16). More complex members of the group 4 enzymes include the 18-subunit formate hydrogen lyase (FHL) system from *Thermococcus onnurineus* (17), which oxidizes formate and evolves hydrogen (80^0C). Six subunits conserved within the group 4 hydrogenases are homologous to six subunits found in the catalytic core of the ubiquitous aerobic respiratory complex NADH quinone oxidoreductase or Complex I (*NuoBCDIHL*: (9-11,18)). This conserved six subunit homology suggests a close evolutionary history between group 4 enzymes and Complex I and shows the importance of the hydrogenases in respiratory processes. However, due to the inherent difficulty of purifying and characterizing large, multi-subunit membrane complexes, little is known about their structure and function (16,19,20).

Hyperthermophilic archaea such as *Pyrococcus furiosus,* which grows optimally at 100°C (21), contain a complex hydrogenase system (11). *P. furiosus* grows by fermenting sugars to acetate, CO_2 and H_2 and its membrane bound hydrogenase (MBH) catalyzes H_2 production using reduced ferredoxin (Fd) generated from sugar oxidation, as the electron donor (11). Previous studies of *P. furiosus* MBH showed that it is encoded by a 14-gene operon (*mbhA-N*: PF1423-PF1436; Fig. 1*;* (22)). Six of the last seven genes in the operon are homologous to those

encoding the "core" subunits of Complex I (*mbhH,J-N*, Fig. 1) while the other eight subunits (*mbhA-H*) are homologous to subunits of the Mrp monovalent cation/proton antiporter of some mesophilic bacteria (23). *MbhI* does not have homology to either Complex I subunits or the Mrp subunits, but *MbhH* has homology to both. Mrp catalyzes the efflux of monovalent cations, such as Na^+, K^+, and Li^+ outward in a coupled reaction that transports protons inwards. Of the 14 subunits of MBH, only *mbhJKLN* are predicted not to encode transmembrane helices (22,24). MbhJ and MbhN are proposed to contain one and two [4Fe-4S] clusters, respectively, where MbhJ is the equivalent of the small subunit of the group 1 dimeric [NiFe]-hydrogenases (Fig. 1). MbhKL are the equivalent to the large subunit and contain the [NiFe] active site, with the four Cys residues provided by MbhL.

The respiratory function of MBH was demonstrated by adding reduced ferredoxin to inverted membrane vesicles of *P. furiosus*, whereby H_2, ATP and an electrochemical gradient were formed (25). Inhibition studies established that MBH evolved H_2 while a membrane bound ATP synthase produced ATP. The much lower reduction potential of ferredoxin (-454 mV (26)) compared to NADH (-320 mV) makes ferredoxin a more thermodynamically favorable electron donor for H_2 production, and allows energy to be conserved by a respiratory mechanism (25). Since *P. furiosus* ATP synthase uses Na^+ ions rather than protons (27), and the MBH complex encodes a Na^+/H^+ antiporter (Mrp), it is thought that the hydrogenase module of MBH evolves H_2 and generates a proton gradient, while the Mrp module transforms it into a Na^+ gradient that in turn drives ATP synthesis via ATP synthase (11). Interestingly, MBH in isolated *P. furiosus* membranes is almost exclusively unidirectional in favor of H_2 production in standard *in vitro* assays (24). This is remarkable as other [NiFe]-hydrogenases preferentially catalyze H_2 oxidation, usually by orders of magnitude (2).

This work defines biochemical and structural information on the solubilized and intact 14-subunit MBH complex of *P. furiosus*. We employed the recent development of genetic tools in this organism (28) that have enabled, for example, its cytoplasmic [NiFe]-hydrogenase to be affinity-labeled, overexpressed and purified by affinity chromatography (29,30). Herein we demonstrate that the same strategy can be applied to the MBH complex and show that the purification efficiency depends on the location of the affinity tag on the complex. This is the first report of the affinity purification and characterization of an entire respiratory system from an archaeon as a single intact complex.

METHODS

Generation of P. furiosus strains expressing affinity tagged MBH -A competent strain of *P. furiosus* (COM1) was used to manipulate the MBH operon (28). A one-step marked knock-in genetic protocol was used in which a polyhistidine (His_9) affinity tag was inserted at the C-terminus of the last gene in the operon (*mbhN*, PF1436) yielding strain MW0403 (Fig. 2*A*), or within the operon at the N-terminus of *mbhJ* (PF1432) yielding strain MW0414 (Fig. 2*B*). The knock-in cassette, which contains the selectable marker and the strong constitutive promoter of the gene encoding the S-layer protein (P_{slp}) with an in frame His_9 tag, were generated by using overlapping PCR (31) and Prime Star HS polymerase premix (Clonetech, USA) was used to make the knock-in cassette. *PyrF* was the selectable marker and was placed under the control of the glutamate dehydrogenase promoter (P_{gdh}). In strain MW0403, expression of the MBH operon was controlled by the native *mbh* promoter, while in strain MW0414, the expression of *mbhJ* and the subsequent five genes (*mbhK-N*) was under control of P_{slp}. Generation of MW0414 required the marker cassette to be placed in front of *mbhJ* within the MBH operon (Fig. 2*B*). Expression of MBH, where *mbhN* was tagged, was under control of the native *mbh* promoter and the tag was

placed at the C-terminus of the operon (Fig. 2*A*). All transformants were PCR screened for correct insertion and the PCR product was sequenced (Macrogen, MD).

Membrane preparation-Cells were lysed using 50 mM EPPS (4-(2-Hydroxyethyl)-1-piperazinepropanesulfonic acid; Sigma-Aldrich, USA), pH 8.0, containing 50 μg/ml Deoxyribonuclease I (DNase I; Sigma-Aldrich, USA), and 2 mM dithiothreitol (DTT; Inalco, Italy) in a 5:1 ratio of buffer to cells in an anaerobic chamber (Coy, MI). After 2 hr incubation at 23°C, cells were passed twice through a French press at a pressure of 1000 psi. The cell lysate was then centrifuged in a Beckman-Coulter Optima L-90K ultracentrifuge at 100,000 x g for 1 hr. The supernatant was removed and the membrane pellet was re-suspended in wash buffer (50 mM EPPS, pH 8.0, containing 5 mM $MgCl_2$, 50 mM NaCl, 10% (v/v) glycerol (all obtained from J.T. Baker), 2 mM DTT & 0.1 mM phenylmethylsulfonyl fluoride (PMSF). The membrane pellet was homogenized using 15 ml Pyrex tissue grinders (Pyrex, USA) and the pellet was collected by ultracentrifugation. The washing procedure was repeated twice more, and the pellet was resuspended in 50 mM Tris-HCl (tris(hydroxymethyl)aminomethane (Sigma, USA), pH 8.0, 5 mM $MgCl_2$, 50 mM NaCl, 5% (v/v) glycerol, 2 mM DTT and 0.1 mM PMSF (resuspension buffer).

Membrane solubilization by different detergents -The detergents tested to solubilize MBH were Cymol, Fos-Choline, sodium deoxycholate, N-dodecyl-β-D-maltoside (Affymetrix, USA), Triton-X 114, Triton-X 100 (Bio-Rad, USA). For Cymol, Fos-Choline, Triton-X 114, Triton-X 100 and N-dodecyl-β-D-maltoside, the detergent was added to a final concentration of 2% (w/v) to washed membranes (6 mg detergent/mg membrane protein) and the suspension was incubated for 16 hr at 40^0C. The same procedure was used for sodium deoxycholate except that the

incubation time was 2 hrs. Concentrations of 5, 10 and 20% (w/v) Triton-X 100 were used and incubations were carried out at both 4 and 40^0C.

Affinity Purification of MBH-All purification steps were carried out anaerobically using a Coy anaerobic chamber (Coy laboratories; Michigan, USA). Triton-X 100 (10%, w/v) was incubated with washed membranes (30 mg detergent/mg membrane protein) for 16 hr at 4^0 C. The sample was centrifuged in a Beckman-Coulter Optima L-90K ultracentrifuge at 100,000 x g for 1 hr. The supernatant was collected, diluted to twice the volume with buffer A (50 mM Tris-HCL, pH 8.0, containing 400 mM NaCl, 0.1% (w/v) Triton X-100 and 4 mM DTT) and applied to a 5 ml FF His-Trap Ni-NTA column (GE Healthcare, USA). The column was washed with buffer A and the bound protein was eluted with a 20-column volume gradient from 100% buffer A to 100% buffer B (buffer A containing 500 mM imidazole).

Superose 6 analysis for determination of MBH molecular weight-The molecular weight of the purified MBH sample was analyzed using a calibrated 24 ml Superose 6 30/100 column (GE Healthcare, USA) equilibrated in buffer C (50 mM Tris-HCL, pH 8.0, containing 300 mM NaCl, 0.02% (w/v) Triton X-100 and 2 mM sodium dithionite (DT)). MBH purified from the superose 6 column was used for the SDS-PAGE gel analysis.

SAXS Data -Small angle X-ray scattering was collected at the SIBYLS beamline at the Advanced Light Source (Berkeley, CA) as described (32,33). The sample was buffer exchanged using an Amicon Ultra centrifugal concentrator (Millipore, USA) in buffer containing 50 mM Tris, pH 8.0, 400 mM NaCl, 0.02% (w/v) Triton-X 100 and 4 mM DTT. Thus Triton-X concentration was below the critical micelle concentration. A sample was collected both before and after buffer equilibration. Subtraction of either buffer sample yielded identical results to within experimental error (~1% of signal). For anaerobic data collection, samples were handled in a positive pressure

helium box (containing less than 0.01% O_2). MBH was prepared at 5.0, 3.3, and 1.6 mg/ml Resulting samples were exposed for 0.5, 0.5, 2 and 4 s for data collection. Minor concentration dependence was observed and corrected for by extrapolating to zero concentration. The MBH samples were placed 1.5 m from a MAR165 CCD detector arranged co-axial with the 12 keV monochromatic beam; 10^{12} photons/second were impingent on the sample. The spot size at the sample was 4 × 1 mm convergent to a 100 μm spot at the detector. Buffer subtraction and raw image data were integrated by beamline software specific for this arrangement (33). Scattering data were plotted on log of X-ray intensity scale vs momentum transfer (q) in inverse Å where $q = (4 \pi \sin(\theta/2))/\lambda$ and θ is the scattering angle relative to the incident beam and λ is the wavelength. Processing of SAXS data was conducted utilizing the Scatter package. GNOM was utilized to extract the P(r) function (34).

The scattering profile used to calculate the pair distribution function and subsequently in GASBOR (35) was a merged profile combining all four exposures from all concentrations. The two 0.5 second exposures for each concentration were referenced against one another to check for radiation damage. As none was observed the two exposures were averaged. The longer exposures were used to reduce noise in the high q region. Once each individual concentration had been merged, the three concentrations were used to apply a concentration dependent correction. Ten GASBOR calculations generated ten models from the scattering curve which were averaged and filtered together using the GASBOR associated package DAMAVER. The DAMAVER reported normalized spatial discrepancy (NSD) which measures agreement between models was 2.1. The individual models are shown in Supplementary Material and all support an elongated and asymmetric molecule (supplemental Table S1, supplemental Fig. S1-3).

Other Methods-Hydrogenase assays were performed at 80^0 C and H_2 was measured using an Agilent Technologies 6850 gas chromatograph. H_2 evolution activity was determined using dithionite-reduced methyl viologen (MV; Sigma-Aldrich, USA) as the electron donor (29) or *P. furiosus* ferredoxin reduced by *P. furiosus* pyruvate ferredoxin oxidoreductase (POR). The POR-linked assay contained 100 mM EPPS pH 8.4, 10 mM Na-pyruvate, 0.2 mM coenzyme A, 0.4 mM TPP, 2 mM $MgCl_2$, and 2 mM DTT, POR (30 μg/ml) and ferredoxin (100 μg/ml). Methyl viologen was used as the electron acceptor in the hydrogen oxidation assays. Oxygen sensitivity assays were carried out by exposing the MBH sample (100 μg/ml) in buffer containing 50 mM Tris, pH 8.0, 400 mM NaCl and 4 mM DTT, to air while shaking (30 rpm) and samples were taken at 0, 2, 4, 8, 16 and 32 hr to determine residual hydrogenase activity. Thermal stability at 90^0C was carried out in the same fashion except that the samples were maintained under anaerobic conditions.

Purified MBH complexes were analyzed by electrophoresis using 4-12% Bis-Tris NUPAGE gels (Invitrogen, USA) and 4-20% Tris-Glycine NUSEP gels (Bio-Rad, USA). Bands were cut from the SDS-PAGE gel and were analyzed by MALDI-TOF. Purified MBH was also digested in solution with trypsin overnight and identified using 2D LC-MS/MS. Nickel and iron were measured using a octopole-based ICP-MS (7500ce Agilent Technologies, Tokyo, Japan)), equipped with a MicorMist nebulizer (36). X-band (~9.6 GHz) electron paramagnetic resonance (EPR) spectroscopy was carried out using a Bruker ESP-300E EPR spectrometer equipped with an ER-4116 dual-mode cavity and an Oxford Instruments ESR-9 flow cryostat.

RESULTS

Construction of affinity-tagged MBH- As shown in Fig. 1, the subunits encoded by the first 8 genes of the MBH operon, together with *mbhI* and *mbhM*, are predicted to be membrane

bound, and therefore these were not considered as targets for affinity tagging. On the other hand, *mbhJKLN* are not predicted to encode transmembrane helices and are thought to be located on the cytoplasmic side of the membrane complex (22). The His_9-affinity tag was inserted either at the C-terminus of the subunit encoded by *mbhN*, which is the last gene in the operon, or at the N-terminus of the subunit encoded by *mbhJ*. The forms of MBH that were generated were designated *N*-MBH (in *P. furiosus* strain MW0403) and *J*-MBH (MW0414), respectively. The His_9 tag was chosen as it has been successfully used to purify a form of the cytoplasmic [NiFe]-hydrogenase from *P. furiosus* (30), suggesting that the tag is unlikely to interfere with synthesis of the [NiFe]-catalytic site of MBH. The recombinant strains generated in this study are summarized in Table 1 and the strategy for constructing *N*-MBH and *J*-MBH is shown in Fig. 2.

Affinity purification of MBH-Previous attempts to solubilize MBH from the membrane were carried out using the detergents dodecyl-β-D-maltoside (DDM) and sodium deoxycholate (22,24). However, DDM was not pursued since at higher concentrations it is not compatible with the Ni-NTA affinity purification step, and was not successful previously in purifying the intact complex. Sodium deoxycholate (2%, w/v) efficiently solubilized MBH but incubation for more than 2 hours led to deactivation of the enzyme (24). Cymol, Fos-Choline and Triton-X 114 were not as efficient as Triton-X 100 at solubilizing MBH as measured by recovery of hydrogenase activity (H_2-production from reduced MV) using 2% (w/v) final detergent concentration (data not shown). Since Triton X-100 is compatible with the Ni-NTA affinity step and was used to successfully purify the ATP synthase from *P. furiosus* (37), it was investigated over the concentration range of 5 - 20% (w/v) at both 4 and 40°C. From this analysis, it was determined that 10% (w/v) Triton-X 100 at 4°C (using 3 mg/ml protein) gave ≥ 90% recovery of the hydrogenase activity in a solubilized form of both *N*-MBH and *J*-MBH. The affinity purification

step was carried out under anaerobic conditions but the placement of the His_9-tag clearly affected the efficiency of purification. The *J*-MBH form yielded ~3 mg of MBH per 50 grams of cells (wet weight) with a yield of activity of 27% (Table 2). In contrast, the yield with *N*-MBH was only 2% with ≤ 1 mg of protein (data not shown). Hence, placing the affinity tag on the N-terminus of the "small" subunit (MbhJ) of this MBH is much more efficient in terms of purification than tagging MbhN. *J*-MBH was therefore utilized for all of the characterization studies described below and it will be referred to as purified or solubilized MBH.

Characterization of purified MBH-The purified MBH obtained from affinity purification was analyzed by SDS-PAGE (Fig. 3). Protein bands consistent with the calculated molecular weights from deduced amino acids sequences were observed for all fourteen subunits. Note that the proposed catalytic subunit, MbhL (calculated MWt of 47,903 Da), undergoes C-terminal proteolysis during the processing of the [NiFe]-site, where 47 amino acids are removed, and the calculated size of the mature subunit is 42,899 Da. Thirteen of fourteen MBH subunits were identified both by cutting protein bands from the SDS gel and by using in-solution trypsin digestion followed by LC-MS/MS. MbhJKL was identified by MALDI-TOF analysis from bands cut from the SDS-PAGE gel. The rest of the subunits (including MbhJKL) were identified by LC-MS/MS analysis of in-solution digested samples (supplemental Table S2). MbhD was the only subunit not identified by the LC-MS/MS or MALDI-TOF analyses. This is a small hydrophobic protein (10,412 Da) that is likely resistant to trypsin digestion. A contaminant protein band was observed around the 47 kDa position of the gel and was identified as elongation factor 1-alpha (EF1-α; PF1375; Fig 3).

Purified MBH was also analyzed using a calibrated Superose 6 gel filtration column and gave rise to a single protein peak corresponding to a mass of 310 ± 11 kDa (supplemental Fig.

S4). The predicted mass of the entire MBH complex calculated from the deduced amino acid sequences is 298 kDa. These results indicate that the entire complex containing a single copy of each of the fourteen subunits has been solubilized and purified.

Purified MBH contained both iron and nickel by analysis using ICP-MS in a ratio of 15.4 ± 0.5:1. This result supports the proposed presence of three [4Fe-4S] clusters in the enzyme (Fig. 1), which together with the [NiFe] active site gives a predicted ratio of 13:1. The protein purified under anaerobic conditions (in the presence of DTT**)** exhibited a rhombic EPR signal at 50K with g-values of 2.39, 2.17 and 2.05 (supplemental Fig. S5) indicative of the Ni-B "ready" state (6). No additional EPR resonances were observed that might be attributable to the iron-sulfur clusters after reduction of the as-purified enzyme with sodium dithionite, and the thionine-oxidized enzyme was also EPR-silent.

MBH uses reduced ferredoxin as an electron donor *in vivo* and, as shown in Fig. 1, the redox protein is proposed to interact with MbhN. In a previous attempt to characterize MBH, its solubilization led to the loss of the ability to use ferredoxin as an electron donor (22). As shown in Table 3, the solubilized enzyme evolved H_2 from reduced ferredoxin, which was reduced using the native pyruvate oxidoreductase (POR) system with specific activities of 0.14 and 0.02 U/mg for the purified and membrane bound enzymes, respectively, in accordance with increase in purity of the MBH complex. These results suggest that the [Fe-S] clusters and [NiFe] site are intact and functional. The enzyme also retained its catalytic preference upon solubilization. The ratio H_2 evolution to H_2 oxidation was similar (25:1) for both the membrane bound and the solubilized forms. The two forms of MBH were similarly insensitive to inactivation by oxygen, with half-lives under air while shaking of approximately 14 hrs. On the other hand, as might be

expected, the solubilized enzyme was much less thermostable with a half-life at 90^0C of 1 hr, compared to 25 hr for the membrane bound form.

SAXS data analysis-The quaternary structure of purified MBH was analyzed by small angle x-ray scattering (SAXS). Analysis of the SAXS profiles as a function of MBH concentration showed only a minor concentration dependence where the lower concentration (1.5 mg/ml) had a higher radius of gyration than the higher concentration sample (5 mg/ml) providing greater confidence that the sample was not aggregating (Fig. 4*A*). Also shown in dashed lines is the profile for the six core subunits of Complex I (PDB 4HEA). From this, we can further see the similarities between MBH and Complex I as the six core Complex I subunits and the MBH calculated profiles agree in much of the low q region, which suggests that there are similar features and dimensions between the two proteins (Fig. 4*A*). Guineir analysis of the low q (momentum transfer in $Å^{-1}$) region of the SAXS profile extrapolated to zero concentration yielded a radius of gyration of 63 ± 2 Å. From the radius of gyration and volume of correlation, the mass of the purified MBH was calculated from the SAXS profile (38) to be 310 kDa, which in good agreement with the predicted value of 298 kDa and the experimental value from the SEC column (310 kDa). In Fourier transform, the real space P(r) function provided an estimated maximum dimension of 288 Å and also suggests a globular shape of the purified MBH (Fig. 4*B*). The scattering profile decayed as q^4 (the value expected for a folded rigid protein (39)). Using ten GASBOR (34) runs an average shape was calculated without symmetry (Fig. 5). With a calculated mass in agreement with the mass of the monomer to within error, the "Z-shaped" structure is expected to characterize the mono-dispersed homogenous species. A comparison to subunits of the atomic resolution structures of NADH quinone oxidoreductase or Complex I (PDB 4HEA) is shown within the MBH SAXS model (Fig. 5). The Complex I homologous

subunits of MBH are drawn in ribbon. These include four cytoplasmic subunits homologous to MbhJKLN (NuoBCDI) and one membrane bound subunit (MbhM/NuoH). The Complex I homolog of MbhH (NuoL) is not continuous with the other homologs within the MBH SAXS model and is shown (green ribbon) with an intervening non-homologous section of Complex I (red space filling). We can distinguish where in the SAXS model the membrane bound subunits (including the Mrp subunits) and soluble subunits (including the catalytic subunit) are located (Fig 5). The overall SAXS analysis reveals as a folded assembled complex suitable for the pursuit of other forms of structural analyses for MBH including crystal structures.

DISCUSSION

We describe here the first successful affinity purification of a membrane bound energy-conserving group 4 hydrogenase with an engineered tag. There is only one previous report of affinity purification of any membrane bound hydrogenase and this is for the group 1 dimeric enzyme from the mesophilic bacterium *Rhizobium japonicum*, although in that case affinity purification took advantage of NAD as a substrate and used a reactive-red 120-agarose column (40). There is only one previous example of affinity purification of an entire respiratory complex: this is the 6-subunit membrane bound NADH quinone oxidoreductase from the mesophilic bacterium *Vibrio cholera*, which compares with the 14-subunit MBH. This also used an engineered His_9 tagged protein that was solubilized with the detergent dodecyl maltoside (DM) (41). Herein we show that the location of the affinity tag is critical, with a much higher recovery of activity with the tag located on MbhJ compared to MbhN. The former tag location is probably more accessible to the Ni-NTA column and results in the improved purification. The high recovery of enzymatic activity with *J*-MBH after both solubilization and the affinity step is also noteworthy. For example, the purification of the *P. furiosus* ATP synthase yielded 2% of the

initial activity with ≤ 1 mg from 50 g of cells (37). This compares with ~3 mg with a yield of activity of 27% for *P. furiosus* MBH (Table 2).

Solubilized *P. furiosus* MBH was purified as an intact complex that evidently contains one copy of each of the 14 subunits encoded by the MBH operon (Fig. 1) with calculated and measured masses of 298 and 310 kDa, respectively. The predicted and measured contents of nickel and iron (13:1 and 15:1, respectively) are also in good agreement with a completely intact complex. Earlier attempts to purify MBH using standard chromatographic techniques resulted in partial purification of complexes containing predominantly MbhLK or MbhJ-N (22,24). Like the intact MBH complex purified herein, these subcomplexes were catalytically active and the as-purified enzyme exhibited a rhombic EPR signal with g-values very similar to what was observed here with intact MBH (22). However, in that case the signal was assigned to the Ni-C state, while from the g-values it is the same Ni-B signal that was observed here (6). Interestingly, in the prior study (22), an EPR signal indicative of reduced iron-sulfur clusters signal was observed, but that was not the case here with the complete complex, suggesting perhaps a change in conformation of the cluster-containing subunits when detached from intact MBH. The oxygen tolerance of purified MBH was similar to that in the membrane bound form, indicating that the infrastructure around metal centers is maintained after detergent extraction. Even though purified MBH was much less thermostable than the membrane bound enzyme, it was still a very stable complex (half-life at 90°C of 1 hr), illustrating an advantage of solubilizing membrane proteins from hyperthermophilic species.

MBH and other group 4 hydrogenases are proposed to have an evolutionary history in common with the aerobic respiratory Complex I (NADH quinone oxidoreductase). This 16-subunit 536 kDa enzyme is the largest complex of the aerobic electron transport chain and

couples NADH oxidation to ubiquinone reduction and proton translocation (42,43). The proton gradient is utilized by ATP synthase to generate ATP. Group 4 hydrogenases have a similar function in generating a proton gradient, while *P. furiosus* MBH has an additional Mrp modules that serves to generate a sodium ion gradient (11). There are six conserved subunits found in the group 4 hydrogenases that are also found in Complex I. These subunits comprise the Complex I core and the subunit that binds quinone is the homolog of the [NiFe]-containing catalytic subunit of the group 4 hydrogenases (9,10). This homology with Complex I allows placement of five of these six core subunits from the crystal structure of Complex I from *Thermus thermophilus* (PDB 4HEA) within the SAXS model as cytoplasmic subunits, including the catalytic subunit of MBH. This fit also allows us to postulate where to place the membrane wall in the model, as shown in Fig. 5. Since Complex I does not contain any homolog of the Mrp subunits, we would not expect the core subunits to completely fit within the MBH SAXS model. Overall, generation of the SAXS model of MBH shows that our purified protein is sufficiently homogenous for low-resolution structural characterization. *P. furiosus* MBH represents a large family of membrane bound respiratory complexes that include those that oxidize formate and carbon monoxide (11). In addition to the Mrp and hydrogenase modules, these enzymes contain additional subunits that oxidize the C-1 substrates. As yet, none of these complexes have been solubilized and purified other than MBH. However, *P. furiosus* was recently used to heterologously express the membrane bound 18-subunit formate hydrogen lyase (FHL) of *Thermococcus onnurineus* to give a functional complex that oxidizes formate and evolves H_2 (17,44). FHL is also encoded by a single operon and in addition to two subunits that show sequence similarity to formate dehydrogenases, the FHL complex contains four homologs of the *mbhH* subunit of *P. furiosus* MBH for reasons that are not at all clear. Otherwise, the subunits of the hydrogenase module of

FHL are very similar to those of *P. furiosus* MBH, suggesting that a similar tagging and purification strategy (with the His_9 tag attached to the *fhlN* subunit) might be successful for the intact FHL complex, and this is currently being investigated. In conclusion, we have devised a one-step affinity purification protocol for the respiratory MBH of *P. furiosus* that gives a high yield of the entire catalytically-active membrane bound complex. The group 4 hydrogenases show little sequence similarity to the structurally characterized group 1 2-subunit enzymes, except for the residues that bind the [NiFe] active site and the [4Fe-4S] proximal cluster (9,10). Further characterization of MBH may therefore provide insight into the diversity of hydrogenase structure and function, such as providing a strategy for the characterization of closely related but even more complex membrane bound respiratory enzymes, as well as providing evolutionary insights into the ubiquitous Complex I of aerobic organisms, both prokaryotic and eukaryotic.

REFERENCES

1. Lee, H. S., Vermaas, W. F., and Rittmann, B. E. (2010) Biological hydrogen production: prospects and challenges. *Biotechnol.* **28**, 262-271

2. Vignais, P., and Billoud, B. (2007) Occurrence, classification, and biological function of hydrogenases: an overview. *Chem. Rev.* **107**, 4206-4272

3. Fontecilla-Camps, J. C. (2009) Structure and function of [NiFe]-hydrogenases. *Met. Ions Life Sci.* **6**, 151-78

4. Friedrich, B., Fritsch, J. and Lenz, O. (2011) Oxygen-tolerant hydrogenases in hydrogen-based technologies. *Curr. Opin. Biotechnol.* **22**, 358-64

5. Shafaat, H. S., Rudiger, O., Ogata, H. and Lubitz, W. (2013) [NiFe] hydrogenases: a common active site for hydrogen metabolism under diverse conditions. *Biochimica et Biophysica Acta.* **1827**, 986-1002

6. Foerster, S., Stein, M., Brecht, M., Ogata, H., Higuchi, Y., and Lubitz, W. (2002) Single Crystal EPR Studies of the Reduced Active Site of [NiFe] Hydrogenase from *Desulfovibrio vulgaris Miyazaki* F. *Journal of the American Chemical Society.* **125**, 83-93

7. Volbeda, A., Charon, M. H., Piras, C., Hatchikian, E. C., Frey, M. and Fontecilla-Camps, J. C. (1995) Crystal structure of the nickel-iron hydrogenase from *Desulfovibrio gigas*. *Nature.* **373**, 580-7

8. Volbeda, A., Darnault, C., Parkin, A., Sargent, F., Armstrong, F. A. & Fontecilla-Camps, J. C. (2013) Crystal structure of the O_2-tolerant membrane-bound hydrogenase 1 from *Escherichia coli* in complex with its cognate cytochrome b. *Structure.* **21**, 184-90

9. Hedderich, R. (2004) Energy-converting [NiFe] hydrogenases from archaea and extremophiles: ancestors of complex I. *J. Bioenerg. Biomembr*. **36**, 65-75

10. Hedderich, R. Forzi, L. (2005) Energy-converting [NiFe] hydrogenases: more than just H_2 activation. *J. Mol. Microbiol. Biotechnol.* **10**, 92-104

11. Schut, G. J., Boyd, E.S., Peters, J.W., and M.W.W. Adams. (2013) The modular respiratory complexes involved in hydrogen and sulfur metabolism by heterotrophic hyperthermophilic archaea and their evolutionary implications. *FEMS Microbiol. Rev.* **37**, 182-203

12. Böhm, R, Sauter, M., Böck A. (1990) Nucleotide sequence and expression of an operon in *Escherichia coli* coding for formate hydrogenlyase components. *Mol. Microbiol.* **4**, 231–243

13. Sauter, M., Böhm, R., Böck A. (1992) Mutational analysis of the operon (hyc) determining hydrogenase 3 formation in *Escherichia coli*. *Mol. Microbiol.* **6**, 1523–1532

14. Singer S. W., Hirst, M. B., Ludden, P. W. (2006) CO-dependent H_2 evolution by *Rhodospirillum rubrum*: role of CODH:CooF complex. *Biochimica et Biophysica Acta.* **1757**, 1582–1591

15. Kurkin S., Meuer. J., Koch, J., Hedderich, R., and Albracht S.P.J. (2002) The membrane-bound [NiFe]-hydrogenase (Ech) from *Methanosarcina barkeri*: unusual properties of the iron-sulphur clusters. *Eur. J. Biochem.* **269**, 6101-6111

16. Meuer, J., Bartoschek, S., Koch, J., Kunkel, A. & Hedderich, R. (1999) Purification and catalytic properties of Ech hydrogenase from *Methanosarcina barkeri*. *Eur. J. Biochem.* **265**, 325-335

17. Kim, M. S., Bae, S. S., Kim, Y. J., Kim, T. W., Lim, J. K., Lee, S. H., Choi, A. R., Jeon, J. H., Lee, J. H., Lee, H. S. & Kang, S. G. (2013) CO-dependent H_2 production by genetically engineered Thermococcus onnurineus NA1. *Appl. Environ. Microbiol.* **79**, 2048-5

18. Marreiros, B. C., Batista, A. P., Duarte, A. M. & Pereira, M. M. (2013) A missing link between complex I and group 4 membrane-bound [NiFe] hydrogenases. *Biochimica et Biophysica Acta.* **1827**, 198-209

19. Soboh B, Linder, D., Hedderich R. (2002) Purification and catalytic properties of a CO-oxidizing:H_2 -evolving enzyme complex from *Carboxydothermus hydrogenoformans. Eur. J. Biochem.* **269**, 5712-5721

20. Soboh B, Linder, D., Hedderich R. (2004) A multisubunit membrane-bound [NiFe] hydrogenase and an NADH-dependent Fe-only hydrogenase in the fermenting bacterium *Thermoanaerobacter tengcongensis*. *Microbiology.* **150**, 2451-2463

21. Fiala, G., and Stetter, K. (1986) *Pyrococcus furiosus* sp. nov. represents a novel genus of marine heterotrophic archaebacteria growing optimally at 100°C. *Arch. Microbiol.* **145**, 56-61

22. Sapra, R., Verhagen, M. F. & Adams, M. W. (2000) Purification and characterization of a membrane-bound hydrogenase from the hyperthermophilic archaeon *Pyrococcus furiosus*. *J. Bacteriol.* **182**, 3423-3428

23. Swartz, T. H., Ikewada, S., Ishikawa, O., Ito, M. & Krulwich, T. A. (2005) The Mrp system: a giant among monovalent cation/proton antiporters? *Extremophiles.* **9**, 345-354

24. Silva, P., Van den Ban, E.C.D., Wassink H., Haaker H., de Castro B., Robb F.T, and Hagen W.R. (2000) Enzymes of hydrogen metabolism in *Pyrococcus furiosus*. *Eur. J. Biochem.* **267**, 6541-6551

25. Sapra, R., Bagramyan, K. & Adams, M. W. (2003) A simple energy-conserving system: proton reduction coupled to proton translocation. *Proc. Natl. Acad. Sci. USA.* **100**, 7545-7550

26. Brereton, P. S., Verhagen, M. F., Zhou, Z. H. & Adams, M. W. (1998) Effect of iron-sulfur cluster environment in modulating the thermodynamic properties and biological function of ferredoxin from *Pyrococcus furiosus*. *Biochemistry.* **37**, 7351-7352

27. Pisa, K. Y., Huber, H., Thomm, M. & Muller, V. (2007) A sodium ion-dependent A1-AO ATP synthase from the hyperthermophilic archaeon *Pyrococcus furiosus*. *FEBS J.* **274**, 3928-3938

28. Lipscomb, G. L., Stirrett, K., Schut, G. J., Yang, F., Jenney, F. E., Jr., Scott, R. A., Adams, M. W., and Westpheling, J. (2011) Natural competence in the hyperthermophilic archaeon *Pyrococcus furiosus* facilitates genetic manipulation: construction of markerless deletions of genes encoding the two cytoplasmic hydrogenases. *Appl. Environ. Microbiol.* **77**, 2232-2238

29. Chandrayan S.K., McTernan. P. M., Hopkins R.C., Sun J., Jenney F.E. and Adams M.W.W. (2012) Engineering hyperthermophilic archaeon *Pyrococcus furiosus* to overproduce its cytoplasmic [NiFe]-Hydrogenase. *J. Biol. Chem.* **287**, 3257-3264

30. Hopkins, R. C., Sun, J., Jenney, F. E., Jr., Chandrayan, S. K., McTernan, P. M., and Adams, M. W. W. (2011) Homologous expression of a subcomplex of *Pyrococcus*

furiosus hydrogenase that interacts with pyruvate ferredoxin oxidoreductase. *PLOS One.* **6**, e26569

31. Horton, R. M., Hunt, H. D., Ho, S. N., Pullen, J. K., and Pease, L. R. (1989) Engineering hybrid genes without the use of restriction enzymes: gene splicing by overlap extension. *Gene.* **77**, 61-68

32. Hura G. L., M. A. L., Hammel M., Rambo R. P., Poole F. P. II, Tsutakawa S. E., Jenney F. E. Jr, Classen S., Frankel K. A., Hopkins R. C., Yang S.-J., Scott J. W., Dillard B. D., Adams M. W. W. and Tainer, J. A. (2009) Robust, high-throughput solution structural analyses by small angle X-ray scattering (SAXS). *Nature Methods.* **6**, 606-612

33. Classen, S., Hura, G. L., Holton, J. M., Rambo, R. P., Rodic, I., McGuire, P. J., Dyer, K., Hammel, M., Meigs, G., Frankel, K. A., and Tainer, J. A. (2013). Implementation and performance of SIBYLS: a dual endstation small-angle X-ray scattering and macromolecular crystallography beamline at the Advanced Light Source. *J. Appl. Crystallogr.* **46,** 1-13

34. Semenyuk, A. V., and Svergun, D. I. (1991) Gnom - a program package for small-angle scattering data-processing. *J. Appl. Crystallogr.* **24**, 537-540

35. Svergun, D. I., Petoukhov, M. V., and Koch, M. H. J. (2001) Determination of domain structure of proteins from X-ray solution scattering. *Biophys. J.* **80**, 2946-2953

36. Cvetkovic, A., Menon, A. L., Thorgersen, M. P., Scott, J. W., Poole, F. L. 2nd, Jenney, F. E., Jr., Lancaster, W. A., Praissman, J. L., Shanmukh, S., Vaccaro, B. J., Trauger, S. A., Kalisiak, E., Apon, J. V., Siuzdak, G., Yannone, S. M., Tainer, J. A., and Adams, M. W. W. (2010) Microbial metalloproteomes are largely uncharacterized. *Nature.* **466**, 779-782

37. Vonck, J., Pisa, K. Y., Morgner, N., Brutschy, B. & Muller, V. (2009) Three-dimensional structure of A1A0 ATP synthase from the hyperthermophilic archaeon *Pyrococcus furiosus* by electron microscopy. *J. Biol. Chem.* **284**, 10110-10119

38. Rambo, R. P., and Tainer J. A. (2013) Accurate assessment of mass, models and resolution by small-angle scattering. *Nature.* **496**, 477-481

39. Rambo, R. P., and Tainer J. A. (2011) Characterizing flexible and intrinsically unstructured biological macromolecules by SAS using the Porod-Debye law. *Biopolymers.* **95**, 559-571

40. Stults, L.W, Moshiri, F. and Maier, R. J. (1986) Aerobic purification of hydrogenase from *Rhizobium japonicum* by affinity chromatography. *J. Bacteriol.* **166**, 795-800

41. Barquera, B., Hellwig, P., Zhou, W., Morgan, J. E., Häse, C. C., Gosink, K. K., Nilges, M., Bruesehoff, P. J., Roth, A., Lancaster, C. R. D., and Gennis, R. B. (2002) Purification and characterization of the recombinant Na+-translocating NADH:quinone oxidoreductase from *Vibrio cholerae*. *Biochemistry.* **41**, 3781-3789

42. Baradaran, R., Berrisford, J. M., Minhas, G. S., and Sazanov, L. A. (2013) Crystal structure of the entire respiratory complex I. *Nature.* **494**, 443-448

43. Efremov, R. G., Baradaran, R., and Sazanov, L. A. (2010) The architecture of respiratory complex I. *Nature.* **465**, 441-445

44. Lipscomb, G. L., Schut, G. J., Thorgersen M. P., Nixon, W. J., Kelly, R. M., and Adams, M. W. W. (2013) Engineering hydrogen gas production from formate in a hyperthermophile by heterologous production of an 18-subunit membrane-bound complex. *J. Biol. Chem.* **289**, 2873-2879

Table 3.1. Strains used in this work.

Strain Designation	Genotype	Deleted Or Inserted ORF/Elements	Parent Strain	Refs
COM1	Δ *pyrF*	PF1114	DSM 3638	(30)
MW0414	*ΔpyrF::*P_{gdh} *pyrF* P_{slp} His_9 *PF1432*	$P_{slp}$$His_9$ *inserted in front of PF1432 (mbhJ)*	COM1	This study
MW0403	*ΔpyrF:: PF1436* His_9 P_{gdh} *pyrF*	His_9 *inserted behind PF1436 (mbhN)*	COM1	This study

COM1 was the competent parent strain. MW0414 and MW0403 were generated by placing the marker cassette at the N-terminus of *mbhJ* and at the C-terminus of the operon at *mbhN*, respectively.

Table 3.2. Purification of *J*-MBH

Step	Total Units[1] (μmol min^{-1})	Total (mg)	Protein	Specific Activity	% Yield	Fold Purification
Wash Membrane	184	172		1.1	100	1.0
Triton-X 100 Extraction	148	147		1	80	0.9
Ni-NTA	50	2.6		19	27	17

Table 3.3. Properties of *J*-MBH

Property	*J*-MBH	Washed Membranes
POR-Fd H_2 Evolution Activity (U/mg)	0.14	0.02
H_2 evolution:H_2 oxidation activity (using MV as electron carrier)	25:1	26:1
Half-life ($t_{1/2}$, hr) at 90°C under argon	1 hr	25 hr
Half-life ($t_{1/2}$, hr) at 25°C under air	15 hr	13 hr
Metal content (Fe:Ni)	15:1	19:1

Figure 3.1

Schematic representation of *P. furiosus* MBH. *Upper:* Operon encoding *P. furiosus* MBH. The Mrp module is encoded by MbhA-H and the hydrogenase module by MbhI-N. *Lower:* The enzyme is predicted to contain three [4Fe-4S] clusters in addition to the [NiFe]-catalytic site. The His_{9x}-affinity tag was attached to either MbhJ or MbhN as indicated. Fd_{red} and Fd_{ox} represent the reduced and oxidized forms of *P. furiosus* ferredoxin. The predicted size (kDa) of each MBH subunit is shown in the table.

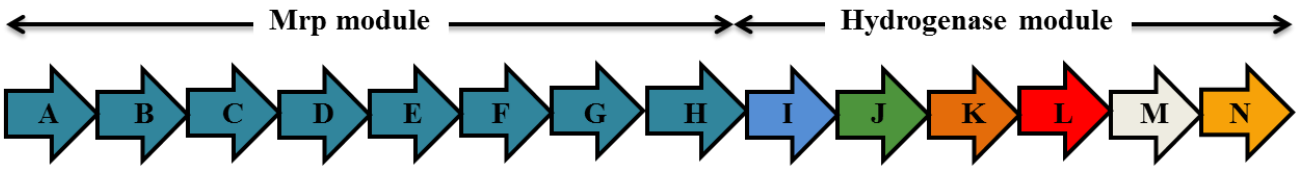

MBH Subunit	Molecular Weight (kDa)
MBH A	18.7
MBH B	9.1
MBH C	13.5
MBH D	10.4
MBH E	11.1
MBH F	15.5
MBH G	12.8
MBH H	54.9
MBH I	13.0
MBH J	18.3
MBH K	20.2
MBH L	47.9
MBH M	35.4
MBH N	15.7

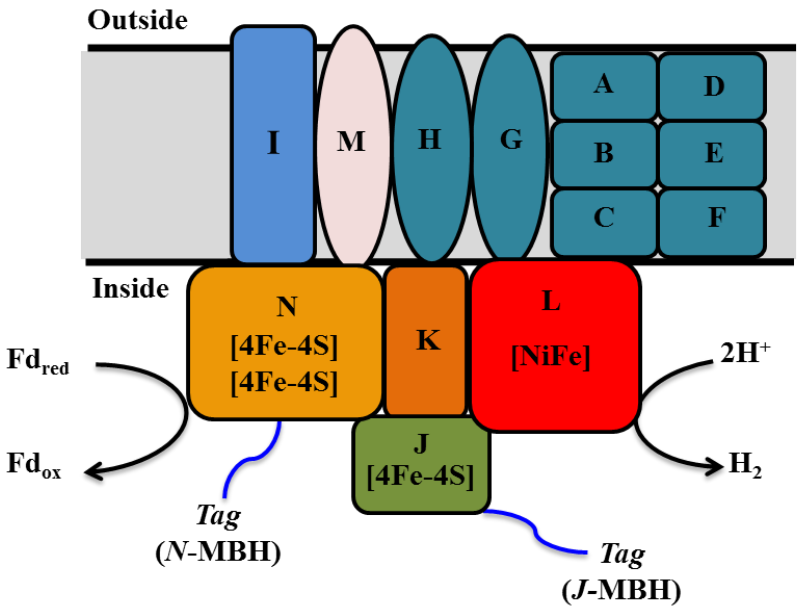

Figure 3.2

The genetic strategy used to insert the His_{9x} tag into MBH. A) The tag is inserted at the C-terminus of *mbhN* (yielding *P. furiosus* strain MW0403) where PF1437 is the gene immediately downstream of the MBH operon. B) The tag is inserted at the N-terminus of *mbhJ* (yielding *P. furiosus* strain MW0414). The abbreviations are: UFR and DFR, upstream and downstream flanking regions (1 kb) of the MBH operon; *pyrF*, selectable marker; P_{gdh} and P_{slp}, promoters for the gene encoding glutamate dehydrogenase and the S-layer protein of *P. furiosus*, respectively. The affinity tag was His_{9x}-tag.

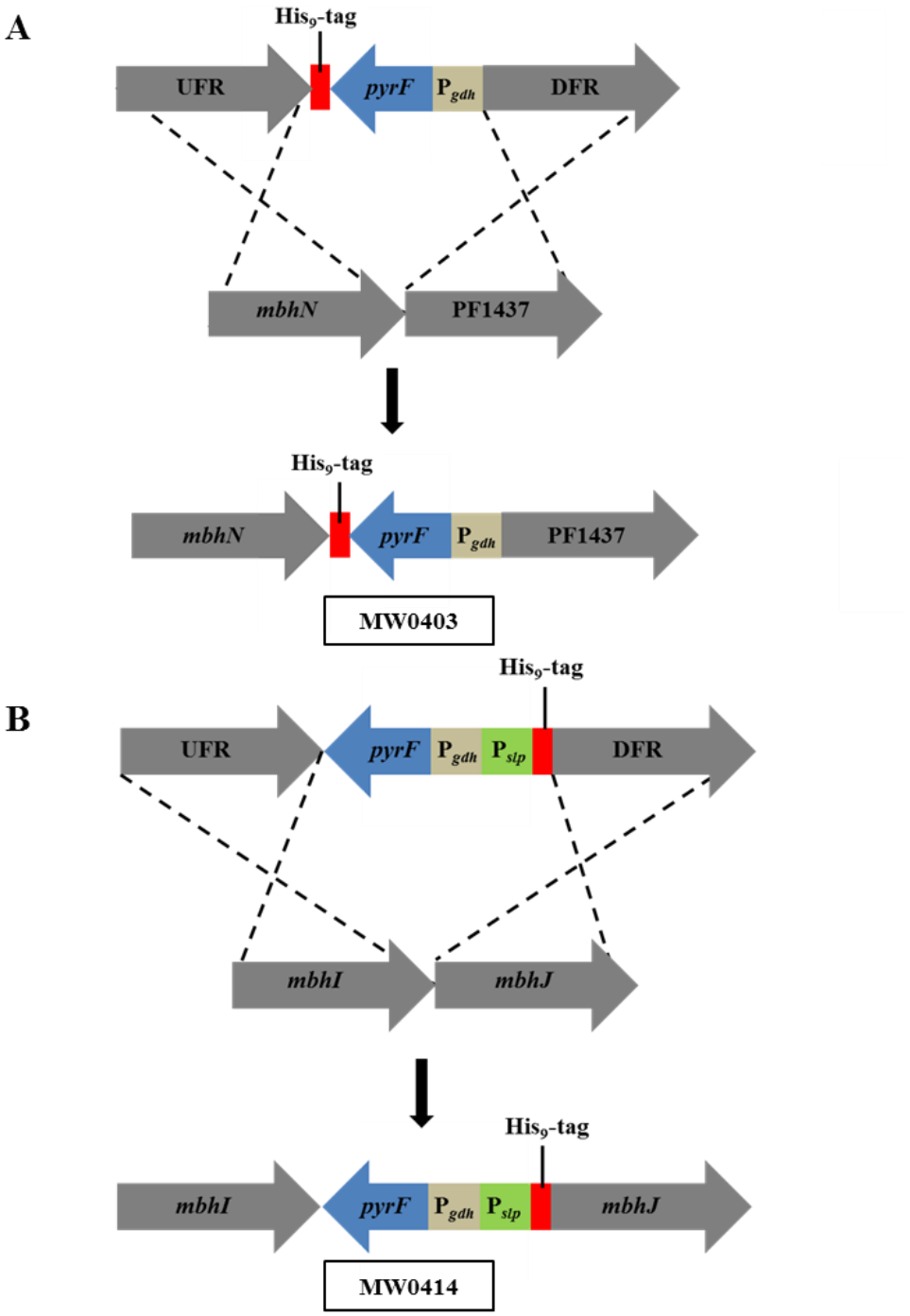
A
His9-tag
UFR
pyrF
Pgdh
DFR
mbhN
PF1437
His9-tag
mbhN
pyrF
Pgdh
PF1437
MW0403
B
His9-tag
UFR
pyrF
Pgdh
Pslp
DFR
mbhI
mbhJ
His9-tag
mbhI
pyrF
Pgdh
Pslp
mbhJ
MW0414

Figure 3.3

SDS-PAGE of purified *J*-MBH. MBH subunits were analyzed from bands cut from gel and from samples that were digested in-solution. MBH subunits identified by either MALDI-TOF or LC-MS/MS are labeled with a black arrow. MbhD is the only subunit not identified and the protein band corresponding to its calculated molecular weight is shown by a dashed arrow.

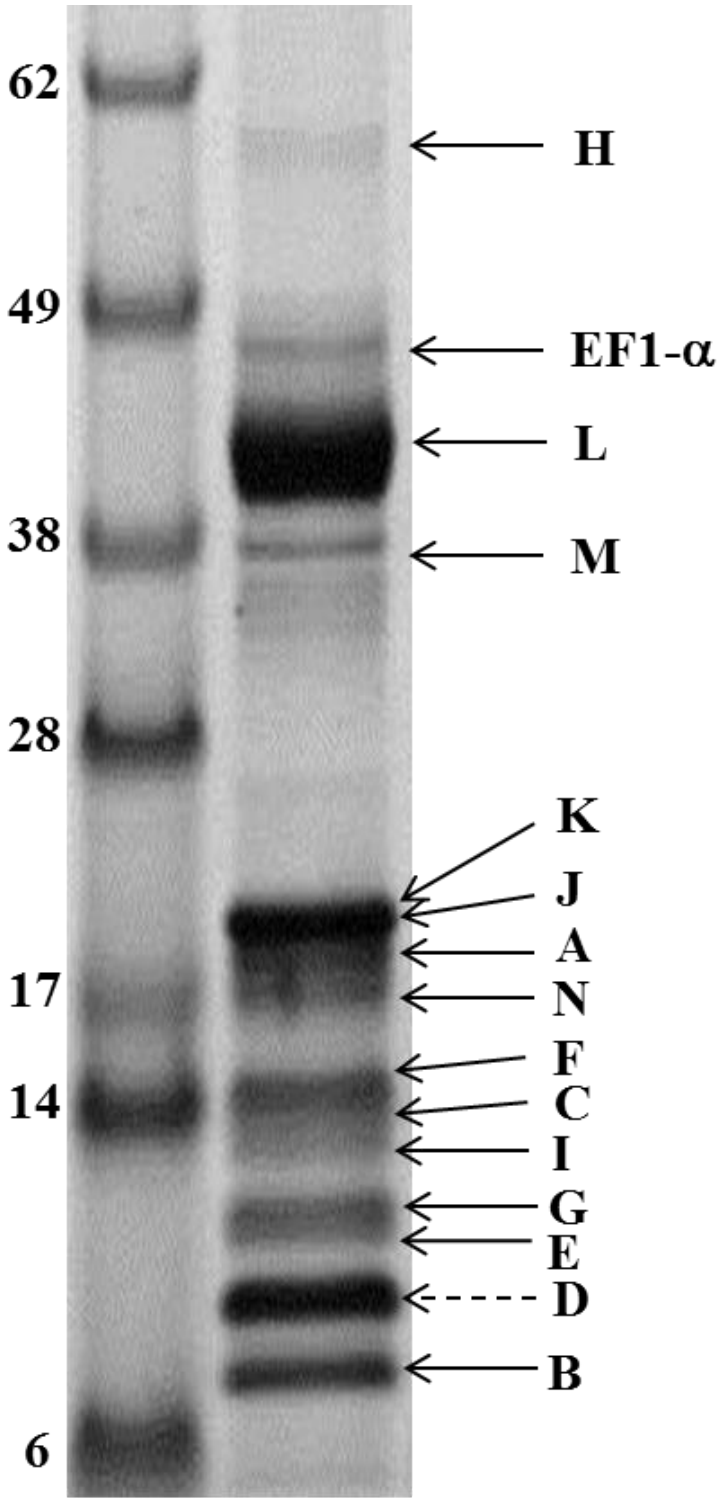
62
49
38
28
17
14
6
H
EF1-α
L
M
K
J
A
N
F
C
I
G
E
D
B

Figure 3.4

SAXS analysis of purified MBH. (A) Experimental SAXS profile of MBH (blue) with the Guineir region plotted on the inset with a linear fit (red). The calculated profile from a portion of Complex I (NADH quinone oxidoreductase, PDB 4HEA; dashed black line) is shown for comparison. (B) The real space pair distribution file extracted from SAXS data.

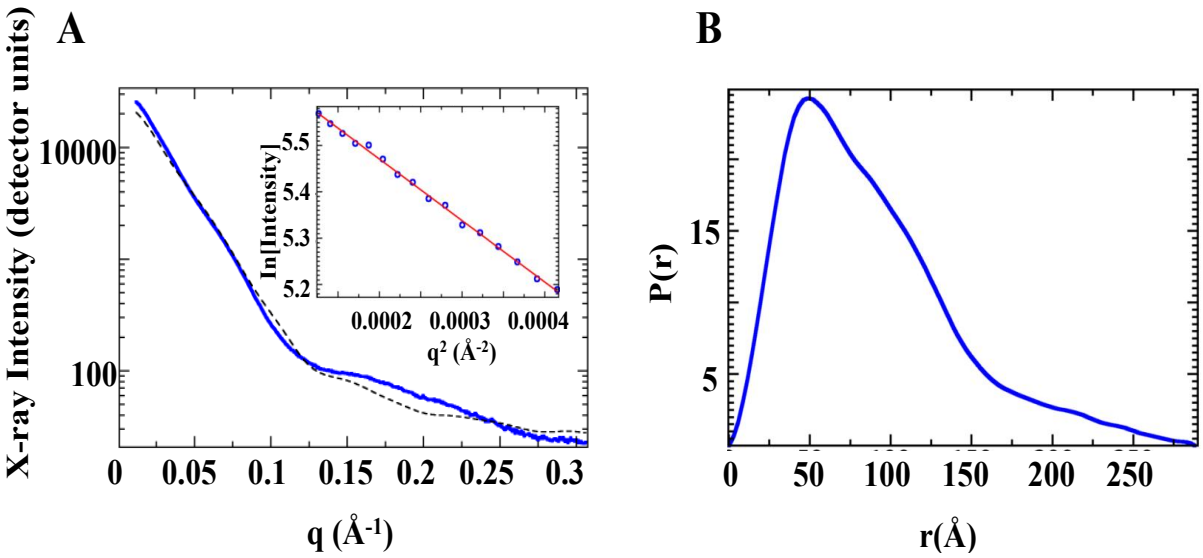
A
X-ray Intensity (detector units)
10000
100
0
0.05
0.1
0.15
0.2
0.25
0.3
q (Å-1)
ln[Intensity]
5.5
5.4
5.3
5.2
0.0002
0.0003
0.0004
q2 (Å-2)
B
P(r)
15
5
0
50
100
150
200
250
r(Å)

Figure 3.5

Shape and assembly of MBH from SAXS. Shapes generated from SAXS are elongated and multi-lobed. The homologous portions of Complex I (NADH quinone oxidoreductase, PDB 4HEA) shown in ribbon were augmented by intervening and non-homologous portions (red spheres) to create an atomic model of equivalent size to MBH. This model was fit into the SAX S generated shape, shown rotated in 3 orientations. By analogy portions of the shape which a likely associated with the cellular membrane (the MRP module) and oxidize Ferredoxin (Fd) are identified.

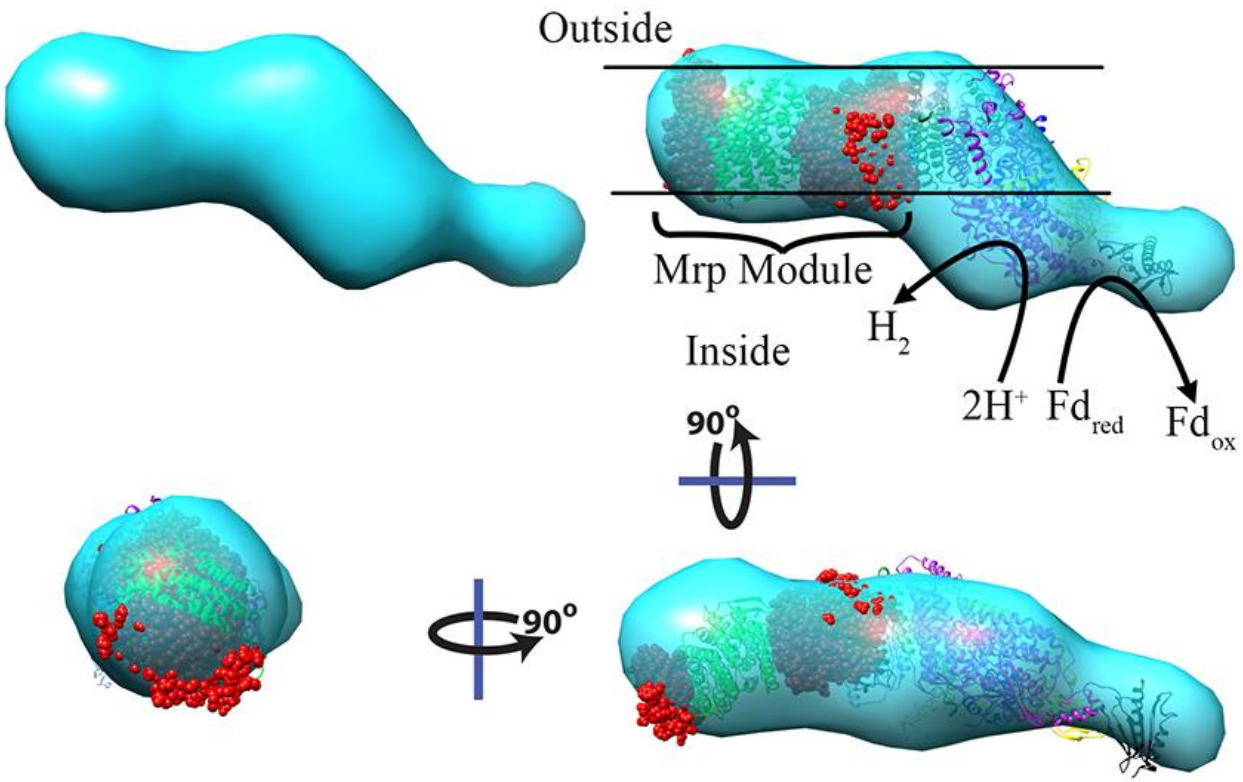
Outside
Mrp Module
Inside
H_2
$2H^+$
Fd_{red}
Fd_{ox}
90°
90°

CHAPTER 4

ENGINEERING THE RESPIRATORY MEMBRANE-BOUND HYDROGENASE OF THE HYPERTHERMOPHILIC ARCHAEON *PYROCOCCUS FURIOSUS* AND CHARACTERIZATION OF THE CATALYTICALLY-ACTIVE CYTOPLASMIC SUBCOMPLEX[1]

[1]McTernan PM, Chandrayan SK, Wu C-H, Vaccaro BJ, Lancaster WA, et al. 2014. Protein Engineering Design and Selection gzu051: 1-8. Reprinted here with permission of the publisher.

ABSTRACT

The archaeon *Pyrococcus furiosus* grows optimally at 100 degrees C by converting carbohydrates to acetate, CO_2 and H_2, obtaining energy from a respiratory membrane-bound hydrogenase (MBH). This conserves energy by coupling H_2 production to oxidation of reduced ferredoxin with generation of a sodium ion gradient. MBH is a group 4 hydrogenase and is encoded by a 14-gene operon that contains hydrogenase and Na^+/H^+ antiporter modules. Herein a His-tagged 4-subunit cytoplasmic version of MBH (C-MBH) was engineered and expressed in *P. furiosus* by differential transcription of the MBH operon. It was purified under anaerobic conditions by affinity chromatography without detergent. Purified C-MBH had a Fe:Ni ratio of 14:1, similar to the predicted value of 13:1. The O_2 sensitivities of C-MBH and the 14-subunit membrane bound version were similar (half-lives of ~15 hr in air), but C-MBH was more thermolabile (half-lives at 90 degrees C of 8 hr and 25 hr, respectively). C-MBH evolved H_2 with the physiological electron donor, reduced ferredoxin, optimally at 60 degrees C. This is the first report of the engineering and characterization of a soluble catalytically-active subcomplex of a membrane bound respiratory hydrogenase.

INTRODUCTION

Due to limiting fossil fuel availability and a growing need for energy, a major push has occurred recently to generate alternative renewable fuels. Such fuels must be energy efficient as well as carbon neutral, and biohydrogen production meets these criteria (Lee *et al*., 2010). Hydrogen gas is metabolized by microbes from all three domains of life using the enzyme hydrogenase, which functions to catalyze the reversible reduction of protons to molecular hydrogen (H_2) (Vignais and Billoud, 2007). Hydrogenases are classified based on the metal content of their active sites into the [NiFe]-, [FeFe]- and the [FeS] cluster free-hydrogenases. The [NiFe]-hydrogenases are ubiquitous in the microbial world and have been extensively studied from numerous mesophilic bacteria (Fontecilla-Camps, 2009; Friedrich *et al*., 2011; Shafaat *et al*., 2013). The minimum structure of the [NiFe] hydrogenase is a heterodimer composed of a large and small subunit. The large subunit contains the [NiFe] catalytic site that is coordinated by the sulfur atoms of four cysteine residues organized into two –CxxC– motifs near the N- and C-termini. The small subunit typically contains three iron-sulfur clusters invariably of the [4Fe-4S] type that shuttle electrons between an acceptor/donor for the enzyme and its active site (Vignais and Billoud, 2007). [NiFe]-hydrogenases are classified into four groups based on the phylogeny of their catalytic subunits (Vignais and Billoud, 2007). The majority of crystal structures for [NiFe]-hydrogenases are available for group 1 hydrogenases (Volbeda *et al*., 1995; Volbeda *et al*., 2013). Recently, the first crystal structure of a group 3 hydrogenase was determined from *Methanothermobacter marburgensis* (PDB code: 4OMF) (Vitt *et al*., 2014).

Group 4 hydrogenases are the least studied of the [NiFe]-hydrogenases. These hydrogenases are defined as the H_2-evolving energy-conserving membrane-associated hydrogenases (Vignais and Billoud, 2007). Very little sequence similarity exists between group 4

hydrogenases and other [NiFe] hydrogenases except for the conserved residues that bind the [NiFe] catalytic site and its proximal [4Fe-4S] cluster, indicating a distinct evolutionary history (Hedderich, 2004; Hedderich, 2005; Schut *et al*., 2013). Group 4 hydrogenases play an important role in conserving energy by establishing ion gradients across membranes that can be used to generate ATP. These enzymes contain at least six subunits and are much more complex than the characterized dimeric hydrogenases. The simplest members include the 6-subunit 'energy-conserving' hydrogenase (Ech) from the archaeon *Methanosarcina barkeri,* which functions in methanogenesis, and the 7-subunit hydrogenase 3 from *Escherichia coli*, which oxidizes formate and evolves H_2 (Kurkin *et al*., 2002; Meuer *et al*., 1999; Böhm *et al*., 1990; Sauter *et al*., 1992). Six subunits conserved within the group 4 hydrogenases are homologous to the catalytic core of the ubiquitous aerobic respiratory complex NADH quinone oxidoreductase or Complex I (*NuoBCDIHL*) (Hedderich, 2004; Hedderich, 2005; Schut *et al*., 2013; Marreiros *et al*., 2013). This conserved homology suggests a close evolutionary history between group 4 enzymes and Complex I.

Pyrococcus furiosus is a hyperthermophilic archaeon that grows optimally at 100°C and contains a complex hydrogenase system (Schut *et al*., 2013; Fiala and Stetter, 1986). It grows by fermenting sugars to acetate, CO_2 and H_2 and its membrane bound hydrogenase (MBH) catalyzes H_2 production using reduced ferredoxin (Fd) generated from sugar oxidation as the electron donor (Schut *et al*., 2013). Previous studies of *P. furiosus* MBH showed that it is encoded by a 14-gene operon (*mbhA-N*: PF1423-PF1436) (Sapra *et al*., 2000). Six of the last seven genes in the operon are homologous to those encoding the "core" subunits of Complex I (*mbhH,J-N*) while another eight subunits (*mbhA-H*) are homologous to subunits of the Mrp monovalent cation/proton antiporter of some mesophilic bacteria (Fig. 1) (Swartz *et al*., 2005). The

exceptions are *mbhI,* which does not have homology to subunits of either Complex I or Mrp, and *mbhH,* which has homology to both (Fig. 1). Mrp catalyzes the efflux of monovalent cations, such as Na^+, K^+, and Li^+ outward in a coupled reaction that transports protons inwards. Of the 14 subunits of MBH, only *mbhJKLN* are predicted to not encode transmembrane helices (Sapra *et al*., 2000; Silva *et al*. 2000). MbhJ and MbhN are proposed to contain one and two [4Fe-4S] clusters, respectively, where MbhJ is the equivalent of the small subunit of the group 1 dimeric [NiFe]-hydrogenases (Fig. 1). MbhKL are equivalent to the large subunit and contain the [NiFe] active site, with the four Cys residues provided by MbhL.

The evolutionary linkage between respiratory complex I and group 4 [NiFe] hydrogenases has been extensively reviewed (Hedderich, 2004; Hedderich, 2005; Schut *et al*., 2013). An "ancestral group 4 [NiFe] hydrogenase" has been proposed that evolved into the archaeal, bacterial and eukaryotic (Nuo or Nqo, respectively) complex I by the shuffling of two distinct modules – Mrp and Mbh. Moreover, another notion of a "universal adaptor molecule" has been proposed to understand the evolution of Nuo or Nqo complex I and group 4 hydrogenases (Batista *et al*., 2013). The universal adaptor molecule is conceived as a set of conserved subunits between group 4 hydrogenases and complex I and contains four subunits (*nuoB*, *nuoD*, *nuoH*, and *nuoL*). *NuoB* and *nuoD* are analogous to the large and small subunits of the group 4 hydrogenases (*mbhL, mbhJ*) while *nuoH* (*mbhM*) is believed to function like a membrane anchor that links the hydrogenase module to the membrane, and *nuoL* (*mbhH*) is homologous to *mrpA* & *mrpD* from the Mrp monovalent cation/proton antiporter (Fig. 1). *NuoM* and *nuoN* also show homology to *mrpA*, *mrpD*, and *mbhH* (Fig. 1). Close evolutionary relationships have also been observed by analyzing the three dimensional structure of the hydrophilic domains of the Nqo Complex I of *Thermus thermophilus* (PDB 2FUG and 3M9S)

(Sazanov and Hinchliffe, 2006; Efremov *et al*. 2010). MBH has significant sequence similarity to the Q-module of Complex I of *T. thermophilus,* which includes Nqo4, 5, 6 and 9 (Fig. 1) (Hedderich, 2004; Hedderich, 2005). The Q-module has a quinone binding grove in Nqo4, which is where the [NiFe] site is located in the large subunit of MBH (MbhL) and the "N2" [FeS] cluster of Nqo6 is analogous to the proximal [FeS] cluster of small subunit of MBH (MbhJ). Nqo9 shares similarity with MbhN and harbors two [FeS] clusters. Nqo5 is homologous to MbhK and is part of the large subunit.

The best characterized group 4 hydrogenases are the 6-subunit *Ech* from *M. barkeri* and the 14-subunit MBH from *P. furiosus.* Biochemical studies of *Ech* have been described but there is no information on its modular structure (Hedderich, 2005; Schut *et al*., 2013; Kurkin *et al*., 2002; Meuer *et al*. 1999), *P. furiosus* MBH was recently affinity tagged and solubilized using detergent to yield an intact and functional 14-subunit complex and a structural model was obtained based on small angle X-ray scattering (SAXS) (McTernan *et al*., 2014). To further understand the modular nature of MBH, engineering the 14-gene operon to generate different forms of the enzyme could have major implications. For example, the generation of subcomplexes of MBH could give insight into which subunits are essential for catalytic activity and the generation of a chemical gradient, as well as providing insights into the evolution of the ubiquitous Complex I.

There are limited reports for the successful engineering of "minimal" versions of hydrogenase. This was achieved with the enzyme from a *Ralstonia* species but involved dissociation of the native complex rather than genetic manipulation (Grzeszik *et al*., 1997). The first successful example of the engineering of a subcomplex of hydrogenase was accomplished using the genetic system established for *P. furiosus* in order to make a dimeric version of its

heterotetrameric cytoplasmic hydrogenase SHI (Hopkins *et al*., 2011; Lipscomb *et al*. 2011). Herein, we have successfully engineered a strain of *P. furiosus* that generates a soluble 4-subunit subcomplex of MBH (C-MBH). Previous attempts to purify the 14-subunit complex led to the purification of subcomplexes of MBH but these were heterogeneous and difficult to characterize (Sapra *et al*., 2000; Silva *et al*. 2000). In this study, we have taken advantage of the same genetic system for *P. furiosus* that has been previously used to make a dimeric version of SHI and to over-express SHI (Hopkins *et al*., 2011; Lipscomb *et al*. 2011; Chandrayan *et al*., 2012). We have engineered a strain of *P. furiosus* by dividing the native MBH 14-gene operon into two different transcriptional units and have incorporated an affinity tag within the operon. This enabled us to purify a subcomplex of MBH from the cytoplasm (C-MBH) without the use of detergents. This is the first description of the engineering of a membrane bound hydrogenase to generate a soluble, catalytically-active enzyme complex.

METHODS

Generation of P. furiosus strains expressing affinity tagged MBH

A competent strain of *P. furiosus* (COM1) was used to manipulate the MBH operon (Lipscomb *et al*. 2011). A one-step marked knock-in genetic protocol was used in which a polyhistidine (His_9) affinity tag was inserted within the operon at the N-terminus of *mbhJ* (PF1432) yielding strain MW0414 (Fig. 2) (McTernan *et al*., 2014). The knock-in cassette, which contains the selectable marker and the strong constitutive promoter of the gene encoding the S-layer protein (P_{slp}) with an in frame His_9 tag, were generated by using overlapping PCR (Horton *et al*., 1989). Prime Star HS polymerase premix (Clonetech, USA) was used to make the knock-in cassette. *PyrF* was the selectable marker and was placed under the control of the glutamate dehydrogenase promoter (P_{gdh}). In strain MW0414, the expression of *mbhJ* and the subsequent

five genes (*mbhK-N*) was under control of P_{slp}, while the first 9 genes are under control of the native MBH promoter (McTernan *et al*., 2014). Generation of MW0414 required the marker cassette to be placed in front of *mbhJ* within the MBH operon (Fig. 2). All transformants were PCR screened for correct insertion and the PCR product was sequenced (Macrogen, MD).

Protein expression and purification

All purification steps were carried out anaerobically using a Coy anaerobic chamber (Coy laboratories; Michigan, USA). Cells were lysed using 50 mM EPPS (4-(2-Hydroxyethyl)-1-piperazinepropanesulfonic acid; Sigma-Aldrich, USA), pH 8.0, containing 50 μg/ml Deoxyribonuclease I (DNase I; Sigma-Aldrich, USA), and 2 mM dithiothreitol (DTT; Inalco, Italy) in a 5:1 ratio of buffer to cells in an anaerobic chamber (Coy, MI). After 2 hr incubation at 23^0C, cells were passed twice through a French press at a pressure of 1000 psi. Cytoplasmic extract (S100) was prepared by centrifugation in a Beckman-Coulter Optima L-90K ultracentrifuge at 100,000 x g for 1 hr. Cytoplasmic extract was loaded on 5 ml FF His-Trap Ni-NTA column (GE Healthcare, USA), which was equilibrated with Ni-NTA buffer A (50 mM Tris-HCl, pH 8.0, containing 400 mM NaCl, 4 mM DTT). The column was washed with buffer A and the bound protein was eluted with a 20-column volume gradient from 100% buffer A to 100% buffer B (buffer A containing 500 mM imidazole). After the Ni-NTA step, the affinity purified C-MBH was further purified using a Mono-Q column (Bio-Scale Q2 Column) The column was equilibrated in 50 mM Tris, pH 8.0 containing 2 mM sodium dithionite (DT). The bound protein was eluted with a 20 column volume gradient from 100 % buffer A to 100 % buffer B (buffer A containing 2 M NaCl).

Gel Filtration chromatography

The molecular weight of C-MBH was determined by analyzing the purified protein on a calibrated Superdex 200 10/300 GL column equilibrated 50 mM Tris pH 8.0, 400 mM NaCl, 2 mM DT. The column was calibrated by using these standards: cytochrome c, bovine serum albumin, and thyroglobulin.

Q-PCR analysis

RNA was isolated using the Absolutely RNA miniprep kit (Agilent technologies, USA). Turbo DNase (Agilent technologies, USA) was used to remove DNA contamination. CDNA was synthesized using Affinityscript QPCR CDNA synthesis kit (Agilent technologies, USA). CDNA was analyzed using Brilliant II SYBR green QPCR master mix (Agilent technologies, USA) and measured using a MX3000P instrument (Stratagene, USA). Ct values were normalized to the internal control pyruvate oxidoreductase (POR (pyruvate oxidoreductase) gamma subunit; PF0971).

Other methods

Hydrogenase assays were performed at 80^0 C and H_2 was measured using an Agilent Technologies 6850 gas chromatograph. H_2 evolution activity was determined using dithionite-reduced methyl viologen (MV; Sigma-Aldrich, USA) as the electron donor or *P. furiosus* ferredoxin reduced by *P. furiosus* POR (Chandrayan *et al*., 2012). The POR-linked assay contained 100 mM EPPS pH 8.4, 10 mM Na-pyruvate, 0.2 mM coenzyme A, 0.4 mM TPP, 2 mM $MgCl_2$, and 2 mM DTT, POR (30 μg/ml) and ferredoxin (100 μg/ml). The DT-ferredoxin assay contained 100 mM EPPS pH 8.4, 5mM sodium dithionite and ferredoxin (100 μg/ml). Hydrogen uptake assay was performed by using methyl viologen as an electron acceptor in vials saturated with hydrogen. Oxygen sensitivity assays were carried out by exposing the MBH

sample (100 μg/ml) in 50 mM Tris, pH 8.0, containing 400 mM NaCl and 4 mM DTT to air while shaking (30 rpm). Samples were taken at 0, 2, 4, 8, 16 and 32 hr to determine residual hydrogenase activity. Thermal stability at 90^0C was carried out in the same fashion except that the samples were maintained under anaerobic conditions. The H_2 evolution assay at different temperatures was done using 50 μg of each form of MBH (C-MBH, S-MBH, and washed membranes).

Purified C-MBH was analyzed by electrophoresis using 4-20% Tris-Glycine NUSEP gels (Bio-Rad, USA). Bands were cut from the SDS-PAGE gel, digested with trypsin and were analyzed by MALDI-TOF. Nickel and iron were measured using an octopole-based ICP-MS (7500ce Agilent Technologies, Tokyo, Japan)), equipped with a MicroMist nebulizer (Cvetkovic *et al*., 2010). X-band (~9.6 GHz) electron paramagnetic resonance (EPR) spectroscopy was carried out using a Bruker ESP-300E EPR spectrometer equipped with an ER-4116 dual-mode cavity and an Oxford Instruments ESR-9 flow cryostat.

Temperature Studies

MW0414 was grown in a 20-L fermenter at 90^0C and switched to 72^0C as previously described (Keller *et al*., 2013). C-MBH was purified as described above.

RESULTS

Construction of P. furiosus to generate C-MBH

We previously deleted the catalytic subunit from MBH (*mbhL*) and showed that a functional complex was required for growth (in the absence of elemental sulfur) (Schut *et al*. 2012). In order to obtain a 'minimal' subcomplex of MBH, we decided to engineer the native MBH operon

by splitting it into two separate transcriptional units. The first nine genes (*mbhA-I*) of the operon would be under the control of the native MBH promoter, while the last five genes (*mbhJ*-N) are under control of the stronger P_{slp} promoter that controls constitutive expression of the gene encoding the S-layer protein (Fig. 2). At the same time, an affinity-purification tag (His_9) was inserted within the operon at the N-terminus of *mbhJ* (the hydrogenase "small" subunit). We decided to tag the small subunit of MBH as this tag position was effective for the affinity purification of the intact 14-subunit complex (S-MBH) (McTernan *et al*., 2014). Hence, as shown in Fig. 3, in the engineered strain MW0414, the 14-gene MBH operon is expressed as two transcripts, *mbhA-I* and *mbhJ-N.* If the two protein products (MbhA-I and MbhJ-N) were able to combine and give a functional 14-subunit complex, then *P. furiosus* would be able to grow (Schut *et al*. 2012). However, due to the relative strengths of the native promoter for MBH (P_{mbh}) and P_{slp}, we expected that there would be excess *mbhJ-N* transcript relative to *mbhA-I.* Assuming that the transcripts were similarly stable (see below) and were translated with the same efficiency, then MbhJ-N, a potentially soluble form of the enzyme, should be generated in excess of that which combines with MbhA-I to generate functional MBH. Moreover, it should be possible to purify soluble MbhJ-N from the cytoplasmic fraction by its affinity tag (on MbhJ).

Q-PCR analysis

There was no difference in growth of MW0414 or the parent strain (data not shown), and the specific activity of washed membranes from COM1 and from MW0414 were the same (approx. 1.0 U/mg). This confirmed that the native MBH complex in MW0414 was intact and functional despite being synthesized and assembled from two different subcomplexes encoded by two different transcriptional units (Fig. 3). We first used Q-PCR analysis to determine if the split MBH operon was indeed differentially expressed. The results showed that the *mbhJ-N* transcript

was approximately 2-fold higher than that of *mbhA-I* (Supplementary Fig. S1). Since SHI in the cytoplasm of *P. furiosus* is a very active enzyme, it was not expected that a soluble form of MBH would be detected by an increase in total cytoplasmic hydrogenase activity, and this proved to be the case. Nevertheless, if an intact soluble form of MBH was produced in the cytoplasm, it should be possible to purify it using its affinity tag.

Affinity purification and characterization of affinity-tagged C-MBH

The cytoplasmic extract of MW0414 was applied to a Ni-NTA column and after washing with buffer a significant amount of hydrogenase activity was eluted with a histidine gradient. Hence, it appeared that a soluble His-tagged subcomplex of MBH had been produced, and this was further purified using a Mono-Q anion exchange column. A total of 21 mg of protein containing 12 units of hydrogenase activity (using methyl viologen as the electron donor) eluted from the Ni-NTA column and 12 mg of protein was obtained from the Mono-Q with no loss of activity.

From the molecular analysis (Fig. 4), the second transcript should yield a 5-subunit MbhJ-N complex but MbhM is predicted to be membrane-associated. Analyses by SDS-PAGE revealed that S-MBH was tetrameric (MbhJKLN) rather than pentameric (MbhJ-N) and lacked MbhM. Protein bands corresponding to the calculated molecular weights for all four subunits were evident on the gel. Note that the catalytic subunit, MbhL (calculated MWt of 47,903 Da) is predicted to undergo C-terminal proteolysis during the processing of the [NiFe]-site with the removal of 47 amino acids. This proved to be the case as the band on the gel was consistent with the calculated mass of the mature processed subunit (42,899 Da). The presence of MbhJKLN in

C-MBH was confirmed by LC-MS/MS analysis from trypsin-digested in-solution samples (Table S1).

Purified C-MBH was analyzed using a calibrated S-200 gel filtration column and eluted as a single peak corresponding to a mass of 85 ± 5 kDa (Supplementary Fig. S2). The predicted mass of the MbhJKLN complex calculated from the deduced amino acid sequences is 97 kDa, suggesting that all four subunits are present but that the subcomplex is not globular in shape. To gain a further understanding as to which subunits are associated with C-MBH, we analyzed the purified protein with both ICP-MS and electron paramagnetic resonance (EPR). Purified C-MBH contained both iron and nickel in a ratio of 14:1 (Table 1). This result supports the proposed presence of three [4Fe-4S] clusters in the enzyme (Fig. 4), which together with the [NiFe] active site should give a predicted Fe:Ni ratio of 13:1. The anaerobically purified protein after reduction with sodium dithionite exhibited a complex rhombic EPR signal at 6K that could be attributed to multiple $[4Fe\text{-}4S]^{1+}$ clusters (Supplementary Fig. S3). A schematic of purified C-MBH containing four subunits (MbhJKLN) is shown in Fig. 4

MBH uses reduced ferredoxin as an electron donor *in vivo* and the redox protein is proposed to interact with MbhN (Fig. 1) (Schut *et al*., 2013). C-MBH also evolves H_2 using ferredoxin as the electron donor at 80°C, both when reduced by sodium dithionite or by the native pyruvate ferredoxin oxidoreductase (Table 1). The ability of the subcomplex to catalyze the physiological reaction is also consistent with all three [4Fe-4S] clusters being intact and functional in C-MBH. The ratio H_2 evolution to H_2 oxidation by C-MBH using methyl viologen as the electron carrier was 13:1, which is lower than that measured for the membrane-bound form (26:1) but this still demonstrates that this subcomplex version of MBH prefers to evolve hydrogen rather than oxidize it. C-MBH and the washed membrane control were similarly

insensitive to inactivation by oxygen, with half-lives under air while shaking of approximately 13 hrs.

Temperature studies of C-MBH

Purified C-MBH was assayed at different temperatures in order to gain a better understanding of its H_2 evolution activity. It was observed that C-MBH had a different temperature profile in comparison to the form of MBH present in washed membranes (WM) or as the solubilized, purified 14-subunit complex (S-MBH) (Fig. 5). With reduced methyl viologen as the electron donor, C-MBH had maximal activity at 60^0C and was inactive at 90^0C. In comparison the S-MBH and WM forms of MBH were maximally active at or above 90°C. Accordingly, H_2 evolution by C-MBH using ferredoxin, the physiological electron donor to MBH, was measured at 60°C (Table 1), and was higher than the activity measured at 80^0C. C-MBH therefore appeared to be less thermostable than MBH in the washed membrane and this proved to be the case during extended incubation at high temperature. Purified C-MBH had a half-life at 90^0C of 8 hr, which compares with 25 hr for MBH in the washed membrane (Table 1).

We therefore wondered if the yield of purified C-MBH could be improved if the recombinant *P. furiosus* strain was grown at a temperature lower than 90°C, where the enzyme might be unstable and subject to proteolytic digestion. The MW0414 strain was therefore grown in a 20-liter fermenter at 72^0C (Keller *et al*., 2013). Cytoplasmic extracts were prepared from cells grown at 90^0C and at 72°C and C-MBH was purified as described above using two chromatography steps. The yield of C-MBH from the cells grown at the lower temperature was more than twice (9.0 mg vs 4.0 mg) that obtained from cells grown at the higher temperature, indicating that thermal degradation of the enzyme does occur during growth at 90°C. Primers for

Q-PCR were designed to bind the first gene under control of either P_{mbh} (PF1423, *mbhA*) or P_{slp} (PF1432, *mbhJ*) of the MBH operon (Fig. 3). The concentration of RNA was 2-fold higher when generated from the P_{slp} promoter throughout growth compared to the native MBH promoter and this was independent of the temperature shift from 90^0C to 72^0C (Supplementary Fig. S1).

DISCUSSION

Herein we describe the first successful attempt to engineer a cytoplasmic "minimal" catalytically-active subcomplex of a membrane bound respiratory hydrogenase. We had previously generated a smaller form of the heterotetrameric cytoplasmic SHI from *P. furiosus* (Hopkins *et al*., 2011). This was achieved by expressing just two of the four genes that encode the enzyme in a strain in which all four genes had been deleted. However, it was not possible to express simply part of the 14-gene operon encoding MBH since it impossible to obtain a strain of *P. furiosus* lacking a functional MBH. We therefore engineered the MBH operon by splitting the 14-gene operon into two separate transcriptional units. This approach was risky as it was not known if the protein products of the two different transcripts would be able to find each other and assemble into a functional MBH complex (Fig. 3), which would enable *P. furiosus* to grow, and if so, would the excess subunits form a functional complex in the cytoplasm. All of this proved to be the case, however, as the over-expressed part of the MBH operon generated a stable cytoplasmic protein with hydrogenase activity, although it contained four (MbhJKLN) rather than the expected five subunits (MbhM was not present). These results show that, surprisingly, splitting and disrupting the MBH operon still produced a functional MBH, and we were able to purify the cytoplasmic subcomplex using the engineered affinity tag.

We also expected to see a 1:1 ratio of MBH activity in the membrane (from 14-subunit MBH) and in the cytoplasmic fraction (from MbhJKLN) based on our Q-PCR data. However, measured at 80°C using the DT-MV H_2 evolution assay, the activity of C-MBH was only about 10% of that of S-MBH purified from the same batch of cells grown at 90°C (McTernan *et al*., 2014). However, the activity of C-MBH roughly doubled when assayed at 60^0C versus 80^0C (Fig. 5), so the Ni-NTA purified C-MBH represents about 20% of the MBH activity present in the membrane in cells grown at 90^0C (with no temperature switch). That this was lower than expected is unlikely to be due to the five-subunit version of C-MBH (MbhJ-N) remaining in the membrane (MbhM is predicted to be membrane-associated) since there was no increase in the hydrogenase activity (measured at 80°C) in the membrane. The lower than expected C-MBH activity is more likely due to the thermolability of the subcomplex, and this is supported by the finding that the yield of C-MBH increased more than two-fold when cells were grown at 72°C. The amounts of activity and protein associated with purified C-MBH doubled when cells were grown at a lower temperature (90^0C then switched to 72^0C). Hence, from cells grown at 72^0C we are able to purify the equivalent of about 40% of MBH found in the membranes. Either the remainder is lost due to the low thermal stability of C-MBH or the two transcripts generated from the MBH operon are not translated with the same efficiency.

That purified C-MBH was less stable than S-MBH is not unexpected given that C-MBH lacked 10 partner subunits. What is surprising, however, is that C-MBH retained the very unusual catalytic preference of S-MBH (Table 1). In *in vitro* assays using dyes such as methyl viologen as electron carriers, [NiFe]-hydrogenases preferentially oxidize H_2, often by orders of magnitude (Vignais and Billoud, 2007). *P. furiosus* MBH is therefore atypical in that it preferentially catalyzes H_2 evolution by a ratio of approximately 26:1 in the standard assays

(Table 1). It was assumed that this may arise because of the large complex nature of this membrane-bound enzyme where electron transfer is coupled to both H^+ and Na^+ pumping, which might account for the catalytic preference for the physiological reaction of H_2 production. However, the results presented herein show that this is a property of the cytoplasmic component of MBH that is independent of the ion-pumping membrane component. Stability assays of C-MBH showed that it was just as resistant to inactivation by O_2 as the native 14-subunit complex, suggesting that the infrastructure of the catalytic subunit is maintained in the cytoplasmic form when it is dissociated from the other ten subunits.

Generation of a cytoplasmic catalytic subcomplex of this respiratory hydrogenase is a significant achievement. In particular, obtaining relatively large amounts of the heterotetrameric soluble complex in the absence of any detergent greatly facilitates structural analyses of this representative of the poorly studied group 4 hydrogenases, with implications for the evolution of complex I, and such studies are in progress.

REFERENCES

1.) Batista,A.P., Marreiros,B.C., and Pereira,M.M. (2013) *Biol. Chem.,* **394**, 659–666.

2.) Böhm,R., Sauter,M., and Böck,A. (1990) *Mol. Microbiol.,* **4**, 231–243.

3.) Chandrayan,S.K., McTernan,P.M., Hopkins,R.C., Sun,J., Jenney,F.E. and Adams,M.W.W. (2012) *J. Biol. Chem.,* **287**, 3257-3264.

4.) Cvetkovic,A. *et al*.(2010) *Nature,* **466**, 779-782.

5.) Efremov,R.G., Baradaran,R. and Sazanov,L.A. (2010) *Nature,* **465**, 441-445.

6.) Fiala,G., and Stetter,K. (1986) *Arch. Microbiol.,* **145**, 56-61.

7.) Fontecilla-Camps,J.C. (2009) *Met. Ions Life Sci.,* **6**, 151-78.

8.) Friedrich,B., Fritsch,J. and Lenz,O. (2011) *Curr. Opin. Biotechnol.,* **22**, 358-64.

9.) Grzeszik,C., Ross,K., Schneider,K., Reh,M., Schlegel,H.G. (1997) *Arch. Microbiol.,* **167**, 172–176.

10.) Hedderich,R. (2004) *J. Bioenerg. Biomembr.,* **36**, 65-75.

11.) Hedderich,R.F.,L. (2005) *J. Mol. Microbiol. Biotechnol.,* **10**, 92-104.

12.) Hopkins,R.C., Sun,J., Jenney,F.E.,Jr., Chandrayan,S.K., McTernan,P.M., and Adams, M.W.W. (2011) *PLOS One,* **6**, e26569.

13.) Horton,R.M., Hunt,H.D., Ho,S.N., Pullen,J.K., and Pease,L.R. (1989) *Gene.,* **77**, 61-68.

14.) Keller,M.W. *et al*. (2013) *Proc. Natl. Acad. Sci.,* **110**, 5840-5845.

15.) Kurkin,S., Meuer,J., Koch,J., Hedderich,R., and Albracht,S.P.J. (2002) *Eur. J. Biochem.,* **269**, 6101-6111.

16.) Lee,H.S., Vermaas,W.F., and Rittmann,B.E. (2010) *Biotechnol.,* **28**, 262-271.

17.) Lipscomb,G.L., Stirrett,K., Schut,G.J., Yang,F., Jenney,F.E.,Jr., Scott,R.A., Adams,M.W., and Westpheling,J. (2011) *Appl. Environ. Microbiol.,* **77**, 2232-2238.

18.) Marreiros,B.C., Batista,A.P., Duarte,A.M. and Pereira,M.M. (2013) *Biochimica et Biophysica Acta.,* **1827**, 198-209.

19.) McTernan, P.M., Chandrayan, S.K., Wu, C.-H., Vaccaro, B.J., Lancaster, W.A., Yang, Q., Fu, D., Hura,G.L., Tainer,J.A. and Adams,M.W.W.(2014) *J. Biol. Chem*., doi:10.1074/jbc.M114.567255.

20.) Meuer,J., Bartoschek,S., Koch,J., Kunkel,A. and Hedderich,R. (1999) *Eur. J. Biochem.,* **265**, 325-335.

21.) Sapra,R., Verhagen,M.F. and Adams,M.W. (2000) *J. Bacteriol.,* **182**, 3423-3428.

22.) Sauter,M., Böhm,R., Böck,A. (1992) *Mol. Microbiol.,* **6**, 1523–1532.

23.) Sazanov,L.A., and Hinchliffe,P. (2006) *Science,* **311,**1430-1436.

24.) Schut,G.J., Nixon,W.J., Lipscomb,G.L., Scott,R.A., and Adams,M.W.W. (2012) *Front. Micro*., **3**, 1-6.

25.) Schut,G.J., Boyd,E.S., Peters,J.W., and Adams,M.W.W. (2013) *FEMS Microbiol. Rev.,* **37**, 182-203.

26.) Shafaat,H.S., Rudiger,O., Ogata,H. and Lubitz,W. (2013) *Biochimica et Biophysica Acta.,* **1827**, 986-1002.

27.) Silva,P., Van den Ban,E.C.D., Wassink,H., Haaker,H., de Castro,B., Robb,F.T, and Hagen,W.R. (2000) *Eur. J. Biochem.,* **267**, 6541-6551.

28.) Swartz,T.H., Ikewada,S., Ishikawa,O., Ito,M. and Krulwich,T.A. (2005) *Extremophiles,* **9**, 345-354.

29.) Vignais,P., and Billoud,B. (2007) *Chem. Rev.,* **107**, 4206-4272.

30.) Vitt,S., Ma,K., Warkentin,E., Moll,J., Pierik,A.J., Shima,S., and Ermler,U. (2014) *J. Mol. Biol.,* **426**, 2813-2826.

31.) Volbeda,A., Charon,M.H., Piras,C., Hatchikian,E.C., Frey,M. and Fontecilla-Camps,J.C. (1995) *Nature,* **373**, 580-7.

32.) Volbeda,A., Darnault,C., Parkin,A., Sargent,F., Armstrong,F.A. and Fontecilla-Camps,J.C. (2013) *Structure,* **21**, 184-90.

Table 4.1. Characterization of Purified C-MBH

Property	C-MBH	Washed Membrane
DT-Fd H_2 evolution activity (U/mg) at 80°C	0.03	0.05
DT-Fd H_2 evolution activity (U/mg) at 60°C	0.06	0.01
POR-Fd H_2 evolution activity (U/mg) at 80°C	0.004	0.02
H_2 evolution:oxidation activity (MV as electron carrier) at 80°C	13:1	26:1
Half-life ($t_{1/2}$, hr) at 90°C under argon	8 hr	25 hr
Half-life ($t_{1/2}$, hr) at 25°C under air	13 hr	13 hr
Metal Content (Fe:Ni)	14:1	19:1

Figure 4.1

Comparison of homologous subunits between MBH, complex I and Mrp antiporter. Nqo numbers are given for each *T. thermophilus* complex I subunit with the correlated *Nuo* letter in parenthesis. Red subunits represent the catalytic subunits and include mbhL and nuoD. Orange subunits represent the Q module and include mbhJKLN and nuoBCDI. Aqua colored subunits are homologous and include mbhH, nuoLMN, and mrpAD. Blue subunits are homologs to mbhM and include nuoH. Light green subunits are homologous to mbhG and include mrpC. Green subunits are homologous to mbhABC and include mrpEFG. Grey subunits are homologous to mbhDEF and include mrpB. Yellow subunits represent the N module of complex I and include nuoEFG. MbhI is shown in red and the dark blue subunits represent nuoAJK. Tan subunits represent two subunits that were observed in the 16-subunit crystal structure of Nqo from *T. thermophiles* (Efremov *et al*., 2010). There is no homology between the three complexes for *mbhI*, *nuoAEFGJK* or *Nqo15-16*. Fd_{red} and Fd_{ox} represent reduced and oxidized ferredoxin, respectively, and QH_2 and Q represent reduced and oxidized ubiquionone, respectively.

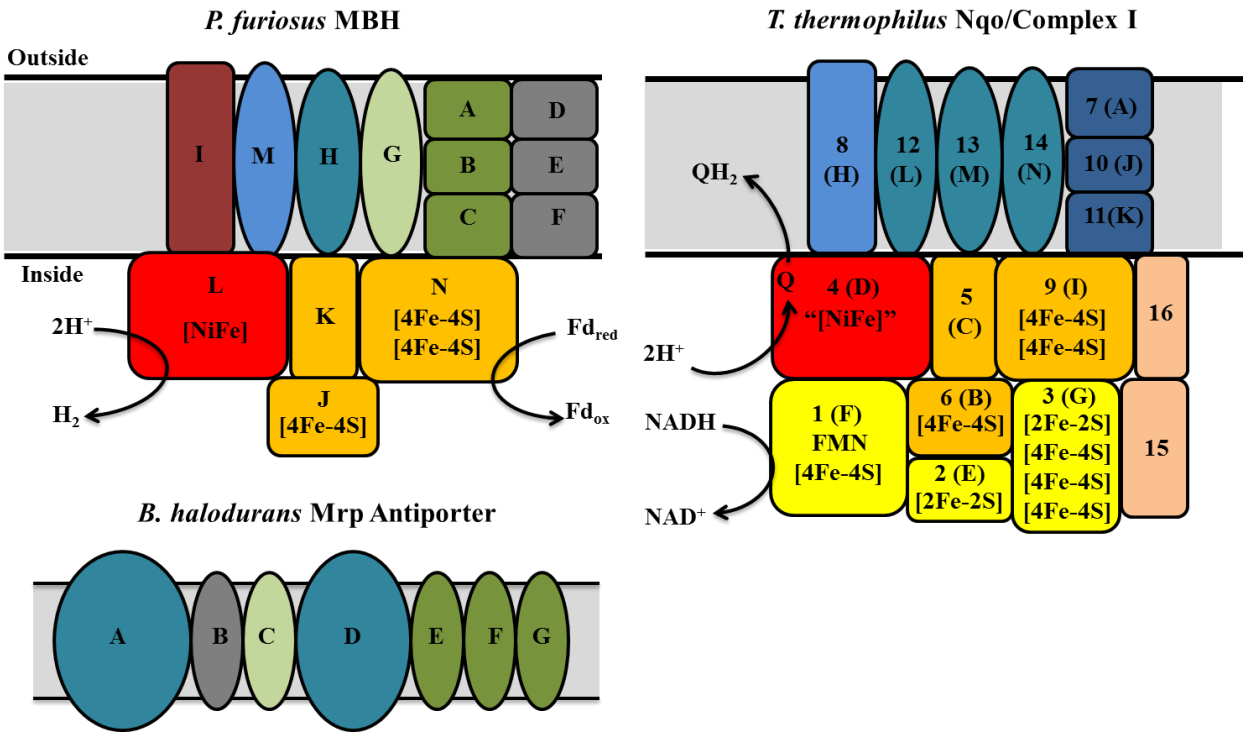
P. furiosus MBH
Outside
Inside
I
M
H
G
A
B
C
D
E
F
L
[NiFe]
K
N
[4Fe-4S]
[4Fe-4S]
J
[4Fe-4S]
2H+
H2
Fdred
Fdox
T. thermophilus Nqo/Complex I
QH2
8
(H)
12
(L)
13
(M)
14
(N)
7 (A)
10 (J)
11(K)
Q
4 (D)
"[NiFe]"
5
(C)
9 (I)
[4Fe-4S]
[4Fe-4S]
16
2H+
NADH
NAD+
1 (F)
FMN
[4Fe-4S]
6 (B)
[4Fe-4S]
2 (E)
[2Fe-2S]
3 (G)
[2Fe-2S]
[4Fe-4S]
[4Fe-4S]
[4Fe-4S]
15
B. halodurans Mrp Antiporter
A
B
C
D
E
F
G

Figure 4.2

The genetic strategy used to insert the His_{9x} tag and to overexpress last five genes (*mbhJ-N*) of the MBH operon relative the first nine genes (*mbhA-I*). The tag is inserted at the N-terminus of *mbhJ*. The abbreviations are: UFR and DFR, upstream and downstream flanking regions (1 kb) of the MBH operon; *pyrF*, selectable marker; P_{gdh} and P_{slp}, promoters for the gene encoding glutamate dehydrogenase and the S-layer protein of *P. furiosus,* respectively.

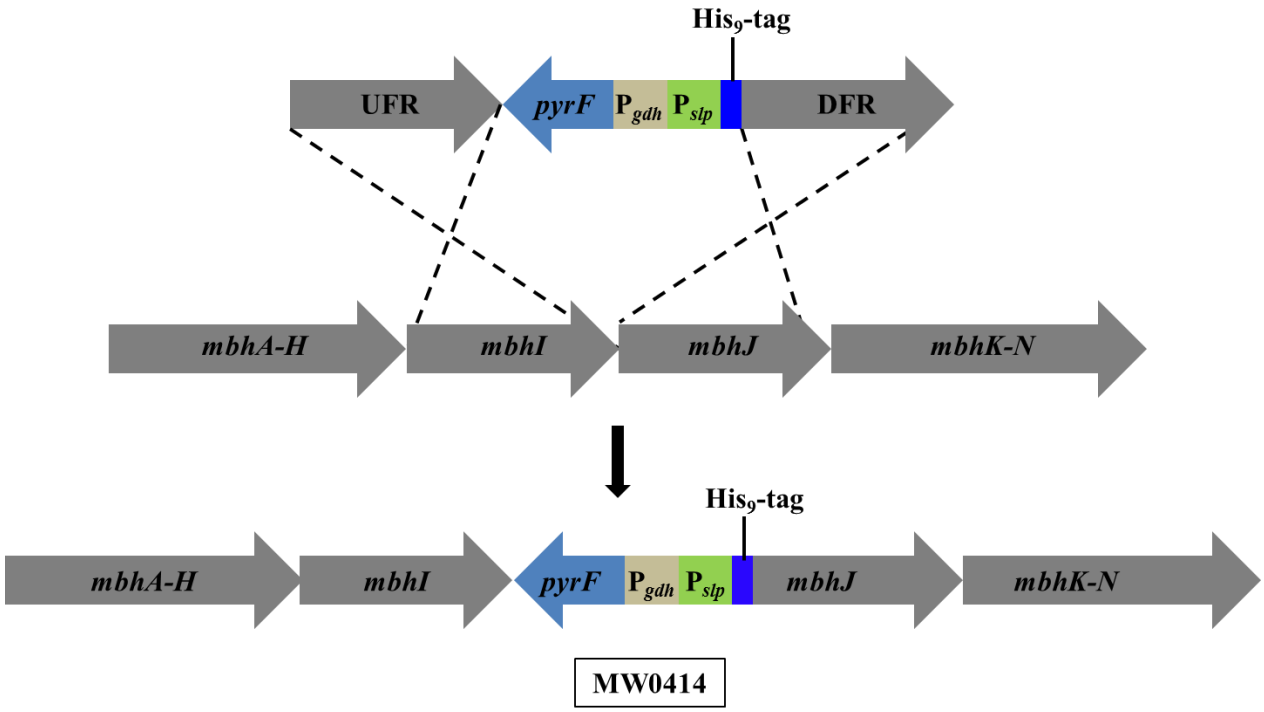
His9-tag
UFR
pyrF
Pgdh
Pslp
DFR
mbhA-H
mbhI
mbhJ
mbhK-N
His9-tag
mbhA-H
mbhI
pyrF
Pgdh
Pslp
mbhJ
mbhK-N
MW0414

Figure 4.3

Transcription of the engineered MBH operon. (A) Schematic showing the transcribed products of the two different transcriptional units of the engineered MBH operon. The abbreviations are: $P_{mbh,}$ the native MBH promoter that controls the expression of *mbhA-I; pyrF*, selectable marker; $P_{gdh,}$ promoter for the gene encoding glutamate dehydrogenase; P_{slp}, promoter for the S-layer protein that controls the expression of *mbhJ-N*. Based on Q-PCR analysis, *mbhJ-N,* under the control of P_{slp}, were expressed at twice the level of *mbhA-I,* under the control of the native P_{mbh}.

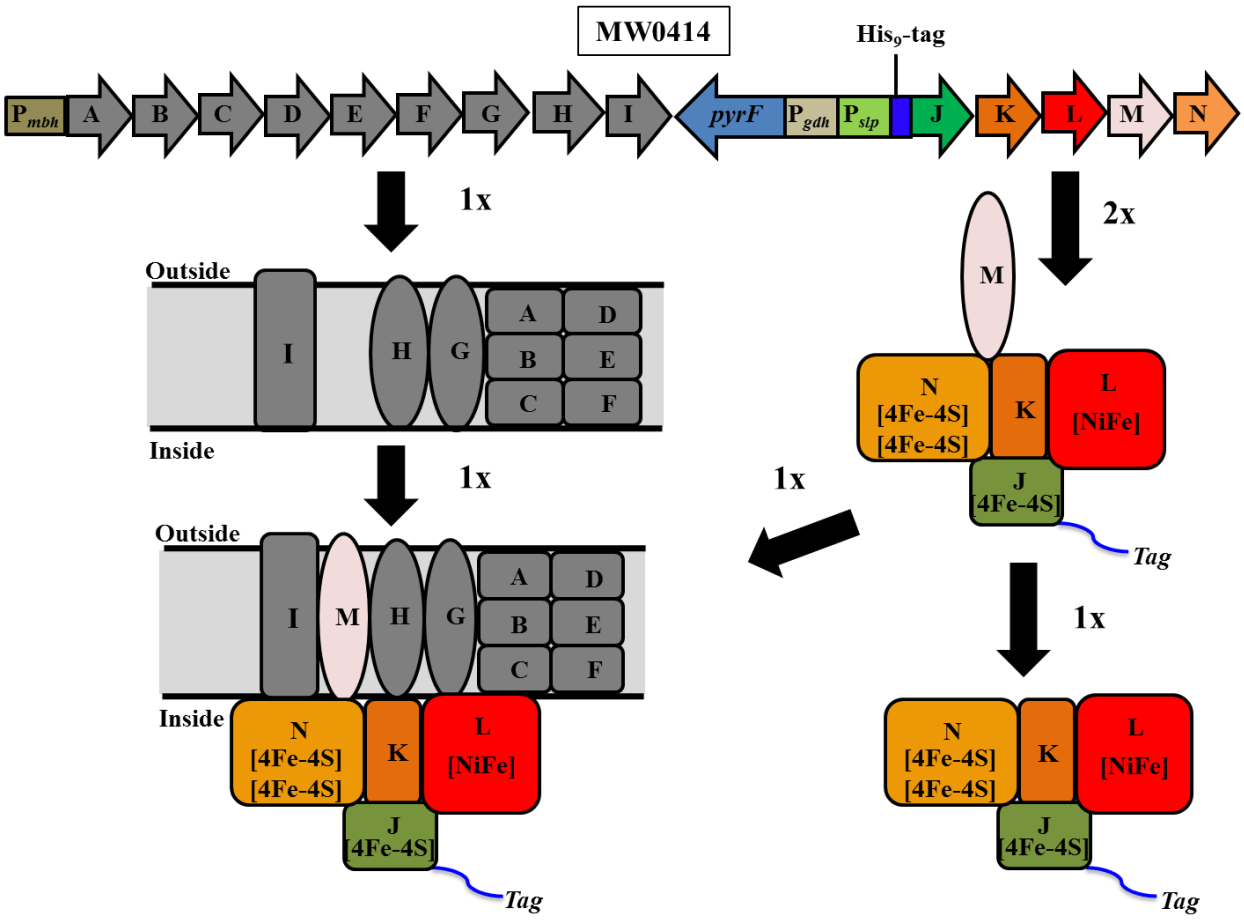
MW0414
His9-tag
Pmbh
A
B
C
D
E
F
G
H
I
pyrF
Pgdh
Pslp
J
K
L
M
N
1x
2x
Outside
Inside
I
H
G
A
B
C
D
E
F
M
N
[4Fe-4S]
[4Fe-4S]
K
L
[NiFe]
J
[4Fe-4S]
Tag

Figure 4.4

SDS-PAGE of purified *C*-MBH. Left: MBH subunits identified by LC-MS/MS are labeled with a black arrow. Right: Schematic of C-MBH showing location of the affinity-tag. MbhL harbors the [NiFe] active site, MbhK is part of the large subunit, MbhJ harbors one [4Fe4S] cluster, and MbhN harbors two [4Fe4S] clusters. Fd_{red} and Fd_{ox} represent reduced and oxidized ferredoxin, respectively.

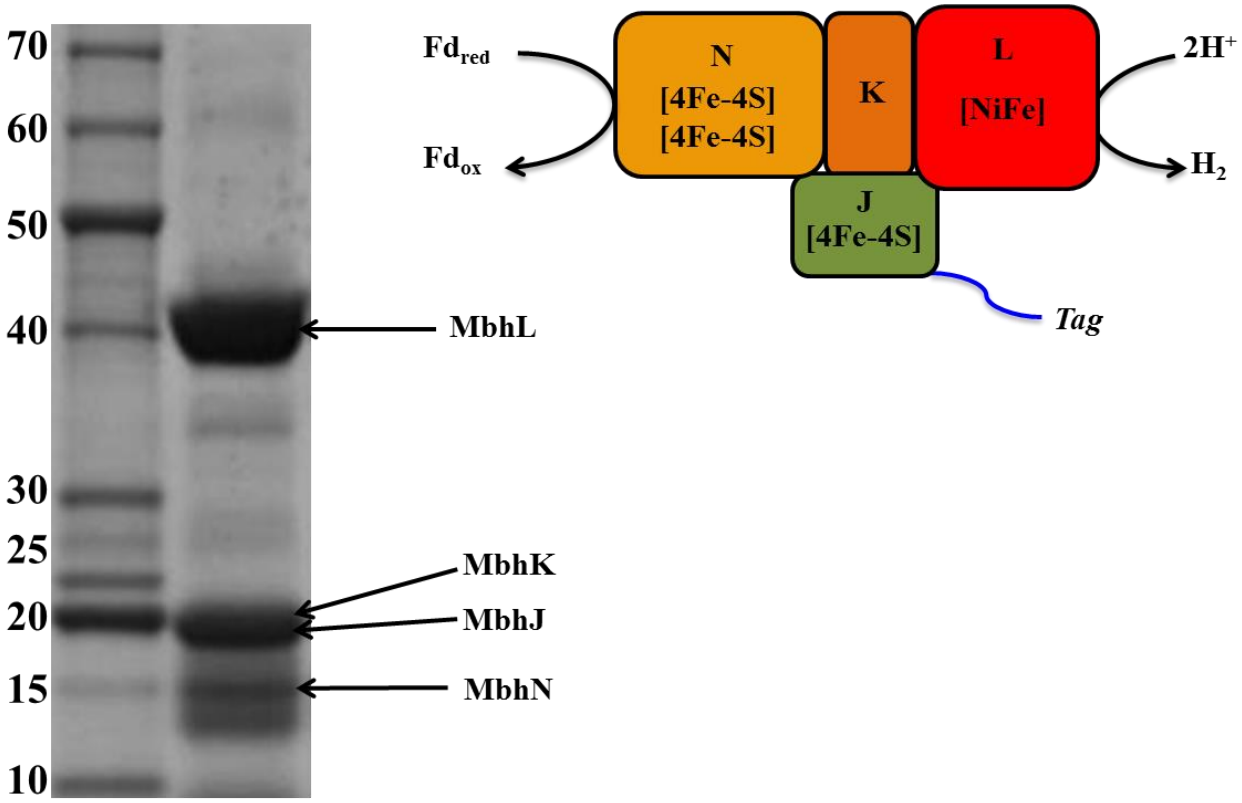
70
60
50
40
30
25
20
15
10
MbhL
MbhK
MbhJ
MbhN
Fd$_{red}$
Fd$_{ox}$
N
[4Fe-4S]
[4Fe-4S]
K
L
[NiFe]
2H$^+$
H$_2$
J
[4Fe-4S]
Tag

Figure 4.5

Temperature profile for C-MBH activity. The H_2 evolution activity using reduced methyl viologen as the electron donor of C-MBH (circular symbols), washed membranes (WM, square symbols) and solubilized and purified MBH (S-MBH, triangles) is shown.

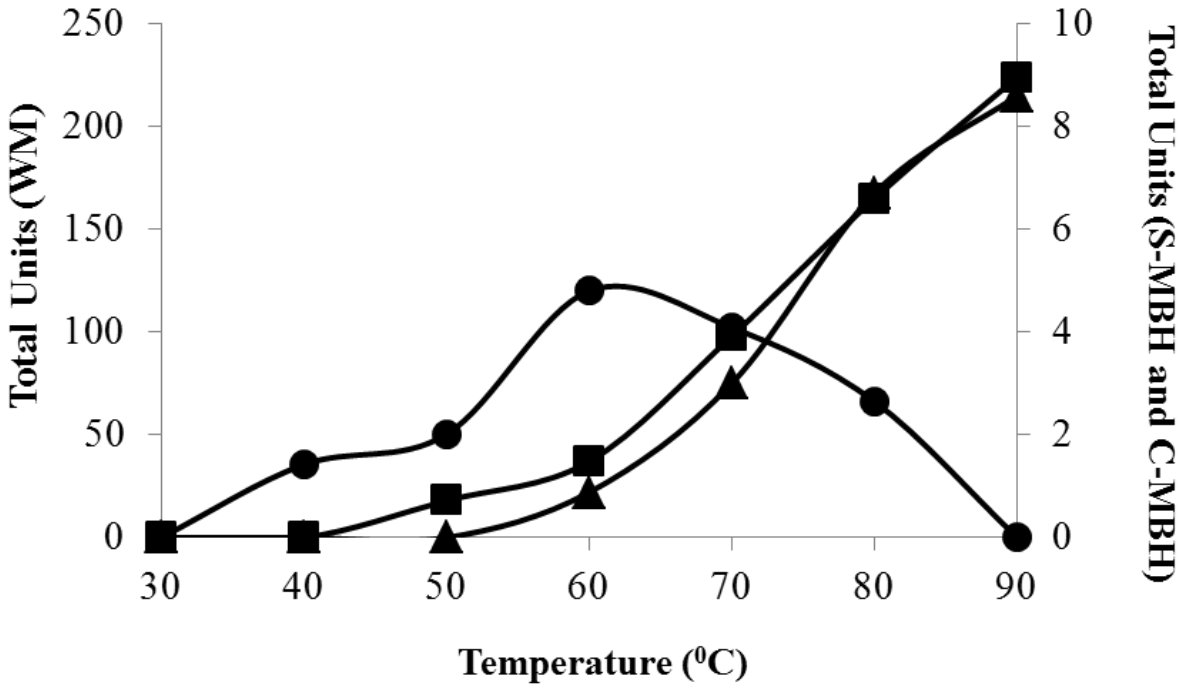
250
200
150
100
50
0
Total Units (WM)
10
8
6
4
2
0
Total Units (S-MBH and C-MBH)
30
40
50
60
70
80
90
Temperature (⁰C)

CHAPTER 5

SUMMARY AND CONCLUSIONS

The genetically competent strain of *P. furiosus*, termed strain COM1, was used for all genetic manipulations of its hydrogenases. I chose to use SHI as a simple model [NiFe]-hydrogenase to see if the *P. furiosus* genetic system could be used for future studies on the much more complex membrane-bound [NiFe]-hydrogenase (MBH). This genetic system used to place different types of affinity tags as well as a stronger promoter in front of the SHI operon. I found that the tag used to purify SHI had a major influence on the yield, as well as the reproducibility of the purification. In Chapter 2, I showed the successful affinity purification of SHI using the strep-II tag. This tag worked but was not very efficient. The purification procedure needed at least three chromatography columns linked together and the flow-through had to be run over the column three times in order to achieve a high yield. This is not ideal for an affinity purification and thus we also investigated the use of a histidine tag for affinity purifications of SHI. We were reluctant to do this initially as the poly-histidine tag might the incorporation of Ni into the catalytic site of the enzyme. However, it was observed that the histidine tag did not have any of the issues that were observed with using the Strep-II tag and was reproducible. Thus, it seems that the histidine tag is better for the purification for the hydrogenases of *P. furiosus* and did not "strip" the Ni of the [NiFe] active site. The tag position is also important when engineering affinity tags and are usually added to the N- or C-terminus of a target protein. In the case of SHI, it was observed that the tagging of the N-terminus of the SHI operon (PF0891) and the N-terminus of PF0894 were accessible to the affinity column, but this is not always the case and will be discussed in more detail in the tagging of MBH below.

The use of the histidine affinity tag and the over-expression of the SHI operon using the strong S-layer protein promoter (P_{slp}) greatly improved the yield of this hydrogenase from *P. furiosus*. With a one-step purification procedure, we could obtain 4.2 mgs from 50 grams of cells. This compares with the standard chromatographic purification of native SHI in the parent strain that, after 4 chromatographic steps, yields 1.3 mgs of SHI from 50 grams of cells. As discussed above, SHI is a member of the group 3 category of [NiFe]-hydrogenases, which are poorly characterized compared to the well-studied group 1 enzymes. The availability of large amounts of SHI will enable structural analysis of this enzyme that will provide insights into how to make hydrogenases that are highly active, oxygen-tolerant, and have tailored enzymatic activity for biofuel production (237). SHI has also been used successfully for industrial and practical applications. One report used SHI, together with a cocktail of 15 other enzymes, in the conversion of sugars to hydrogen gas (238, 239). Sucrose and water were converted into hydrogen gas and in batch reactions yielded 23.2 moles of dihydrogen per mole of sucrose, which is very close to 100% of the theoretical yield of 12 dihydrogen per hexose (239). Another application of SHI has been proposed to use this enzyme for the generation of NADPH at an industrial scale, which is the physiological reaction of the enzyme (240).

Based on the success of using the *P. furiosus* genetic system to tag an overproduce SHI, I then decided to use the same approach to purify the entire 14-subunit MBH. Previous attempts to purify MBH had met with limited success due to the complexity of this large membrane bound complex and their attempts yielded only 2-5 of its 14 subunits (187, 188). This was a start but the purification of the entire complex is needed in order to gain a better understanding of these enzymes, as not much is known about the structure and function of group 4 hydrogenases. These enzymes have very limited homology to other [NiFe]-hydrogenases, including those

hydrogenase that already have crystal structures. In chapter 3, I showed that I can purify the entire 14-subunit MBH complex to homogeneity using a histidine tag and have characterized the purified enzyme both enzymatically and structurally. MBH is unique compared to other [NiFe]-hydrogenases in that it has a high preference to catalyze H_2 evolution over H_2 oxidation (25:1). From a biofuel standpoint, understanding why MBH prefers to evolve hydrogen could be a major breakthrough in the development of new biocatalysts that evolve large quantities of hydrogen. One of the best ways to understand this preference of MBH would be to obtain a crystal structure of the entire enzyme complex and compare its active site structure to the structure of those available for the conventional group 1 hydrogenases, all of which preferentially catalyze hydrogen oxidation in the standard dye-linked assays.

An important factor in the purification of MBH was the use of the correct detergent in order to solubilize the entire complex from the membrane. In previous studies of MBH, the detergents tested were sodium deoxycholate and n-dodecyl-β-D-maltoside (DDM). Sodium deoxycholate is an ionic detergent that yielded approximately five subunits of MBH (MbhJKLMN), but the detergent was found to "kill" the activity of the solubilized complex if incubated with it for more than 2 hours (188). DDM on the other hand is a non-ionic detergent that was shown to solubilize roughly just 2 subunits of MBH (MbhKL), although the activity is stable in this detergent (187). I chose to test another non-ionic detergent Triton-X 100, which had been successfully used previously to extract the entire ATP synthase complex from *P. furiosus* (190, 191). As shown in Chapter 3, use of this detergent (10%) at a low temperature (4^0C) lead to near complete (~80%) extraction of the complete 14-subunit MBH complex from the membrane. The lower temperature had a large effect on the amount of activity that was extracted from the membrane since at room temperature the yield of activity was only 30-40%.

The use of a low temperature to solubilize membrane proteins has been noted before in the literature as the protein of interest may be more stable at a lower temperature, which thus allows a higher chance to extract the entire membrane-bound complex (241). It is also interesting to note that the non-ionic detergent Triton-X 100 is the only detergent that has been shown to work in successfully extracting entire intact protein complexes from the membrane of *P. furiosus*. This suggests that it is best to work with non-ionic detergents for the extraction of membrane proteins from *P. furiosus*.

Unlike the tagging of SHI described above, the position of the tag in MBH was very important. My first attempt to tag MBH was done by engineering the tag at the C-terminus of the last gene in the MBH operon, *mbhN*. Attempts to purify MBH using this tag position were not efficient and the issues with this purification were assumed to be caused by the inaccessibility of the tag to the affinity column. Since the N-terminus of the first gene of the MBH operon, *mbhA*, encodes for a membrane bound protein, it was not ideal to try to tag this locus. Thus, in order to place the tag within the operon on one of the soluble MBH subunits, I split the operon into two different transcriptional pieces using the S-layer protein promoter (P_{slp}) to over-express the last 5 subunits encoded by the operon (MbhJ-N). The splitting of the operon will be discussed further below, but the placement of the tag at the N-terminus of MbhJ proved to be much more accessible to the affinity column and yielded an order of magnitude more MBH protein after affinity purification.

The new affinity purification protocol for MBH also opens the door for purifying other membrane proteins from *P. furiosus*. One potential candidate is the membrane-bound complex termed MBX, which is expressed exclusively when *P. furiosus* is grown in the presence of elemental S^0 (181). The physiological function of this protein is unknown and the purification of

the entire 13-subunit complex has still not been reported. Therefore, in order to gain a better understanding of the function of this protein, the established protocol for MBH could be used in order to purify the entire MBX complex. Besides native membrane-bound proteins in *P. furiosus*, heterologously-expressed membrane proteins might also be purified from *P. furiosus*. Recently, the 18-subunit membrane-bound formate hydrogen lyase (FHL) complex from *Thermococcus onnurineus* was expressed in *P. furiosus* and shown to be active when formate was added to the growth medium (242). This heterologously-expressed FHL complex could also be tagged using the MBH approach and attempts could be made to purify the entire 18-subunit complex. Thus, by using the established purification protocol for MBH, we can now purify any membrane-bound protein from *P. furiosus* whether it is natively or heterologously expressed.

Another advantage of having a method to tag and purify MBH is that we can now construct different types of MBH variants in order to better understand the function of each of its subunits. In a previous report, the catalytic subunit (MbhL) of MBH was deleted and the resulting strain grew on S^0 (when MBH is not expressed) but did not grow in the absence of sulfur (when MBH is highly expressed and evolves H_2) (243). Two potential mutants that could be generated would involve the removal of MbhA-G and MbhA-H. The ΔMbhA-G mutant would be predicted to evolve H_2 and generate a proton gradient as MbhH is thought to be the proton pump of MBH, but the Na^+-dependent ATP synthase would not be able to generate ATP. Thus, this mutant would generate only 2 ATP/glucose rather than the 3.2 ATP/glucose of the parent strain and is predicted not to grow as well as the parent strain. The ΔMbhA-H would not be expected to generate any proton gradient and would also be interesting to see if the MBH variant would be incorporated into the membrane. Both of these mutants could help in gaining a better understanding of the pumping properties of the Mrp subunits of MBH.

In Chapter 3, some insight into the structure of MBH was provided by small angle X-ray scattering (SAXS). From this approach, the shape of the entire 14-subunit MBH was determined and compared to the crystal structure of complex I from *Thermus thermophilus*. This "L-shaped" SAXS model fit very well with the crystal structure of Complex I and shows that these structures share a common structural shape. Although the SAXS model gave some good insights into the structure of MBH, a more refined structure at the amino acid level would give much more insight into the common themes found between MBH and Complex I. Further studies are needed for the structural characterization of the entire 14-subunit complex. Unfortunately, Triton-X 100 is not a compatible detergent for crystallography and thus further tests are needed to try and purify the entire 14-subunit complex from the membrane with a crystallography compatible detergent such as DDM (241). Triton-X 100 is not ideal for protein crystallography as huge protein-detergent complexes (PDC) are known to form using this detergent. These large PDCs cause major issues with interpreting structures of membrane proteins, as they basically "mask" any observable structure. Although Triton-X 100 is not compatible with crystallographic studies, it can be used for electron microscopy studies (191). This approach should be pursued further in order to generate a structure of MBH.

Another strategy to gain a structure of MBH would be to engineer a "minimal" soluble version of MBH that could be purified without the use of detergent. One report of the successful engineering of a "minimal" version of a hydrogenase complex was from our laboratory, wherein we generated a dimeric version of the heterotetrameric SHI from *P. furiosus* (216). In Chapter 4, I have shown the successful generation, by genetic manipulation, of a 4-subunit version of MBH that can be purified from the cytoplasm (C-MBH) without the use of detergent. This is a major development in the research of MBH as it allows us to characterize large amounts of a soluble

version of a normally membrane-bound protein that can be affinity purified very easily without the use of detergent.

As shown in Chapter 4, the engineering of C-MBH was done by splitting the native MBH operon into two different transcriptional units. Generally, when planning to engineer an affinity tag on a protein, the targets are the extremities of the protein of interest at either the N- or C-terminus of genes at the beginning or end, respectively, of the operon. This is believed to be the best course of action as interrupting the operon sequence with a "foreign" sequence would cause the operon not to be transcribed correctly. As shown in Chapter 4, I show an example of splitting the operon into two transcriptional units that yielded complete intact functional enzyme, while placing an affinity tag within the operon. From this strain, I was able purify both the entire 14-subunit MBH complex and the "soluble" MBH complex using a histidine tag at the small subunit (MbhJ). Thus, in the case of MBH, the position of the tag proved to be very important and this example should be useful for the tagging of other proteins in *P. furiosus*, as this shows there are more options for where to place an affinity tag on a target protein then just tagging the genes at the end of an operon.

C-MBH was characterized and was found to still harbor the catalytic preference to evolve hydrogen rather than oxidation (13:1). This observation was important from a structural perspective as it shows that the Mrp antiporter subunits are not responsible for constraining the hydrogenase subunits to function in only one direction. This suggests that the preference of MBH to evolve hydrogen over oxidizing it like "standard" hydrogenases is dependent on the structure and electronic environment of the active site of this enzyme. C-MBH was still active with reduced ferredoxin without the other partner subunits, which suggests that the interaction of reduced ferredoxin with the soluble subunits of MBH is independent from the rest of the

membrane-bound complex. From a structural perspective, this observation suggests that a crystal structure of C-MBH would be extremely useful as the protein is still correctly folded, active and should harbor all of the predicted metals. Comparison of such a structure with the structures of the group 1 "standard" hydrogen-oxidizing hydrogenases could have a major impact in understanding the preference of MBH to evolve hydrogen. This understanding could be very beneficial as it could be used to engineer these "standard" hydrogenases into an efficient hydrogen evolving-catalyst like MBH.

C-MBH was supplied to Dr. John Peters (Montana State University). His group obtained crystals and solved the structure to a resolution of 3.2 angstrom (Figure 5.1; 244). This is the first crystal structure of a group 4 hydrogenase and represents the hydrogenase subunits of MBH (MbhJKLMN). One interesting observation that has come from this crystal structure is the presence of a "membrane-bound" subunit (MbhM) with the four hydrophilic subunits of MBH (MbhJKLN). As shown in Figure 5.1, all five subunits (MbhJ-N) were observed in the structure, which suggests that MbhM is not the membrane anchor that holds these soluble hydrogenase subunits to the membrane, as previously predicted based on sequence comparisons with complex I. This suggests that MbhH and MbhM may be the subunits responsible for anchoring the four soluble subunits to the membrane. Comparison of this 5-subunit version of C-MBH with a crystal structure of the entire 14-subunit complex, if that could be obtained, could help answer these questions and enlighten us on how MBH is properly assembled into the membrane.

As stated in the introduction, MBH shares an evolutionary history with Complex I from the electron transport chain (Chapter 1). Complex I is found in all aerobic organisms, including higher eukaryotes, and one of the closest homologs of its catalytic subunit is the catalytic subunit of MBH. As stated in the introduction, the hydrophilic subunit MbhL is homologous to the

Figure 5.1

Crystal structure of *C*-MBH solved at 3.2 angstroms resolution. A schematic of the *C*-MBH units observed in the crystal structure is shown on the right. Modified from (244)

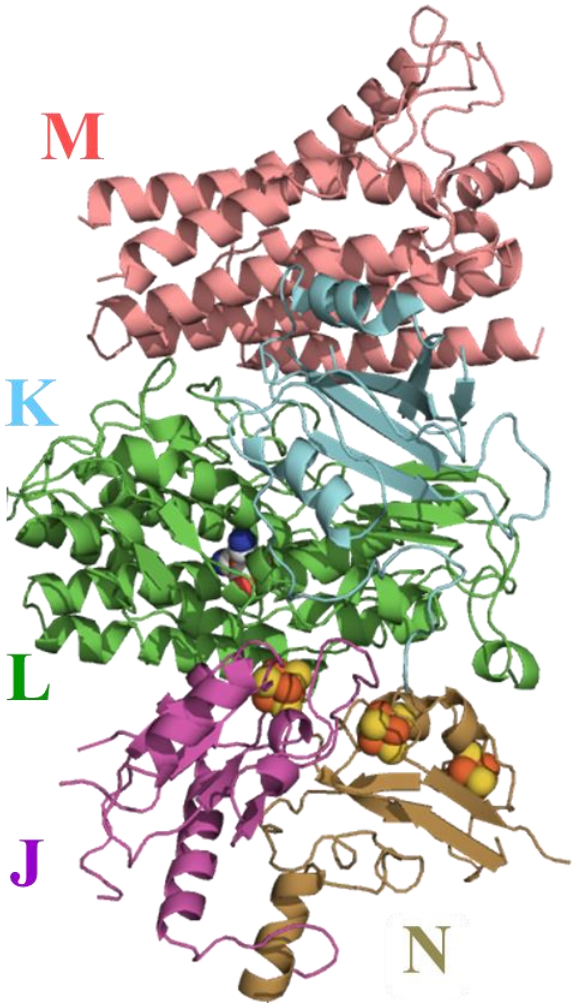
M
K
L
J
N

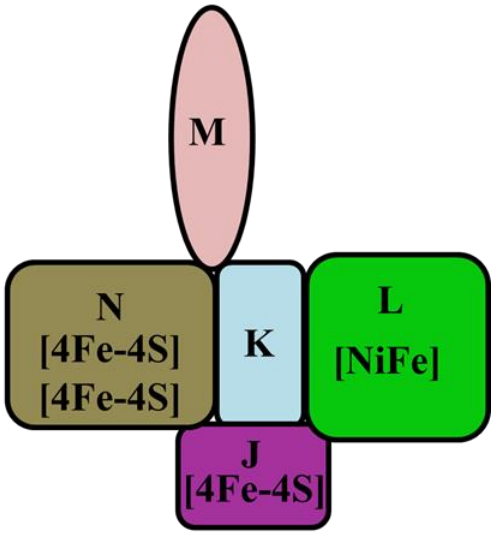
M
N
[4Fe-4S]
[4Fe-4S]
K
L
[NiFe]
J
[4Fe-4S]

catalytic subunit NuoD. The great similarity between these subunits is evident from their respective crystal structures. From an overlay of the two subunits, we can see where the cysteine residues of the hydrogenase that bind the [NiFe] site have been replaced in the Nuo structure. Specifically, the cysteines that coordinate the [NiFe] site, Cys 68, 71, 374, 376, have been replaced in NuoD with Asp 86, His89, Val403 and Asp406 respectively (244). These residues, as well as a critical tyrosine (Tyr87), are important in Nuo for binding quinone. This evolutionary transition from a [Ni-Fe] active site to a quinone binding site can be explained by the energetic need of more complex organisms to generate higher energy yields from their metabolism, which can be done by reducing quinones (E_0'= ~0 mV) instead of protons (E_0' = -420 mV, pH 7.0). Quinones can be "trapped" and used for subsequent oxidoreductase reactions, in which they are the electron donor, unlike hydrogen gas that diffuses from the cell. This transition in respiratory processes also lead to the use of quinones in other respiratory complexes such as arsenate reductase, polysulfide reductase, or nitrate reductases, which allowed organisms to use a variety of electron accepters to conserve energy. Thus, this transition of Nuo from MBH is believed to be a fundamental step in the generation of higher energy yields from respiration processes and is now used in almost all forms of life.

The development of a crystal structure of the hydrogenase module of MBH is potentially of great significance, as this enzyme and structure represent a huge step forward in hydrogenase research. From this structure, we can gain insight into why MBH prefers to evolve hydrogen compared to "standard" [NiFe]-hydrogenases. Also, this structure will help us understand how MBH and Complex I are similar/different at the structural level and shed insight into how these enzymes have evolved from a common ancestor over time. My project has also demonstrated the power of the *P. furiosus* genetic system and shows that this organism could be extremely

useful in the future for research of hyperthermophilic enzymes and proteins. Now that we have a protocol for the purification of MBH, the expression of recombinant membrane proteins from other hyperthermophiles can now be attempted using affinity tags and strong promoters for overexpression. This allows for the heterologous expression and purification of hyperthermophilic enzymes that cannot be purified from their native host. *P. furiosus* has the potential to be the hyperthermophilic "*E. coli*" of the future and can be engineered to express thermophilic proteins of all types for biochemical analysis and biofuel production.

REFERENCES

1. Leigh JA, Albers SV, Atomi H, Allers T (2011) Model organisms for genetics in the domain archaea: methanogens, halophiles, thermococcales and sulfolobales. FEMS Microbiology Reviews 35: 577-608.
2. Winker S, Woese C (1991) A definition of the domains Archaea, Bacteria, and Eucarya in terms of small subunit ribosomal RNA characteristics. Systematic Applied Microbiology 14: 305-310.
3. Blöchl E, Burggraf S, Fiala G, Lauerer G, Huber G, et al. (1995) Isolation, taxonomy and phylogeny of hyperthermophilic microorganisms. World Journal Microbiology and Biotechnology 11: 9-16.
4. Garrett RA, Klenk H-P (2008) Archaea: evolution, physiology, and molecular biology. John Wiley & Sons.
5. Woese CR, Fox GE (1977) Phylogenetic structure of the prokaryotic domain: the primary kingdoms. Proceedings National Academy of Sciences 74: 5088-5090.
6. Woese CR, Kandler O, Wheelis ML (1990) Towards a natural system of organisms: proposal for the domains Archaea, Bacteria, and Eucarya. Proceedings National Academy of Sciences 87: 4576-4579.
7. Huet J, Schnabel R, Sentenac A, Zillig W (1983) Archaebacteria and eukaryotes possess DNA-dependent RNA polymerases of a common type. European Molecular Biology Organization 2: 1291.
8. Olsen GJ, Woese CR (1996) Lessons from an archaeal genome: what are we learning from *Methanococcus jannaschii*? Trends Genetics 12: 377-379.

9. Rivera MC, Jain R, Moore JE, Lake JA (1998) Genomic evidence for two functionally distinct gene classes. Proceedings National Academy of Sciences 95: 6239-6244.
10. Yutin N, Makarova KS, Mekhedov SL, Wolf YI, Koonin EV (2008) The deep archaeal roots of eukaryotes. Molecular Biological and Evolution 25: 1619-1630.
11. Huber R, Dyba D, Huber H, Burggraf S, Rachel R (1998) Sulfur-inhibited *Thermosphaera aggregans* sp. nov., a new genus of hyperthermophilic archaea isolated after its prediction from environmentally derived 16S rRNA sequences. International Journal of Systematic Bacteriology 48: 31-38.
12. Brochier C, Gribaldo S, Zivanovic Y, Confalonieri F, Forterre P (2005) Nanoarchaea: representatives of a novel archaeal phylum or a fast-evolving euryarchaeal lineage related to *thermococcales*? Genome Biology 6: R42.
13. Brochier-Armanet C, Boussau B, Gribaldo S, Forterre P (2008) Mesophilic *crenarchaeota*: proposal for a third archaeal phylum, the *thaumarchaeota*. Nature Reviews Microbiology 6: 245-252.
14. Auchtung TA, Takacs-Vesbach CD, Cavanaugh CM (2006) 16S rRNA phylogenetic investigation of the candidate division "korarchaeota". Applied Environmental Microbiology 72: 5077-5082.
15. Barns SM, Delwiche CF, Palmer JD, Pace NR (1996) Perspectives on archaeal diversity, thermophily and monophyly from environmental rRNA sequences. Proceedings National Academy of Sciences 93: 9188-9193.
16. Zillig W, Tu J, Holz I (1981) *Thermoproteales*—a third order of thermoacidophilic archaebacteria. Nature 293: 85 - 86
17. Huber H, Stetter KO (2006) *Desulfurococcales*. The prokaryotes: Springer. pp. 52-68.

18. Zillig W, Stetter KO, Wunderl S, Schulz W, Priess H, et al. (1980) The *Sulfolobus*-"*caldariella*" group: taxonomy on the basis of the structure of DNA-dependent RNA polymerases. Archives Microbiology 125: 259-269.
19. Forterre P, Brochier C, Philippe H (2002) Evolution of the archaea. Theoretical Population Biology 61: 409-422.
20. Klenk H-P, Clayton RA, Tomb J-F, White O, Nelson KE, et al. (1997) The complete genome sequence of the hyperthermophilic, sulphate-reducing archaeon A*rchaeoglobus fulgidus*. Nature 390: 364-370.
21. Jones WJ, Nagle Jr DP, Whitman WB (1987) Methanogens and the diversity of archaebacteria. Microbiological Reviews 51: 135.
22. Zillig W, Reysenbach A (1992) The order *thermococcales*. The Prokaryotes: 702-706.
23. Segerer AH, Burggraf S, Fiala G, Huber G, Huber R, et al. (1993) Life in hot springs and hydrothermal vents. Origins of Life and Evolution of the Biosphere 23: 77-90.
24. Stetter KO (1996) Hyperthermophiles in the history of life. In Ciba Foundation Symposium 202-Evolution of Hydrothermal Ecosystems on Earth (And Mars?) John Wiley & Sons: 1-23.
25. Takai K, Nakamura K, Toki T, Tsunogai U, Miyazaki M, et al. (2008) Cell proliferation at 122^0C and isotopically heavy CH_4 production by a hyperthermophilic methanogen under high-pressure cultivation. Proceedings National Academy of Sciences 105: 10949-10954.
26. Kristjánsson JK, Hreggvidsson GO (1995) Ecology and habitats of extremophiles. World Journal of Microbiology and Biotechnology 11: 17-25.

27. Völkl P, Huber R, Drobner E, Rachel R, Burggraf S, et al. (1993) *Pyrobaculum aerophilum* sp. nov., a novel nitrate-reducing hyperthermophilic archaeum. Applied and Environmental Microbiology 59: 2918-2926.

28. Sako Y, Nomura N, Uchida A, Ishida Y, Morii H, et al. (1996) *Aeropyrum pernix* gen. nov., sp. nov., a novel aerobic hyperthermophilic archaeon growing at temperatures up to 100^0 C. International Journal of Systematic Bacteriology 46: 1070-1077.

29. Nakagawa S, Takai K, Horikoshi K, Sako Y (2004) *Aeropyrum camini* sp. nov., a strictly aerobic, hyperthermophilic archaeon from a deep-sea hydrothermal vent chimney. International Journal Systematic and Evolutionary Microbiology 54: 329-335.

30. Schönheit P, Schäfer T (1995) Metabolism of hyperthermophiles. World Journal of Microbiology and Biotechnology 11: 26-57.

31. Schäfer G, Meyering-Vos M (1992) F-type or V-type? The chimeric nature of the archaebacterial ATP synthase. Biochimica et Biophysica Acta (BBA)-Bioenergetics 1101: 232-235.

32. Verhees C, Kengen S, Tuininga J, Schut G, Adams M, et al. (2003) The unique features of glycolytic pathways in archaea. Biochemical Journal 375: 231-246.

33. Adams M (1998) The biochemical diversity of life near and above 100^0C in marine environments. Journal of Applied Microbiology 85: 108S-117S.

34. Mehta MP, Baross JA (2006) Nitrogen fixation at 92^0C by a hydrothermal vent archaeon. Science 314: 1783-1786.

35. Spring S, Rachel R, Lapidus A, Davenport K, Tice H, Copeland A, Klenk HP (2010) Complete genome sequence of *Thermosphaera aggregans* type strain (M11TLT). Standards in Genomic Sciences 2: 245-259.

36. Amend JP, Shock EL (2001) Energetics of overall metabolic reactions of thermophilic and hyperthermophilic archaea and bacteria. FEMS Microbiology Reviews 25: 175-243.
37. Slobodkin A (2005) Thermophilic microbial metal reduction. Microbiology 74: 501-514.
38. Kawarabayasi Y, Hino Y, Horikawa H, Yamazaki S, Haikawa Y, et al. (1999) Complete genome sequence of an aerobic hyper-thermophilic crenarchaeon, *Aeropyrum pernix* K1. DNA Research 6: 83-101.
39. Stetter KO (1996) Hyperthermophilic procaryotes. FEMS Microbiology Reviews 18: 149-158.
40. Adams MW (1990) The metabolism of hydrogen by extremely thermophilic, sulfur-dependent bacteria. FEMS Microbiology Letters 75: 219-237.
41. Stetter KO (1988) "*Archaeoglobus fulgidus*" gen. nov., sp. nov.: a new taxon of extremely thermophilic archaebacteria. Systematic and Applied Microbiology 10: 172-173.
42. Itoh T, Suzuki K-i, Sanchez PC, Nakase T (1999) *Caldivirga maquilingensis* gen. nov., sp. nov., a new genus of rod-shaped crenarchaeote isolated from a hot spring in the Philippines. International Journal of Systematic Bacteriology 49: 1157-1163.
43. Pihl T, Schicho R, Black L, Schulman B, Maier R, et al. (1990) Hydrogen-sulfur autotrophy in the hyperthermophilic archaebacterium, *Pyrodictium brockii*. Biotechnology and Genetic Engineering Reviews 8: 345-378.
44. Pihl T, Black L, Schulman B, Maier R (1992) Hydrogen-oxidizing electron transport components in the hyperthermophilic archaebacterium *Pyrodictium brockii*. Journal of Bacteriology 174: 137-143.

45. Fiala G, Stetter KO (1986) *Pyrococcus furiosus* sp. nov. represents a novel genus of marine heterotrophic archaebacteria growing optimally at 100^0C. Archives of Microbiology 145: 56-61.

46. Stetter KO (1999) Extremophiles and their adaptation to hot environments. FEBS Letters 452: 22-25.

47. Robb FT, Maeder DL, Brown JR, DiRuggiero J, Stump MD, et al. (2000) Genomic sequence of hyperthermophile, *Pyrococcus furiosus*: implications for physiology and enzymology. Methods in Enzymology 330: 134-157.

48. Schut GJ, Bridger SL, Adams MW (2007) Insights into the metabolism of elemental sulfur by the hyperthermophilic archaeon *Pyrococcus furiosus*: characterization of a coenzyme A-dependent NAD (P) H sulfur oxidoreductase. Journal of Bacteriology 189: 4431-4441.

49. Lipscomb GL, Keese AM, Cowart DM, Schut GJ, Thomm M, et al. (2009) SurR: a transcriptional activator and repressor controlling hydrogen and elemental sulphur metabolism in *Pyrococcus furiosus*. Molecular Microbiology 71: 332-349.

50. Kengen S, Stams AJ (1994) Growth and energy conservation in batch cultures of *Pyrococcus furiosus*. FEMS Microbiology Letters 117: 305-309.

51. Kengen S, Stams AJ, Vos WM (1996) Sugar metabolism of hyperthermophiles. FEMS Microbiology Reviews 18: 119-137.

52. Koning SM, Elferink MG, Konings WN, Driessen AJ (2001) Cellobiose uptake in the hyperthermophilic archaeon *Pyrococcus furiosus* is mediated by an inducible, high-affinity ABC transporter. Journal of Bacteriology 183: 4979-4984.

53. Xavier KB, Peist R, Kossmann M, Boos W, Santos H (1999) Maltose metabolism in the hyperthermophilic archaeon *Thermococcus litoralis*: purification and characterization of key enzymes. Journal of Bacteriology 181: 3358-3367.

54. DiRuggiero J, Dunn D, Maeder DL, Holley-Shanks R, Chatard J, et al. (2000) Evidence of recent lateral gene transfer among hyperthermophilic archaea. Molecular Microbiology 38: 684-693.

55. Schut GJ, Brehm SD, Datta S, Adams MW (2003) Whole-genome DNA microarray analysis of a hyperthermophile and an archaeon: *Pyrococcus furiosus* grown on carbohydrates or peptides. Journal of Bacteriology 185: 3935-3947.

56. Brown SH, Kelly RM (1993) Characterization of amylolytic enzymes, having both α-1, 4 and α-1, 6 hydrolytic activity, from the thermophilic archaea *Pyrococcus furiosus* and *Thermococcus litoralis*. Applied Environmental Microbiology 59: 2614-2621.

57. Bauer MW, Bylina EJ, Swanson RV, Kelly RM (1996) Comparison of a β-Glucosidase and a β-Mannosidase from the hyperthermophilic archaeon *Pyrococcus furiosus* purification, characterization, gene cloning, and sequence analysis. Journal of Biological Chemistry 271: 23749-23755.

58. Voorhorst W, Eggen R, Luesink EJ, De Vos W (1995) Characterization of the celB gene coding for beta-glucosidase from the hyperthermophilic archaeon *Pyrococcus furiosus* and its expression and site-directed mutation in *Escherichia coli*. Journal of Bacteriology 177: 7105-7111.

59. Kengen S, De Bok F, Van Loo N, Dijkema C, Stams A, et al. (1994) Evidence for the operation of a novel Embden-Meyerhof pathway that involves ADP-dependent kinases

during sugar fermentation by *Pyrococcus furiosus*. Journal of Biological Chemistry 269: 17537-17541.

60. Mukund S, Adams M (1996) Molybdenum and vanadium do not replace tungsten in the catalytically active forms of the three tungstoenzymes in the hyperthermophilic archaeon *Pyrococcus furiosus*. Journal of Bacteriology 178: 163-167.
61. Siebers B, and Schönheit P (2005) Unusual pathways and enzymes of central carbohydrate metabolism in Archaea. Current Opinion in Microbiology 8: 695-705.
62. Verhaart MR, Bielen AA, Oost Jvd, Stams AJ, Kengen SW (2010) Hydrogen production by hyperthermophilic and extremely thermophilic bacteria and archaea: mechanisms for reductant disposal. Environmental Technology 31: 993-1003.
63. Hansen T, Oehlmann M, Schönheit P (2001) Novel type of glucose-6-phosphate isomerase in the hyperthermophilic archaeon *Pyrococcus furiosus*. Journal of Bacteriology 183: 3428-3435.
64. Tuininga JE, Verhees CH, van der Oost J, Kengen SW, Stams AJ, et al. (1999) Molecular and biochemical characterization of the ADP-dependent phosphofructokinase from the hyperthermophilic archaeon *Pyrococcus furiosus*. Journal of Biological Chemistry 274: 21023-21028.
65. Aono S, Bryant F, Adams M (1989) A novel and remarkably thermostable ferredoxin from the hyperthermophilic archaebacterium *Pyrococcus furiosus*. Journal of Bacteriology 171: 3433-3439.
66. Blamey JM, Adams MW (1994) Characterization of an ancestral type of pyruvate ferredoxin oxidoreductase from the hyperthermophilic bacterium, *Thermotoga maritima*. Biochemistry 33: 1000-1007.

67. Mai X, Adams M (1996) Purification and characterization of two reversible and ADP-dependent acetyl coenzyme A synthetases from the hyperthermophilic archaeon *Pyrococcus furiosus*. Journal of Bacteriology 178: 5897-5903.
68. Ward DE, Kengen SW, van der Oost J, de Vos WM (2000) Purification and characterization of the alanine aminotransferase from the hyperthermophilic archaeon *Pyrococcus furiosus* and its role in alanine production. Journal of Bacteriology 182: 2559-2566.
69. Schäfer T, Schönheit P (1991) Pyruvate metabolism of the hyperthermophilic archaebacterium *Pyrococcus furiosus*. Archives of Microbiology 155: 366-377.
70. Klump H, Di Ruggiero J, Kessel M, Park J, Adams M, et al. (1992) Glutamate dehydrogenase from the hyperthermophile *Pyrococcus furiosus*. Thermal denaturation and activation. Journal of Biological Chemistry 267: 22681-22685.
71. Mai X, Adams M (1996) Characterization of a fourth type of 2-keto acid-oxidizing enzyme from a hyperthermophilic archaeon: 2-ketoglutarate ferredoxin oxidoreductase from *Thermococcus litoralis*. Journal of Bacteriology 178: 5890-5896.
72. Heider J, Mai X, Adams M (1996) Characterization of 2-ketoisovalerate ferredoxin oxidoreductase, a new and reversible coenzyme A-dependent enzyme involved in peptide fermentation by hyperthermophilic archaea. Journal of Bacteriology 178: 780-787.
73. Kletzin A, Adams M (1996) Molecular and phylogenetic characterization of pyruvate and 2-ketoisovalerate ferredoxin oxidoreductases from *Pyrococcus furiosus* and pyruvate ferredoxin oxidoreductase from *Thermotoga maritima*. Journal of Bacteriology 178: 248-257.

74. Vignais, P., and Billoud, B. (2007) Occurrence, classification, and biological function of hydrogenases: an overview. Chemical Reviews 107: 4206-4272.

75. Vignais P, Colbeau A (2004) Molecular biology of microbial hydrogenases. Current Issues in Molecular Biology 6: 159-188.

76. Lubitz W, Ogata H, Rüdiger O, Reijerse E (2014) Hydrogenases. Chemical Reviews 114: 4081-4148.

77. Adams MWW (1990) The structure and mechanism of iron-hydrogenases. Biochemica et Biophysica Atca 1020: 115-145.

78. Nicolet Y, Piras C, Legrand P, Hatchikian CE, Fontecilla-Camps JC *Desulfovibrio desulfuricans* iron hydrogenase: the structure shows unusual coordination to an active site Fe binuclear center. Structure 7: 13-23.

79. Hatchikian EC, Forget N, Fernandez VM, Williams R, Cammack R (1992) Further characterization of the [Fe]-hydrogenase from *Desulfovibrio desulfuricans* ATCC 7757. European Journal of Biochemistry 209: 357-365.

80. Peters JW, Lanzilotta WN, Lemon BJ, Seefeldt LC (1998) X-ray crystal structure of the Fe-only hydrogenase (CpI) from *Clostridium pasteurianum* to 1.8 angstrom resolution. Science 282: 1853-1858.

81. Mulder DW, Boyd ES, Sarma R, Lange RK, Endrizzi JA, et al. (2010) Stepwise [FeFe]-hydrogenase H-cluster assembly revealed in the structure of HydA[Dgr]EFG. Nature 465: 248-251.

82. Fontecilla-Camps JC, Volbeda A, Cavazza C, Nicolet Y (2007) Structure/function relationships of [NiFe]-and [FeFe]-hydrogenases. Chemical Reviews 107: 4273-4303.

83. Pandey AS, Harris TV, Giles LJ, Peters JW, Szilagyi RK (2008) Dithiomethylether as a ligand in the hydrogenase H-cluster. Journal of the American Chemical Society 130: 4533-4540.

84. Mulder David W, Shepard Eric M, Meuser Jonathan E, Joshi N, King Paul W, et al. Insights into [FeFe]-hydrogenase structure, mechanism, and maturation. Structure 19: 1038-1052.

85. Nicolet Y, Lemon BJ, Fontecilla-Camps JC, Peters JW (2000) A novel FeS cluster in Fe-only hydrogenases. Trends in Biochemical Sciences 25: 138-143.

86. Lambertz C, Leidel N, Havelius KG, Noth J, Chernev P, et al. (2011) O_2 reactions at the six-iron active site (H-cluster) in [FeFe]-hydrogenase. Journal of Biological Chemistry 286: 40614-40623.

87. Cohen J, Kim K, King P, Seibert M, Schulten K (2005) Finding gas diffusion pathways in proteins: application to O_2 and H_2 transport in CpI [FeFe]-hydrogenase and the role of packing defects. Structure 13: 1321-1329.

88. Mulder DW, Ortillo DO, Gardenghi DJ, Naumov AV, Ruebush SS, et al. (2009) Activation of HydAΔEFG requires a preformed [4Fe-4S] cluster. Biochemistry 48: 6240-6248.

89. Nicolet Y, Fontecilla-Camps JC (2012) Structure-function relationships in [FeFe]-hydrogenase active site maturation. Journal of Biological Chemistry 287: 13532-13540.

90. Posewitz MC, King PW, Smolinski SL, Zhang L, Seibert M, et al. (2004) Discovery of two novel radical S-adenosylmethionine proteins required for the assembly of an active [Fe] hydrogenase. Journal of Biological Chemistry 279: 25711-25720.

91. Posewitz M, King P, Smolinski S, Smith RD, Ginley A, et al. (2005) Identification of genes required for hydrogenase activity in *Chlamydomonas reinhardtii*. Biochemical Society Transactions 33: 102-104.

92. McGlynn SE, Ruebush SS, Naumov A, Nagy LE, Dubini A, et al. (2007) In vitro activation of [FeFe] hydrogenase: new insights into hydrogenase maturation. Journal of Biological Inorganic Chemistry 12: 443-447.

93. Brazzolotto X, Rubach JK, Gaillard J, Gambarelli S, Atta M, et al. (2006) The [FeFe]-hydrogenase maturation protein HydF from *Thermotoga maritima* is a GTPase with an iron-sulfur cluster. Journal of Biological Chemistry 281: 769-774.

94. King PW, Posewitz MC, Ghirardi ML, Seibert M (2006) Functional studies of [FeFe] hydrogenase maturation in an *Escherichia coli* biosynthetic system. Journal of Bacteriology 188: 2163-2172.

95. Rubach JK, Brazzolotto X, Gaillard J, Fontecave M (2005) Biochemical characterization of the HydE and HydG iron-only hydrogenase maturation enzymes from *Thermatoga maritima*. FEBS Letters 579: 5055-5060.

96. Sofia HJ, Chen G, Hetzler BG, Reyes-Spindola JF, Miller NE (2001) Radical SAM, a novel protein superfamily linking unresolved steps in familiar biosynthetic pathways with radical mechanisms: functional characterization using new analysis and information visualization methods. Nucleic Acids Research 29: 1097-1106.

97. Nicolet Y, Rubach JK, Posewitz MC, Amara P, Mathevon C, et al. (2008) X-ray structure of the [FeFe]-hydrogenase maturase HydE from *Thermotoga maritima*. Journal of Biological Chemistry 283: 18861-18872.

98. Pilet E, Nicolet Y, Mathevon C, Douki T, Fontecilla-Camps JC, et al. (2009) The role of the maturase HydG in [FeFe]-hydrogenase active site synthesis and assembly. FEBS Letters 583: 506-511.

99. Shepard EM, Duffus BR, George SJ, McGlynn SE, Challand MR, et al. (2010) [FeFe]-hydrogenase maturation: HydG-catalyzed synthesis of carbon monoxide. Journal of the American Chemical Society 132: 9247-9249.

100. Peters JW, Szilagyi RK, Naumov A, Douglas T (2006) A radical solution for the biosynthesis of the H-cluster of hydrogenase. FEBS Letters 580: 363-367.

101. Shepard EM, Mus F, Betz JN, Byer AS, Duffus BR, et al. (2014) [FeFe]-hydrogenase maturation. Biochemistry. 53: 4090-4104.

102. Nicolet Y, Martin L, Tron C, Fontecilla-Camps JC (2010) A glycyl free radical as the precursor in the synthesis of carbon monoxide and cyanide by the [FeFe]-hydrogenase maturase HydG. FEBS Letters 584: 4197-4202.

103. Vallese F, Berto P, Ruzzene M, Cendron L, Sarno S, et al. (2012) Biochemical analysis of the interactions between the proteins involved in the [FeFe]-hydrogenase maturation process. Journal of Biological Chemistry 287: 36544-36555.

104. Kuchenreuther JM, Stapleton JA, Swartz JR (2009) Tyrosine, cysteine, and S-adenosyl methionine stimulate in vitro [FeFe] hydrogenase activation. PLoS One 4: e7565.

105. Kuchenreuther JM, George SJ, Grady-Smith CS, Cramer SP, Swartz JR (2011) Cell-free H-cluster synthesis and [FeFe] hydrogenase activation: all five CO and CN− ligands derive from tyrosine. PloS One 6: e20346.

106. McGlynn SE, Shepard EM, Winslow MA, Naumov AV, Duschene KS, et al. (2008) HydF as a scaffold protein in [FeFe] hydrogenase H-cluster biosynthesis. FEBS Letters 582: 2183-2187.

107. Czech I, Silakov A, Lubitz W, Happe T (2010) The [FeFe]-hydrogenase maturase HydF from *Clostridium acetobutylicum* contains a CO and CN− ligated iron cofactor. FEBS Letters 584: 638-642.

108. Czech I, Stripp S, Sanganas O, Leidel N, Happe T, et al. (2011) The [FeFe]-hydrogenase maturation protein HydF contains a H-cluster like [4Fe4S]–2Fe site. FEBS Letters 585: 225-230.

109. Shepard EM, McGlynn SE, Bueling AL, Grady-Smith CS, George SJ, et al. (2010) Synthesis of the 2Fe subcluster of the [FeFe]-hydrogenase H-cluster on the HydF scaffold. Proceedings of the National Academy of Sciences 107: 10448-10453.

110. Berto P, Di Valentin M, Cendron L, Vallese F, Albertini M, et al. (2012) The [4Fe–4S]-cluster coordination of [FeFe]-hydrogenase maturation protein HydF as revealed by EPR and HYSCORE spectroscopies. Biochimica et Biophysica Acta (BBA)-Bioenergetics 1817: 2149-2157.

111. Thauer RK, Kaster A-K, Goenrich M, Schick M, Hiromoto T, et al. (2010) Hydrogenases from methanogenic archaea, nickel, a novel cofactor, and H_2 storage. Annual Review of Biochemistry 79: 507-536.

112. Afting C, Kremmer E, Brucker C, Hochheimer A, Thauer RK (2000) Regulation of the synthesis of H_2-forming methylenetetrahydromethanopterin dehydrogenase (Hmd) and of HmdII and HmdIII in *Methanothermobacter marburgensis*. Archives of Microbiology 174: 225-232.

113. Lyon EJ, Shima S, Boecher R, Thauer RK, Grevels F-W, et al. (2004) Carbon monoxide as an intrinsic ligand to iron in the active site of the iron−sulfur-cluster-free hydrogenase H_2-forming methylenetetrahydromethanopterin dehydrogenase as revealed by infrared spectroscopy. Journal of the American Chemical Society 126: 14239-14248.

114. Thauer RK, Klein AR, Hartmann GC (1996) Reactions with molecular hydrogen in microorganisms: evidence for a purely organic hydrogenation catalyst. Chemical Reviews 96: 3031-3042.

115. Thauer RK, Kaster A-K, Seedorf H, Buckel W, Hedderich R (2008) Methanogenic archaea: ecologically relevant differences in energy conservation. Nature Review Microbiology 6: 579-591.

116. Vogt S, Lyon E, Shima S, Thauer R (2008) The exchange activities of [Fe] hydrogenase (iron–sulfur-cluster-free hydrogenase) from methanogenic archaea in comparison with the exchange activities of [FeFe] and [NiFe] hydrogenases. Journal of Biological Inorganic Chemistry 13: 97-106.

117. Pilak O, Mamat B, Vogt S, Hagemeier CH, Thauer RK, et al. (2006) The crystal structure of the apoenzyme of the iron–sulphur cluster-free hydrogenase. Journal of Molecular Biology 358: 798-809.

118. Hiromoto T, Ataka K, Pilak O, Vogt S, Stagni MS, et al. (2009) The crystal structure of C176A mutated [Fe]-hydrogenase suggests an acyl-iron ligation in the active site iron complex. FEBS Letters 583: 585-590.

119. Shima S, Lyon EJ, Thauer RK, Mienert B, Bill E (2005) Mössbauer studies of the iron-sulfur cluster-free hydrogenase: the electronic state of the mononuclear Fe active site. Journal of the American Chemical Society 127: 10430-10435.

120. Fontecilla-Camps, J. C. (2009) Structure and function of [NiFe]-hydrogenases. Metal Ions in Life Sciences 6: 151-78.

121. Shafaat HS, Rüdiger O, Ogata H, Lubitz W (2013) [NiFe] hydrogenases: A common active site for hydrogen metabolism under diverse conditions. Biochimica et Biophysica Acta (BBA)-Bioenergetics 1827: 986-1002.

122. Foerster S, Stein M, Brecht M, Ogata H, Higuchi Y, and Lubitz W (2002) Single crystal EPR studies of the reduced active site of [NiFe] hydrogenase from *Desulfovibrio vulgaris Miyazaki* F. Journal of the American Chemical Society 125: 83-93.

123. Volbeda A, Charon MH, Piras C, Hatchikian EC, Frey M and Fontecilla-Camps JC (1995) Crystal structure of the nickel-iron hydrogenase from *Desulfovibrio gigas*. Nature 373: 580-7.

124. Volbeda A, Darnault C, Parkin A, Sargent F, Armstrong FA & Fontecilla-Camps JC (2013) Crystal structure of the O_2-tolerant membrane-bound hydrogenase 1 from *Escherichia coli* in complex with its cognate cytochrome b. Structure 21: 184-90.

125. Nicolet Y, Cavazza C, Fontecilla-Camps J (2002) Fe-only hydrogenases: structure, function and evolution. Journal of Inorganic Biochemistry 91: 1-8.

126. Ogata H, Lubitz W, Higuchi Y (2009) [NiFe] hydrogenases: structural and spectroscopic studies of the reaction mechanism. Dalton Transactions: 7577-7587.

127. Böck A, King PW, Blokesch M, and Posewitz MC (2006) Maturation of hydrogenases. Advances in Microbial Physiology 51: 1-225.

128. Forzi L, Sawers RG (2007) Maturation of [NiFe]-hydrogenases in *Escherichia coli*. BioMetals 20: 565-578.

129. Casalot L, Rousset M (2001) Maturation of the [NiFe] hydrogenases. Trends in Microbiology 9: 228-237.

130. Blokesch M, Magalon A, Böck A (2001) Interplay between the specific chaperone-like proteins HybG and HypC in maturation of hydrogenases 1, 2, and 3 from *Escherichia coli*. Journal of Bacteriology 183: 2817-2822.

131. Butland G, Zhang JW, Yang W, Sheung A, Wong P, et al. (2006) Interactions of the *Escherichia coli* hydrogenase biosynthetic proteins: HybG complex formation. FEBS Letters 580: 677-681.

132. Paschos A, Glass RS, Böck A (2001) Carbamoylphosphate requirement for synthesis of the active center of [NiFe]-hydrogenases. FEBS Letters 488: 9-12.

133. Reissmann S, Hochleitner E, Wang H, Paschos A, Lottspeich F, et al. (2003) Taming of a poison: biosynthesis of the NiFe-hydrogenase cyanide ligands. Science 299: 1067-1070.

134. Shomura, Y. and Y. Higuchi (2012). Structural basis for the reaction mechanism of S-carbamoylation of HypE by HypF in the maturation of [NiFe]-hydrogenases. Journal of Biological Chemistry 34: 28409-28419.

135. Rosano C, Zuccotti S, Bucciantini M, Stefani M, Ramponi G, et al. (2002) Crystal structure and anion binding in the prokaryotic hydrogenase maturation factor HypF acylphosphatase-like domain. Journal of Molecular Biology 321: 785-796.

136. Shomura Y, Komori H, Miyabe N, Tomiyama M, Shibata N, et al. (2007) Crystal structures of hydrogenase maturation protein HypE in the apo and ATP-bound forms. Journal of Molecular Biology 372: 1045-1054.

137. Watanabe S, Matsumi R, Arai T, Atomi H, Imanaka T, et al. (2007) Crystal structures of [NiFe] hydrogenase maturation proteins HypC, HypD, and HypE: insights into cyanation reaction by thiol redox signaling. Molecular Cell 27: 29-40.

138. Rangarajan ES, Asinas A, Proteau A, Munger C, Baardsnes J, et al. (2008) Structure of [NiFe] hydrogenase maturation protein HypE from *Escherichia coli* and its interaction with HypF. Journal of Bacteriology 190: 1447-1458.

139. Roseboom W, Blokesch M, Böck A, Albracht SP (2005) The biosynthetic routes for carbon monoxide and cyanide in the Ni–Fe active site of hydrogenases are different. FEBS Letters 579: 469-472.

140. Forzi L, Hellwig P, Thauer RK, Sawers RG (2007) The CO and CN− ligands to the active site Fe in [NiFe]-hydrogenase of *Escherichia coli* have different metabolic origins. FEBS Letters 581: 3317-3321.

141. Bürstel I, Hummel P, Siebert E, Wisitruangsakul N, Zebger I, et al. (2011) Probing the origin of the metabolic precursor of the CO ligand in the catalytic center of [NiFe] hydrogenase. Journal of Biological Chemistry 286: 44937-44944.

142. Soboh B, Stripp ST, Muhr E, Granich C, Braussemann M, et al. (2012) [NiFe]-hydrogenase maturation: isolation of a HypC–HypD complex carrying diatomic CO and CN ligands. FEBS Letters 586: 3882-3887.

143. Bürstel I, Siebert E, Winter G, Hummel P, Zebger I, et al. (2012) A universal scaffold for synthesis of the Fe (CN) 2 (CO) moiety of [NiFe] hydrogenase. Journal of Biological Chemistry 287: 38845-38853.

144. Watanabe S, Arai T, Matsumi R, Atomi H, Imanaka T, et al. (2009) Crystal structure of HypA, a nickel-binding metallochaperone for [NiFe] hydrogenase maturation. Journal of Molecular Biology 394: 448-459.

145. Xia W, Li H, Sze K-H, Sun H (2009) Structure of a nickel chaperone, HypA, from *Helicobacter pylori* reveals two distinct metal binding sites. Journal of the American Chemical Society 131: 10031-10040.

146. Chan Chung KC and Zamble DB (2011) The *Escherichia coli* metal-binding chaperone SlyD interacts with the large subunit of [NiFe]-hydrogenase 3. FEBS Letters 585(2): 291-294.

147. Herbst RW, Perovic I, Martin-Diaconescu V, O'Brien K, Chivers PT, et al. (2010) Communication between the zinc and nickel sites in dimeric HypA: metal recognition and pH sensing. Journal of the American Chemical Society 132: 10338-10351.

148. Douglas CD, Ngu TT, Kaluarachchi H, Zamble DB (2013) Metal transfer within the *Escherichia coli* HypB–HypA complex of hydrogenase accessory proteins. Biochemistry 52: 6030-6039.

149. Leach MR, Sandal S, Sun H, Zamble DB (2005) Metal binding activity of the *Escherichia coli* hydrogenase maturation factor HypB. Biochemistry 44: 12229-12238.

150. Leach MR, Zhang JW, Zamble DB (2007) The role of complex formation between the *Escherichia coli* hydrogenase accessory factors HypB and SlyD. Journal of Biological Chemistry 282: 16177-16186.

151. Theodoratou E, Paschos A, Magalon A, Fritsche E, Huber R, et al. (2000) Nickel serves as a substrate recognition motif for the endopeptidase involved in hydrogenase maturation. European Journal of Biochemistry 267: 1995-1999.

152. Theodoratou E, Huber R, Böck A (2005) [NiFe]-hydrogenase maturation endopeptidase: structure and function. Biochemical Society Transactions 33: 108-111.

153. Kumarevel T, Tanaka T, Bessho Y, Shinkai A, Yokoyama S (2009) Crystal structure of hydrogenase maturating endopeptidase HycI from *Escherichia coli*. Biochemical and Biophysical Research Communications 389: 310-314.

154. Lubitz W, Reijerse E, van Gastel M (2007) [NiFe] and [FeFe] hydrogenases studied by advanced magnetic resonance techniques. Chemical reviews 107: 4331-4365.

155. Schröder O, Bleijlevens B, de Jongh TE, Chen Z, Li T, et al. (2007) Characterization of a cyanobacterial-like uptake [NiFe] hydrogenase: EPR and FTIR spectroscopic studies of the enzyme from *Acidithiobacillus ferrooxidans*. Journal of Biological Inorganic Chemistry 12: 212-233.

156. Pandelia ME, Ogata H, Lubitz W (2010) Intermediates in the catalytic cycle of [NiFe] hydrogenase: functional spectroscopy of the active site. ChemPhysChem 11: 1127-1140.

157. Pandelia M-E, Fourmond V, Tron-Infossi P, Lojou E, Bertrand P, et al. (2010) Membrane-bound hydrogenase I from the hyperthermophilic bacterium *Aquifex aeolicus*: enzyme activation, redox intermediates and oxygen tolerance. Journal of the American Chemical Society 132: 6991-7004.

158. Shomura Y, Yoon K-S, Nishihara H, Higuchi Y (2011) Structural basis for a [4Fe-3S] cluster in the oxygen-tolerant membrane-bound [NiFe]-hydrogenase. Nature 479: 253-256.

159. Fritsch J, Scheerer P, Frielingsdorf S, Kroschinsky S, Friedrich, B, et al. (2011) The crystal structure of an oxygen-tolerant hydrogenase uncovers a novel iron-sulphur centre. Nature 479: 249-252.

160. Shomura Y, Higuchi Y (2013) Structural aspects of [NiFe]-hydrogenases. Reviews in Inorganic Chemistry 33: 173-192.

161. Goris T, Wait AF, Saggu M, Fritsch J, Heidary N, et al. (2011) A unique iron-sulfur cluster is crucial for oxygen tolerance of a [NiFe]-hydrogenase. Nature Chemical Biology 7: 310-318.

162. Buhrke T, Lenz O, Krauss N, Friedrich B (2005) Oxygen tolerance of the H_2-sensing [NiFe] hydrogenase from *Ralstonia eutropha* H16 is based on limited access of oxygen to the active site. Journal of Biological Chemistry 280: 23791-23796.

163. Dross F, Geisler V, Lenger R, Theis F, Krafft T, et al. (1992) The quinone-reactive [NiFe]-hydrogenase of *Wolinella succinogenes*. European Journal of Biochemistry 206: 93-102.

164. Brugna-Guiral M, Tron P, Nitschke W, Stetter K-O, Burlat B, et al. (2003) [NiFe] hydrogenases from the hyperthermophilic bacterium *Aquifex aeolicus*: properties, function, and phylogenetics. Extremophiles 7: 145-157.

165. Guiral M, Tron P, Aubert C, Gloter A, Iobbi-Nivol C, et al. (2005) A membrane-bound multienzyme, hydrogen-oxidizing, and sulfur-reducing complex from the hyperthermophilic bacterium *Aquifex aeolicus*. Journal of Biological Chemistry 280: 42004-42015.

166. Rodrigue A, Chanal A, Beck K, Müller M, Wu L-F (1999) Co-translocation of a periplasmic enzyme complex by a hitchhiker mechanism through the bacterial tat pathway. Journal of Biological Chemistry 274: 13223-13228.

167. Garcin E, Vernede X, Hatchikian E, Volbeda A, Frey M, et al. (1999) The crystal structure of a reduced [NiFeSe] hydrogenase provides an image of the activated catalytic center. Structure 7: 557-566.

168. Marques MC, Coelho R, De Lacey AL, Pereira IA, Matias PM (2010) The three-dimensional structure of [NiFeSe] hydrogenase from *Desulfovibrio vulgaris* Hildenborough: a hydrogenase without a bridging ligand in the active site in its oxidized, "as-isolated" state. Journal of Molecular Biology 396: 893-907.

169. Appel, J. and R. Schulz (1998). Hydrogen metabolism in organisms with oxygenic photosynthesis: hydrogenases as important regulatory devices for a proper redox poising? Journal of Photochemistry and Photobiology: Biology 47: 1-11.

170. Ludwig M, Schulz-Friedrich R, Appel J (2006) Occurrence of hydrogenases in cyanobacteria and anoxygenic photosynthetic bacteria: implications for the phylogenetic origin of cyanobacterial and algal hydrogenases. Journal of Molecular Evolution 63: 758-768.

171. Montet Y, Amara P, Volbeda A, Vernede X, Hatchikian EC, et al. (1997) Gas access to the active site of Ni-Fe hydrogenases probed by X-ray crystallography and molecular dynamics. Nature Structural Biology 4: 523-526.

172. Dementin Sb, Leroux F, Cournac L, Lacey ALd, Volbeda A, et al. (2009) Introduction of methionines in the gas channel makes [NiFe] hydrogenase aero-tolerant. Journal of the American Chemical Society 131: 10156-10164.

173. Duché O, Elsen S, Cournac L, Colbeau A (2005) Enlarging the gas access channel to the active site renders the regulatory hydrogenase HupUV of *Rhodobacter capsulatus* O_2 sensitive without affecting its transductory activity. FEBS Journal 272: 3899-3908.

174. Buhrke T, Löscher S, Lenz O, Schlodder E, Zebger I, et al. (2005) Reduction of unusual iron-sulfur clusters in the H_2-sensing regulatory Ni-Fe hydrogenase from *Ralstonia eutropha* H16. Journal of Biological Chemistry 280: 19488-19495.

175. Vitt S, Ma K, Warkentin E, Moll J, Pierik A, et al. (2014) The F_{420}-reducing [NiFe]-hydrogenase complex from *Methanothermobacter marburgensis*, the first X-ray structure of a group 3 family member. Journal of Molecular Biology. 426: 2813-2826

176. Burgdorf T, van der Linden E, Bernhard M, Yin QY, Back JW, et al. (2005) The soluble NAD^+-reducing [NiFe]-hydrogenase from *Ralstonia eutropha* H16 consists of six subunits and can be specifically activated by NADPH. Journal of Bacteriology 187: 3122-3132.

177. Bryant F, Adams M (1989) Characterization of hydrogenase from the hyperthermophilic archaebacterium, *Pyrococcus furiosus*. Journal of Biological Chemistry 264: 5070-5079.

178. Ma K, Adams M (2000) Hydrogenases I and II from *Pyrococcus furiosus*. Methods in Enzymology 331: 208-216.

179. Hedderich R (2004) Energy-converting [NiFe] hydrogenases from archaea and extremophiles: ancestors of complex I. Journal of Bioenergetics and Biomembranes 36: 65-75.

180. Hedderich R, Forzi L (2005) Energy-converting [NiFe] hydrogenases: more than just H_2 activation. Journal of Molecular Microbiology and Biotechnology 10: 92-104.

181. Schut GJ, Boyd ES, Peters JW, and Adams MWW. (2013) The modular respiratory complexes involved in hydrogen and sulfur metabolism by heterotrophic hyperthermophilic archaea and their evolutionary implications. FEMS Microbiology Reviews 37: 182-203.

182. Böhm R, Sauter M, Böck A (1990) Nucleotide sequence and expression of an operon in *Escherichia coli* coding for formate hydrogenlyase components. Molecular Microbiology 4: 231–243.

183. Sauter M, Böhm R, Böck A (1992) Mutational analysis of the operon (hyc) determining hydrogenase 3 formation in *Escherichia coli*. Molecular Microbiology 6: 1523–1532.

184. Singer SW, Hirst MB, Ludden PW (2006) CO-dependent H_2 evolution by *Rhodospirillum rubrum*: role of CODH:CooF complex. Biochimica et Biophysica Acta. 1757: 1582–1591.

185. Kurkin S, Meuer J, Koch J, Hedderich R, Albracht SPJ (2002) The membrane-bound [NiFe]-hydrogenase (Ech) from *Methanosarcina barkeri*: unusual properties of the iron-sulphur clusters. European Journal of Biochemistry 269: 6101-6111.

186. Meuer J, Bartoschek S, Koch J, Kunkel A, Hedderich R (1999) Purification and catalytic properties of Ech hydrogenase from *Methanosarcina barkeri*. European Journal of Biochemistry 265: 325-335.

187. Sapra R, Verhagen MF, Adams MW (2000) Purification and characterization of a membrane-bound hydrogenase from the hyperthermophilic archaeon *Pyrococcus furiosus*. Journal of Bacteriology 182: 3423-3428.

188. Silva P, Van den Ban ECD, Wassink H, Haaker H, de Castro B, Robb FT, Hagen WR (2000) Enzymes of hydrogen metabolism in *Pyrococcus furiosus*. European Journal of Biochemistry 267: 6541-6551.

189. Swartz TH, Ikewada S, Ishikawa O, Ito M, Krulwich TA (2005) The Mrp system: a giant among monovalent cation/proton antiporters? Extremophiles 9: 345-354.

190. Pisa KY, Huber H, Thomm M, Muller V (2007) A sodium ion-dependent A1-AO ATP synthase from the hyperthermophilic archaeon *Pyrococcus furiosus*. FEBS Journal 274: 3928-3938.

191. Vonck J, Pisa KY, Morgner N, Brutschy B, Müller V (2009) Three-dimensional structure of A_1A_0 ATP synthase from the hyperthermophilic archaeon *Pyrococcus furiosus* by electron microscopy. Journal of Biological Chemistry 284: 10110-10119.

192. Jenney FE, Adams MW (2008) Hydrogenases of the model hyperthermophiles. Annals of the New York Academy of Sciences 1125: 252-266.

193. Sapra R, Bagramyan K, Adams MW (2003) A simple energy-conserving system: proton reduction coupled to proton translocation. Proceedings of the National Academy of Sciences 100: 7545-7550.

194. Mitchell P (1961) Coupling of phosphorylation to electron and hydrogen transfer by a chemi-osmotic type of mechanism. Nature 191: 144-148.

195. Silver S, Nucifora G, Chu L, Misra TK (1989) Bacterial resistance ATPases: primary pumps for exporting toxic cations and anions. Trends in Biochemical Sciences 14: 76-80.

196. Müller V, Grüber G (2003) ATP synthases: structure, function and evolution of unique energy converters. Cellular and Molecular Life Sciences 60: 474-494.

197. Grüber G, Manimekalai MSS, Mayer F, Müller V (2014) ATP synthases from archaea: the beauty of a molecular motor. Biochimica et Biophysica Acta 1837: 940-952.

198. Cross RL, Müller V (2004) The evolution of A-, F-, and V-type ATP synthases and ATPases: reversals in function and changes in the H^+/ATP coupling ratio. FEBS Letters 576: 1-4.

199. Grüber G, Wieczorek H, Harvey WR, Müller V (2001) Structure–function relationships of A-, F-and V-ATPases. Journal of Experimental Biology 204: 2597-2605.

200. Ma K, Adams MW (2001) Ferredoxin: NADP oxidoreductase from *Pyrococcus furiosus*. Methods in Enzymology 334: 40-45.

201. Lipscomb GL, Stirrett K, Schut GJ, Yang F, et al. (2011) Natural competence in the hyperthermophilic archaeon *Pyrococcus furiosus* facilitates genetic manipulation: construction of markerless deletions of genes encoding the two cytoplasmic hydrogenases. Applied and Environmental Microbiology 77: 2232-2238.

202. Efremov RG, Baradaran R, Sazanov LA (2010) The architecture of respiratory complex I. Nature 465: 441-445.

203. Marreiros BC, Batista AP, Duarte AM, Pereira MM (2013) A missing link between complex I and group 4 membrane-bound [NiFe] hydrogenases. Biochimica et Biophysica Acta 1827: 198-209.

204. Kim MS, Bae SS, Kim YJ, Kim TW, Lim JK, et al. (2013) CO-dependent H_2 production by genetically engineered *Thermococcus onnurineus* NA1. Applied Environmental Microbiology 79: 2048-5.

205. Soboh B, Linder D, Hedderich R (2002) Purification and catalytic properties of a CO oxidizing: H_2-evolving enzyme complex from *Carboxydothermus hydrogenoformans*. European Journal Biochemistry 269: 5712-5721.

206. Soboh B, Linder D, Hedderich R. (2004) A multisubunit membrane-bound [NiFe] hydrogenase and an NADH-dependent Fe-only hydrogenase in the fermenting bacterium *Thermoanaerobacter tengcongensis*. Microbiology 150: 2451-2463.

207. Schneider D, Schmidt CL, Seidler A (2003) Expression of membrane-bound iron-sulfur proteins. Membrane Protein Protocols Springer: 37-47.

208. Shaw AZ, Miroux B. (2003) A general approach for heterologous membrane protein expression in *Escherichia coli*. Membrane Protein Protocols Springer: 23-35.

209. Grisshammer R (2006) Understanding recombinant expression of membrane proteins. Current Opinion in Biotechnology 17: 337-340.

210. Kiefer H, Maier K, Vogel R (1999) Refolding of G-protein-coupled receptors from inclusion bodies produced in *Escherichia coli*. Biochemical Society Transactions 27: 908-912.

211. Padan E, Hunte C, Reilander H (2003) Production and purification of recombinant membrane proteins. Membrane Protein Purification and Crystallization: A Practical Guide: 55.

212. Klammt C, Löhr F, Schäfer B, Haase W, Dötsch V, et al. (2004) High level cell-free expression and specific labeling of integral membrane proteins. European Journal of Biochemistry 271: 568-580.

213. Eshaghi S, Hedrén M, Nasser MIA, Hammarberg T, Thornell A, et al. (2005) An efficient strategy for high-throughput expression screening of recombinant integral membrane proteins. Protein Science 14: 676-683.

214. Lenz O, Gleiche A, Strack A, Friedrich B (2005) Requirements for heterologous production of a complex metalloenzyme: the membrane-bound [NiFe] hydrogenase. Journal of Bacteriology 187: 6590-6595.

215. Sun J, Hopkins RC, Jenney Jr FE, McTernan PM, Adams MW (2010) Heterologous expression and maturation of an NADP-dependent [NiFe]-hydrogenase: a key enzyme in biofuel production. Plos One 5: e10526.

216. Hopkins RC, Sun J, Jenney Jr FE, Chandrayan SK, McTernan PM, et al. (2011) Homologous expression of a subcomplex of *Pyrococcus furiosus* hydrogenase that interacts with pyruvate ferredoxin oxidoreductase. Plos One 6: e26569.

217. Kuchenreuther JM, Grady-Smith CS, Bingham AS, George SJ, Cramer SP, et al. (2010) High-yield expression of heterologous [FeFe] hydrogenases in *Escherichia coli*. Plos One 5: e15491.

218. Boyer ME, Stapleton JA, Kuchenreuther JM, Wang Cw, Swartz JR (2008) Cell-free synthesis and maturation of [FeFe] hydrogenases. Biotechnology and Bioengineering 99: 59-67.

219. Ghirardi ML, King PW, Posewitz MC, Seibert M, Smolinski SL (2006) Process and genes for expression and overexpression of active [FeFe] Hydrogenases. U.S. Patent No. 8,835,153.

220. Sybirna K, Antoine T, Lindberg P, Fourmond V, Rousset M, et al. (2008) *Shewanella oneidensis*: a new and efficient system for expression and maturation of heterologous [Fe-Fe] hydrogenase from *Chlamydomonas reinhardtii*. BMC Biotechnology 8: 73.

221. Stapleton JA, Swartz JR (2010). A cell-free microtiter plate screen for improved [FeFe] hydrogenases. Plos One 5: e10554.

222. Meuer J, Kuettner HC, Zhang JK, Hedderich R, Metcalf WW (2002) Genetic analysis of the archaeon *Methanosarcina barkeri* Fusaro reveals a central role for Ech hydrogenase

and ferredoxin in methanogenesis and carbon fixation. Proceedings of the National Academy of Sciences 99: 5632-5637.

223. Cline SW, Doolittle WF (1992) Transformation of members of the genus *Haloarcula* with shuttle vectors based on *Halobacterium halobium* and *Haloferax volcanii* plasmid replicons. Journal of Bacteriology 174: 1076-1080.

224. Pfeifer F, Gregor D, Hofacker A, Plosser P, Zimmermann P (2002) Regulation of gas vesicle formation in halophilic archaea. Journal of Molecular Microbiology and Biotechnology 4: 175-181.

225. Hechler T, Pfeifer F (2009). Anaerobiosis inhibits gas vesicle formation in halophilic archaea. Molecular Microbiology 71: 132-145.

226. Martusewitsch E, Sensen CW, Schleper C (2000) High spontaneous mutation rate in the hyperthermophilic archaeon *Sulfolobus solfataricus* is mediated by transposable elements. Journal of Bacteriology 182: 2574-2581.

227. Albers S-V, Jonuscheit M, Dinkelaker S, Urich T, Kletzin A, et al. (2006) Production of recombinant and tagged proteins in the hyperthermophilic archaeon *Sulfolobus solfataricus*. Applied and Environmental Microbiology 72: 102-111.

228. Deng L, Zhu H, Chen Z, Liang YX, She Q (2009) Unmarked gene deletion and host–vector system for the hyperthermophilic crenarchaeon *Sulfolobus islandicus*. Extremophiles 13: 735-746.

229. She Q, Zhang C, Deng L, Peng N, Chen Z, et al. (2009) Genetic analyses in the hyperthermophilic archaeon *Sulfolobus islandicus*. Biochemical Society Transactions 37: 92.

230. Wagner M, Berkner S, Ajon M, Driessen AM, Lipps G, Albers SV (2009). Expanding and understanding the genetic toolbox of the hyperthermophilic genus *Sulfolobus*. Biochemical Society Transactions 37: 97-101.

231. Lucas S, Toffin L, Zivanovic Y, Charlier D, Moussard H, et al. (2002) Construction of a shuttle vector for, and spheroplast transformation of, the hyperthermophilic archaeon *Pyrococcus abyssi*. Applied and Environmental Microbiology 68: 5528-5536.

232. Santangelo TJ, Matsumi R, Atomi H, Imanaka T, Reeve JN (2008) Polarity in archaeal operon transcription in *Thermococcus kodakaraensis*. Journal of Bacteriology 190: 2244-2248.

233. Bridger SL, Lancaster WA, Poole FL, Schut GJ, Adams MW (2012) Genome sequencing of a genetically tractable *Pyrococcus furiosus* strain reveals a highly dynamic genome. Journal of Bacteriology 194: 4097-4106.

234. Cammack R, Frey M, Robson R (2002) Hydrogen as a fuel: learning from nature: CRC Press.

235. Sigfusson TI (2007). Pathways to hydrogen as an energy carrier. Philosophical Transactions of the Royal Society A: Mathematical, Physical and Engineering Sciences 365: 1025-1042.

236. Lee H-S, Vermaas WF, Rittmann BE (2010) Biological hydrogen production: prospects and challenges. Trends in Biotechnology 28: 262-271.

237. Chandrayan SK, Wu C-H, McTernan PM, Adams MW (2014) High yield purification of a tagged cytoplasmic [NiFe]-hydrogenase and a catalytically-active nickel-free intermediate form. Protein Expression and Purification 107: 90-94.

238. Zhang Y-HP, Evans BR, Mielenz JR, Hopkins RC, Adams MW (2007) High-yield hydrogen production from starch and water by a synthetic enzymatic pathway. Plos One 2: e456.

239. Myung S, Rollin J, You C, Sun F, Chandrayan S, et al. (2014) In vitro metabolic engineering of hydrogen production at theoretical yield from sucrose. Metabolic Engineering 24: 70-77.

240. Mertens R, Greiner L, van den Ban EC, Haaker HB, Liese A (2003) Practical applications of hydrogenase I from *Pyrococcus furiosus* for NADPH generation and regeneration. Journal of Molecular Catalysis B: Enzymatic 24: 39-52.

241. Privé GG (2007) Detergents for the stabilization and crystallization of membrane proteins. Methods 41: 388-397.

242. Lipscomb GL, Schut GJ, Thorgersen MP., Nixon WJ, et al. (2013) Engineering hydrogen gas production from formate in a hyperthermophile by heterologous production of an 18-subunit membrane-bound complex. Journal of Biological Chemistry 289: 2873-2879.

243. Schut GJ, Nixon WJ, Lipscomb GL, Scott RA, Adams MW (2012). Mutational analyses of the enzymes involved in the metabolism of hydrogen by the hyperthermophilic archaeon *Pyrococcus furiosus*. Frontiers in Microbiology 3: 1-6.

244. Zadvornyy OA, Eilers BJ, Boyd ES, Artz JH, McTernan PM, et al. (2015) Evolution of ubiquitous respiratory complex I from a membrane bound hydrogenase ancestor. *Science*: "submitted, March 2015".